Dissertation zur Erlangung des Doktorgrades
der Fakultät für Chemie und Pharmazie
der Ludwig-Maximilians-Universität München

Integrin mediated regulation of vascular maturation and atherogenesis

Ina Rohwedder
aus
München

2013

Erklärung

Diese Dissertation wurde im Sinne von § 7 der Promotionsordnung vom 28. November 2011 von Herrn Prof. Dr. Reinhard Fässler betreut.

Eidesstattliche Versicherung

Diese Dissertation wurde eigenständig und ohne unerlaubte Hilfe erarbeitet.

München, ..15.03.2013.....

……

(Ina Rohwedder)

Dissertation eingereicht am 15.03.2013
1. Gutachterin / 1. Gutachter: Prof. Dr. Reinhard Fässler
2. Gutachterin / 2. Gutachter: Prof. Dr. Christian Wahl-Schott
Mündliche Prüfung am 03.12.2013

Die vorliegende Arbeit wurde in der Zeit von Januar 2009 bis Februar 2013 in der Arbeitsgruppe von Herrn Prof. Dr. Reinhard Fässler in der Abteilung für Molekulare Medizin am Max-Planck-Institut für Biochemie angefertigt.

Im Verlauf dieser Arbeit wurden folgende Veröffentlichungen publiziert oder zur Publikation vorbereitet:

Rohwedder I, Montanez E, Beckmann K, Bengtsson E, Dunér P, Nilsson J, Soehnlein O, Fässler R: ***Plasma fibronectin deficiency impedes atherosclerosis progression and fibrous cap formation***. EMBO Mol Med. 2012 Jul;4(7):564-76.

Rohwedder I; Tolde O.; Zent R.; Fässler R.: ***α-Parvin controls contraction and actin organization in smooth muscle cells***. Manuscript in preparation

Abbreviations

aa amino acid

ABD actin-binding domain

ABP actin-binding protein

ADMIDAS adjacent to metal-ion-dependent adhesion site

Ala alanine

Alk activin-receptor-like kinase

ANK ankyrin

aPKC atypical protein kinase C

Arg arginine

Arp2/3 complex actin-related protein 2/3 complex

Asp asparagine

ATP adenosine triphosphate

ATPase adenosine triphosphatase

bFGF basic fibroblast growth factor

BM basement membrane

Ca2+ calcium-ion

Cdc42 Cell division control protein 42 homolog

CH calponin homology domain

CH-ILKBP CH domain-containing ILK-binding protein

Col collagen

Crk v-crk sarcoma virus CT10 oncogene homolog

DLL4 Delta-like-4

DNA deoxyribonucleic acid

Dock180 180-kDa protein downstream of CRK

DRF diaphanous-related formin

E embryonic day

EB embryoid bodies

EC endothelial cell

ECM extracellular matrix

Ena/Vasp enabled/vasodilator-stimulated phosphoprotein

EPC endothelial precursor cell

EST expressed sequence tag

FA focal adhesion

F-actin filamentous actin

FAK focal adhesion kinase

FC focal complexes

FERM 4.1, ezrin, radixin, moesin

FN fibronectin

FRET fluorescence energy transfer

G-actin globular actin

GAP GTPase activating protein

GEF guanine nucleotide exchange factor

GDI guanine nucleotide dissociation inhibitor

GDP guanosine diphosphate

GIT G-protein-coupled receptor kinase interacting protein

GSK3β glycogen-synthase kinase-3β

GTP guanosine triphosphate

GTPase guanosine triphosphatase

HeLa Henrietta Lacks

ICAM1 intercellular adhesion molecule-1

Ig immunoglobulin

IL interleukin

ILK integrin linked kinase

ILKAP ILK-associated phosphatase

IPP complex ILK-PINCH-Parvin complex

JNK c-Jun N-terminal kinase

kDa kilodalton

LAD-III leukocyte-adhesion deficiency type III

LDV leucine-aspartic acid-valine

LLC Lewis lung carcinoma

LIM Lin11, Isl1, Mec3

LIMBS ligand-induced metal ion binding site

LIMK LIM kinase

LN laminin

LTBP latent TGFβ-binding protein

MAdCAM-1 mucosal addressin cell adhesion molecule-1

MC Mesangial cell

MCP-1 monocyte chemotactic protein 1

Mg2+ magnesium-ion

MHC myosin heavy chain

MIDAS metal-ion-dependent adhesion site

MLC myosin regulatory light chain

MLCK MLC kinase

MLCP MLC phosphatase

MMP matrix metalloproteinase

µm micrometer

Mn2+ manganese-ion

mRNA messenger RNA

MTOC microtubule organizing centre

MYPT1 myosin phosphatase-targeting subunit 1

NLS nuclear localization signals

P postnatal day

PAK p21-activated kinase

PAR6 polarity-protein-partitioning-defective-6

PAT paralyzed and arrested at the twofold stage

PDGF platelet-derived growth factor

PDGFRβ PDGF receptor β

PH Pleckstrin Homology

PINCH particularly interesting Cys-His-rich protein

PIX PAK-interacting exchange factor

PKB protein kinase B/Akt

PKL paxillin-kinase linker

PLGF placental growth factor

PSI plexin-semaphorin-integrin

PTB phospho-tyrosine binding

PtdIns(3,4,5)P3 phosphatidylinositol-3,4,5-trisphosphate

Rac1 Ras-related C3 botulinum toxin substrate 1

Ras rat sarcoma

RGD arginine-glycine-aspartic acid

RhoA Ras homologous

Rif Rho in filopodia/RhoF

RNA ribonucleic acid

RNAi RNA interference

ROCK Rho-associated kinase

s second

S1P sphingosine-1-phosphate

Ser serine

SFK Src family of tyrosine kinases

SH2 Src-homology 2

SH3 Src homology 3

SRF serum response factor

TESK1 testicular protein kinase 1

TGFβ transforming growth factor β

THD talin head domain

Thr Threonine

TM transmembrane

TNFα tumor necrosis factor α

UB ureteric bud

UC Ureter smooth muscle cell

UNC uncoordinated

VCAM1 vascular cell adhesion molecule 1

VN Vitronectin

vSMC vascular smooth muscle cell

vWFA von Willebrand factor A

WASP Wiskott-Aldrich syndrome protein

WAVE WASP-family verprolin-homologous protein

WIP WASP-interacting protein

Y2H yeast two hybrid

Summary

Migration on and adhesion of cells to extracellular matrix (ECM) componentss or neighboring cells is crucial for development and homeostasis of multicellular organisms. The binding to the ECM is mainly mediated by integrins, a class of α/β heterodimeric transmembrane receptors. Integrins possess only a short cytoplasmatic tail and lack enzymatic activity or actin binding ability. Thus, they rely on adaptor and signaling molecules to transmit extracellular signals into the cell or vice versa and thereby control proliferation, survival and differentiation. The precise function of integrin associated proteins is still not fully known, but in most cases a missregulation of one member of this protein cluster results in severe abnormalities in embryonic development or leads to disease.

First we investigated the impact of plasma derived fibronectin (pFN) on the development of atherosclerosis in mice. It was known, that atherosclerotic plaques develop preferentially at areas of turbulent blood flow in the aorta, at vessel branches and bifurcations. FN depositions were observed at these areas, even before plaques developed, but the source and concrete function of FN remained unknown. *In vitro* experiments suggested that FN deposits at the vessel endothelium enforce and maintain a pro-atherogenic milieu through integrin binding and signaling. We used a conditional knockout approach to delete the FN gene in either hepatocytes and/or haematopoietic cells of atherosclerosis-prone (ApoE)-null mice. These mice are commonly used for atherosclerosis studies, since they develop all stages of lesions throughout their lifespan when being fed a high fat containing diet. While deleting FN in haematopoietic cells did not affect plaque formation, loss of pFN resulted in reduced FN deposits in the subendothelial space of atherosclerosis-prone regions and diminished the number and size of atherosclerotic lesions. Without these FN deposits we observed a downegulation of inflammatory and adhesion markers for monocytes at the endothelium. In addition pFN deletion blocked the migration of vSMC and led to a strongly diminished fibrous cap formation. We could show with our experiments, that pFN has two opposing roles in disease initiation and progression. It promotes disease by enhancing inflammation and monocyte adhesion but also stabilizes developing plaques by promoting fibrous cap formation.

Second, we investigated the *in vivo* function of α-parvin (αpv) in vascular smooth muscle cells (vSMC). αpv is a focal adhesion (FA) protein and forms together with its binding partners integrin linked kinase (ILK) and particularly interesting Cysteine-Histidin-rich-protein (PINCH) a ternary protein complex, the IPP complex. Constitutive deletion of αpv has been shown to result in embryonic lethality due to severe cardiovascular defects. vSMC, crucial for stabilizing vessels, were not properly recruited to their destination on the endothelial layer of vessels and adherent cells remained round and not properly spread. *In vitro* isolated cells were round, with multiple retraction fibers and elevated levels of phospho-Myosin light chain 2 (pMLC2) and RhoA indicated hypercontraction after αpv deletion. Comparable results were obtained after ILK and integrin β1 deletion conditional from vSMC. The conditional αpv deletion from vSMC results in vascular defects, similar to αpv null mice, but mice survive until 4 weeks of age. As expected we could detect elevated pMLC2 levels in αpv null vSMC but also higher matrix degradation in the absence of αpv, which is further weakening vascular structures. The proposed role for αpv in regulating contraction is also applying to intestinal SMC (iSMC), but not to ureter SMC (UC)

and mesangial cells (MC), which *in vivo* results in the formation of a paralytic ileus and subsequent death of mice.

Introduction

The Integrin family of adhesion receptors

In almost all tissues, cells are surrounded by a three-dimensional crosslinked network of macromolecules that form the extracellular matrix (ECM). This network is secreted and constantly remodeled by the cells themselves. The ECM provides the cell with environmental information, but also acts as signaling platform and is capable of binding growth factors and chemokines. There are multiple cellular receptors, which enable the cell to bind to the ECM and transmit signals into the cell. Integrins belong to the family of type I transmembrane adhesion receptors, and are the major receptor family in all metazoans for mediating cell adhesion to proteins of the ECM. In vertebrates they can additionally interact with cellular counter receptors and thus mediate cell-cell interaction. Integrins are heterodimeric proteins, consisting of one α- and one β-subunit, which form with their head domains a shared binding platform for different ECM molecules. Their name “integrins” refers to their ability to act as a bridge between the ECM and the intracellular cytoskeleton. This linkage to various intracellular binding proteins enables integrins not only to act as simple adhesion molecules, but additionally induces signaling events in the cell mediating cell shape, contraction but also proliferation, survival and differentiation. Because of this central role they are of great importance for development and immune response. Not surprisingly therefore, that misregulations in integrin signaling can lead to cancer and other diseases. In line with their importance for the organism, they are evolutionary conserved and the number of integrin subunits rises with the complexity of the organism. In the nematode *Caenorhabditis elegans* only two integrins are known, formed by two α- and one β-subunits. In the fruit fly *Drosophila melanogaster* already five different integrins can be assembled out of five α-subunits and two β-subunits (Hynes et al. 2000). In all mammals 24 integrins are known, made up by combining 18 α- and 8 β-subunits. These different integrins heterodimers are subdivided into 4 distinct categories, grouped by specificity to a specific ligand and also cell-specific expression patterns. (Fig. 1)

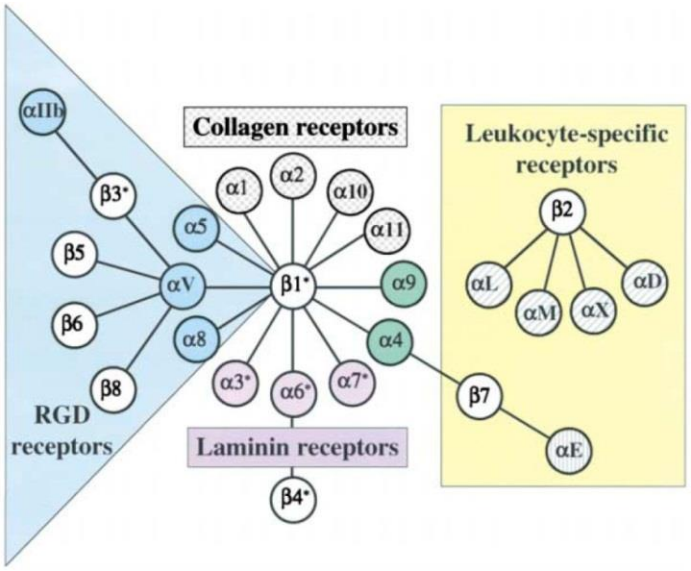

Figure 1: The Integrin receptor family

Depicted are the 24 mammalian integrin heterodimers arranged to their main ligands (RGD containing ligands, Collagen and Laminin) and a 4th group containing integrins specifically expressed on leucocytes only. Gray hatchings indicate the presence of an inserted I/A domain. (taken from Hynes, 2002)

Class 1) These integrins bind preferentially to ligands containing the RGD (arginine-glycine-aspartic acid) tripepdide sequence. All αV containing heterodimers (αvβ1, αvβ3, αvβ5, αvβ6 and αvβ8) belong to this group and in addition α5β1, α8β1 as well as αIIbβ3, an integrin specific for platelets. Ligands, which contain RGD are fibronectin (FN), vitronectin (VN), thrombospondin, osteopontin, tenascin and many other proteins. Although this subset of integrins shares a large number of ligands, there is a variance of affinity to the receptor, most likely regulated by how precise the RGD conformation fits to the integrin binding pocket.

Class 2) Collagen (Col) binding integrins are the β1 heterodimers α1β1, α2β1, α10β1 and α11β1. All of these α-subunits contain a special αA/I domain, critical for ligand binding. The different heterodimers vary in their preference to different Col types.

Class 3) The β1 heterodimers α3β1, α6β1, α7β1 together with α6β4 integrin are highly specific receptors for laminin (LN). It has been demonstrated with LN fragments, that different binding regions exist for distinct integrin dimers (Nishiuchi et al. 2006). In addition the Col-receptors α1β1, α2β1 and α10β1 can also bind LN (Humphries et al., 2006).

Class 4) The α4β7 and αEβ7 heterodimers as well as the β2 heterodimers αLβ2, αMβ2, αXβ2, αDβ2 are specific for leucocytes. They recognize the tripeptide motif LDV (leucine-aspartic acidvaline) or structurally related motifs. Besides FN, this sequence is found in VCAM1 (vascular cell adhesion molecule 1), mucosal addressin cell adhesion molecule-1 (MAdCAM-1) and intercellular adhesion molecule 1 (ICAM1). The latter three are surface proteins expressed by endothelial cells enabling leucocytes to bind to the EC layer and transmigrate into the tissue. The related integrins α9β1 and α4β1 can bind both: ECM such as FN and additionally recognize Ig-superfamily counter receptors like VCAM1.

Integrin structure, activation and ligand binding

Both Integrin subunits, α as well as β, consist of very large extracellular domains of up to 1104 amino acids (aa) for α- and 778 aa for β-subunits, that contribute to ligand binding, a helical transmembrane (TM) domain of 25-29 aa and only a very short C-terminal cytoplasmic segment of about 20-50 aa. The only exception is the β4 subunit which contains a long cytoplasmatic segment of around 1000 aa. β4 is - as integrin α6β4 the only heterodimer that is connected to intermediate filaments instead of the actin cytoskeleton.

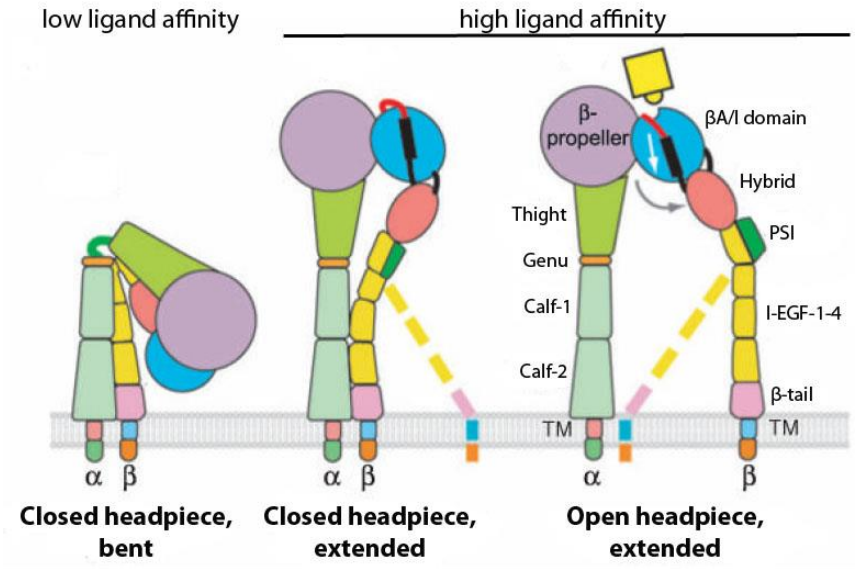

Figure 2: Integrin structure

Integrin domain structure and rearrangements during activation are shown. The leg region of β subunits separate during activation. The picture shows what may be the predominant (solid representation) and less predominant (dashed lines) orientations. (modified from Luo et al. 2007).

The extracellular head domain of α subunits is folded into 7-bladed β propellers, followed by the stalk consisting of an Ig-like (thigh) and two calf (1 & 2) domains (β sandwich domains) (Fig. 2). The head domain of the β subunit is organized in a βI/A domain, which is inserted into an immunoglobulin (Ig)-like "hybrid" domain. The stalk consists of a PSI (plexin, semaphorins, and integrins) domain, four tandem cysteine-rich EGF-like repeats and a β-tail domain. The βI/A domain together with the β propellers of the α-subunits forms the integrin head domain, with the ligand binding pocket, where ligand binding itself is taking place. It is commonly accepted, that integrins can exist in a low-, intermediate- and high affinity state. Based on electron microscopy studies it is believed, that a bent head domain represents the low affinity state, while integrins with an extended ectodomain are on high affinity for ligands. There are two models proposed for this change in affinity: The "deadbolt model" describes a scenario where the head is still bent in an activated integrin. The TM regions perform a piston-like movement that results in sliding of the extracellular stalks of the α and β subunits, and the interaction between headpiece β stalk is disrupted just beyond the membrane (Luo et al. 2007). Until now no experimental evidence for this theory could be found (Luo et al. 2006). In the "switchblade model", first the α and β cytoplasmic and TM regions dissociate, which then results in a dislocation of an epidermal growth factor (EGF)-like

repeat in the β stalk and causes the head region to extend in a switchblade-like movement. Additionally, the Hybrid domain of the β-subunit performs a “swing-out” movement, that results in a shift from a closed (low affinity) to an open (high affinity) conformation of the βA/I domain. The Col-binding and the leukocyte specific α-subunits have in addition an N-terminal von Willebrand factor A (vWFA) domain inserted into their β-propeller, referred to as the αA/I domain. It has a strong similarity to the βA/I domain and can as well change from a closed and low affinity to an open and high affinity state. The βA/I domain and also the αA/I domain contain a central Mg2+ binding site (MIDAS - metal-ion-dependent adhesion site), which is regulating the switch between the affinity conformations. Only on the βA/I domain two flanking additional Ca2+ binding sites are present: one called SyMBS (synergistic metal ion binding site) and the other AdMIDAS (adjacent to MIDAS). At integrins lacking the αA/I domain, the βA/I domain is mainly mediating ligand binding, but for these 9 integrins with αA/I domain, this domain is stronger contributing to ligand binding. Concerning the cytoplasmatic domain (integrin tail) of β-subunits, a strong sequence homology was described, whereas the α-subunit tails show more variance in sequence apart from the conserved GFFKR motif. It was shown by mutation studies that this motif is important for the association with the β-tail (Takada et al. 2007), since any changes in this motif activates integrins by destabilizing the association of α- and β-TM domain (O’Toole et al. 1994, Lu et al. 2001). A recognition sequence for phosphotyrosine-binding (PTB) domains is found on most integrin β tails:a membrane proximal NPxY motif and a membrane distal NxxY motif. These protein sequences can be found in a large variety of cytoskeleton adaptors and signaling proteins, that are necessary to transmit signals from the ECM to the cytoskeleton or are critical for integrin activation (Hynes 2002).

Bidirectional signaling

Integrins have the ability to signal in both directions (bidirectionally) across the plasma membrane. In general this means that ligand binding to the integrin head triggers signaling within the cell through recruitment of different integrin tail binding proteins (outside-in signaling). This then induces changes in the cytoskeleton or various signal transduction pathways and can lead to cell spreading, contraction or migration. In the other direction, inside-out signaling describes a process where intracellular signals induce the conformational changes in integrins, necessary for ligand binding.

Inside-Out signaling

The affinity for integrins to bind their corresponding ligand is a tightly regulated process. The best example for inside-out signaling is the activation of integrins themselves. Especially for cells of the hematopoietic system it is important to keep their integrins in the inactive conformation and to prevent unwanted strong cell-cell/ECM interactions. Leukocytes travel through the blood stream and do not adhere to the endothelial cell (EC) layer, until inflammatory stimuli like T-cell receptor activation or ligation of selectins on neutrophils emerge. This induces a signal cascade, resulting in the translocation of the adaptor proteins talin and kindlin to the cytoplasmatic tail of β-subunit and subsequent tail separation, switching the integrin into a high affinity state. Only then, firm leucocyte adhesion to EC surface proteins like ICAM1 and VCAM1 by the LDV-binding class of integrins will occur and lead to the

transmigration into the tissue. Also for platelets, where integrin activation leads to clot formation, an intracellular stimulus is required for ligand binding. Here the binding of glycoprotein VI on platelets to exposed Col is preceding the activation of their integrin αIIbβ3 and fibrinogen binding.

The two cytoplasmatic integrin adaptor molecules talin and more recently also kindlin have emerged as critical regulators of integrin activity. Orthologs of talin were identified in all multicellular eukaryotes studied. Whereas lower eukaryotes only have one talin, vertebrates encode two talin isoforms (talin1 and talin2). Talin is 270 kDa protein, composed of a 50 kDa N-terminal globular head domain (THD) and a 220 kDa C-terminal rod domain. The THD contains three FERM (protein 4.1, ezrin, radixin, moesin) subdomains: F1, F2, and F3, and a non-homologous F0 domain. Binding to the conserved membrane-proximal NPxY (x can be any aa) motif of β integrin cytoplasmic tail occurs via a PTB (phosphotyrosine binding) domain that is located in the F3 subdomain. Talin binding was abolished after mutating the NPxY motif in β1 or β3 integrins, or mutating the PTB domain resulting in decreased integrin affinity (Moser et al. 2009). FRET (Fluorescence energy transfer) studies suggested that talin head binding induces separation of the two integrin tails and TM domains, a final step in integrin activation (Kim et al. 2003). But still, the head domain of talin is not enough to trigger also clustering of integrins after ligand binding and the formation of focal adhesions (FA). This was shown with reexpression of THD in talin deficient cells and proposes an independent function of the talin tail (Zhang et al. 2008a). The talin rod domain is composed of a series of helical bundles that contain binding sites for vinculin and actin and it is therefore regarded as an important linker between the ECM and the cytoskeleton. Its ability to also bind integrins along with the presence of a homodimerization motif suggests that the tail of talin is necessary for integrin clustering and FA-Formation.
Although talin is essential for integrin activation it is not enough and further co-factors are required. It was for example shown, that mutations and truncations of the β3 integrin tail C-terminal to the talin binding site results in decreased ligand affinity of the integrin, suggesting that also other proteins can modulate the affinity state (Ma et al. 2006). More recent studies showed that kindlin is one of these proteins, also binding to integrins and controlling integrin activation (Ussar et al. 2008, Montanez et al. 2008, Moser et al. 2008,). The kindlin family consists of three members: kindlin1/Unc-112-Related Protein 1 (URP1), which is expressed in epithelial cells; kindlin2/Mig-2, which is ubiquitously expressed; and Kindlin3/URP2, whose expression is restricted to hematopoietic cells. Like talin, kindlins have a C-terminal FERM domain, but the F2 subdomain is split by an inserted pleckstrin homology (PH) domain. Binding to the integrin tail again works via the PTB domain in the F3 subdomain in kindlin. Unlike talin that interacts with the membrane proximal NPxY motif, the F3 subdomain of kindlin interacts with the more distal NxxY motif. Interestingly, kindlin2 is not able to activate integrins like the THD does, but further enhances activation when co-expressed with THD (Montanez et al. 2008). Studies further showed that both proteins critically depend on the presence of each other, because THD domain cannot achieve integrin activation in kindlin2 knockdown cells (Ma et al. 2008). It is not yet fully understood, how this synergistical effect is achieved and if both proteins bind simultaneously or subsequently to the tail of β integrin. Mutations in kindlin1 cause a skin-blistering disease in humans called Kindler syndrome. A knockout model of the ubiquitously expressed kindlin2, led to peri-implantion lethality due to a severely decreased function of β1 and β3 integrin. Kindlin3 was shown to be required for leukocyte adhesion and extravasation and in humans. Mutations in kindlin3 leads to a rare disease known as

leukocyte-adhesion deficiency type III (LAD-III) characterized by severe bleedings, leukocyte adhesion and extravasation defects (Kuijpers et al., 2009, Svensson et al., 2009).

Integrin clustering and FA formation

After being activated, integrins are able to bind their corresponding ligand and thus form a link between the cell and the ECM. Nevertheless, the adhesion force of one integrin is too weak to realize firm adhesion of the cell to the matrix. Lateral association of integrins to the point of adhesion unites numerous weak links to the ECM in a synergistic manner, also called “avidity”. It has been shown, that activation of integrins as well as their clustering is required for transmitting signals from the ECM into the cell (Zhu et al. 2007), but how this integrin clustering is mechanistically executed, is not known yet. On 2D cultured cells, several distinct types of adhesive structures can be observed: nascent adhesions appear at the leading edge of cells, where new interactions to the ECM are formed (Choi et al. 2011). These small adhesions can mature in a Rac1 driven manner into focal complexes (found at the lamellopodiums edge). Under the influence of RhoA activity and tension, focal complexes grow in size to become FAs (localized at the cell periphery) and finally mature into fibrillar adhesions (center of cells) (Geiger et al. 2001). The mechanism of this maturation process is still not perfectly clear, but several proteins have been identified, which serve as a marker for some of these subtypes. Talin and also paxillin are already found in nascent focal adhesions and focal complexes, whereas the LIM-domain protein zyxin is first present in large FAs. While αv integrin is more associated to FA, α5 integrin and tensin are typical components of fibrillar adhesions (Zamir et al. 1999). Although these defined structures are only observed *in vitro* on solid surfaces, comparable adhesive units were observed *in vivo*, for example the adhesions to the basement membrane (BM) formed by aortic EC (Kano et al. 1996), or the adhesive structures of SMC (Turner et al. 1991). A large number of proteins in recruited to the place of FA formation, actin linkers as well as signaling proteins, in a process named outside-in signaling.

Outside-In signaling

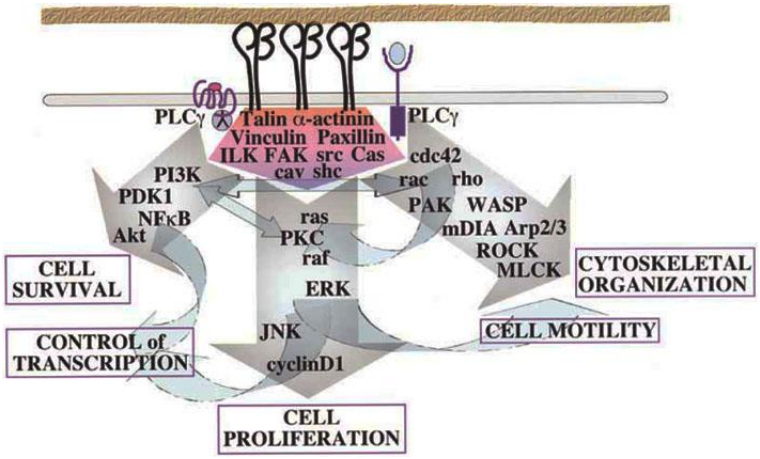

Figure 3: Outside-in signaling.

Depicted are the major signal pathways and key players. They often act in concert with G protein-coupled or kinase receptors. The major integrin associated proteins are highlighted with a pink-purple pentagon beneath the clustered integrins. (modified from Hynes et al. 2002)

Integrins have a central role for adhesion and signaling in all cells and are therefore crucial for the survival of the organism (Fig. 3). However their short cytoplasmatic tail lacks catalytic activity of its own. Instead integrins bind a huge number of proteins either directly or via adaptor molecules. So far over 700 molecules, associated to integrin mediated adhesion were identified (Zaidel-Bar et al. 2007 and 2010, Schiller et al. 2011), also called the integrin "adhesome". Out of them more than 40 proteins were shown to bind directly to β integrin cytoplasmic tails (Legate et al. 2009). Interestingly much fewer proteins interact directly with the tails of α-subunits. Since not all of these proteins bind simultaneously there is a spatiotemporal control of assembly/disassembly of the molecular composition of the FA adhesome (Legate et al. 2009). Integrin activation results in downstream signaling events that can be divided into three temporal stages The first effects of integrin activation is the up-regulation of lipid kinase activity that then increases the concentrations of PtdIns-4,5-P2 and PtdIns-3,4,5-P3 as well as the induction of rapid phosphorylation of specific protein substrates. Among them are the important kinases FAK and src. Their phosphorylation leads to FAK/src activation and several minutes after the first stage to phosphorylation of more FA proteins like paxillin and activation of signaling pathways like Ras/MAPK. Also Rho family GTPases and other actin regulatory proteins are activated, resulting in the reorganization of the actin cytoskeleton. The last stage represents the long-term consequences of integrin outside-in signaling, like proliferation and survival as well as alterations in cell morphology.

Actin binding and regulation via Integrins

The link of integrins to the actin cytoskeleton is one of the key functions of the adhesome proteins. Integrins are unable to bind directly to actin but proteins of the adhesome serve as a mechanical link between actin and the ECM and also regulate actin remodeling. According to Legate et al. 2009 they can be roughly divided into 4 classes:

1) integrin-bound proteins that directly bind actin, such as talin, α-actinin, and filamin;

2) integrin-bound proteins that indirectly associate with the cytoskeleton or in its regulation such as kindlin, integrin-linked kinase (ILK), paxillin, and FAK;
3) non-integrin-bound actin binding proteins, like vinculin;
4) adaptor and signaling molecules that regulate the interactions of the proteins from the groups mentioned above.

The first linkage to the cytoskeleton after integrin-ligand-binding is the recruitment of talin to the NPxY motiv of β-integrin tails. A 2-pN slip bond is established, providing the initial force from the cytoskeleton to the ECM (Jiang et al. 2003). As a next step, vinculin is recruited to nascent adhesions, which is binding to several sites in the talin rod domain. Interestingly these binding sites are normally not exposed and probably mechanical stretch is required for binding. Along with this finding, expression of the THD in talin null cells, which is not able to bind vinculin, activates integrins but fails to form detectable focal contacts (Zhang et al. 2008a). This suggests that talin is required for the initial contact, but vinculin, which can bind to both actin and talin is critical for maintaining and strengthening this connection. α-actinin is a protein, able to bind to vinculin, as well as talin and even to β-integrin itself. It was shown, that α-actinin incorporation into FAs is increasing in a force-dependent manner (Laukaitis et al 2001) and matching to this theory α-actinin has been shown to have an essential role in adhesion strengthening *in vivo*: In mammals, which express four isoforms of α-actinin, α-actinin2 and α-actinin3 can cross-link actin filaments in the region of Z discs in striated muscles where they regulate force coupling of muscle fibers (MacArthur et al. 2007). α-actinin 4 was shown to be essential for kidney function by strengthening the adhesion of podocytes to the glomerular basement membrane (Kos et al. 2004). Another FA protein, being able to bind to the tail of β-integrin is the adaptor protein ILK. Through binding to its main binding partner parvin, ILK is also acting as a link between ECM and actin. This link is additionally working via ILK binding to paxillin, which is also an actin binding protein. Since the main focus of the second publication is on parvin and the IPP complex, these proteins will be presented in more detail in an own paragraph.

Actin dynamics and Rho / Rac signaling

The attachment of integrins to F-actin not only critical for the force dependent formation of FA, it is also needed for the precise control of cell protrusion and retraction during cell migration, cell shape regulation, wound healing or cell contraction. Although actin dynamics are highly dependent on Rho-GTPase signaling, which will be further discussed below, there are many actin binding proteins (ABP), which regulate actin assembly and disassembly during cell migration. The lamellopodium forms at the leading edge of cells, a dendritic actin network in a thin membrane leaflet. There, nascent adhesions are formed between integrins and the ECM and membrane protrusions are formed by the polymerization of actin. This assembly of new actin fibers requires the polymerization of G-actin into F-actin. As short dimeric or trimeric actin intermediates are very unstable, this process is highly dependent on the presence of actin nucleators.

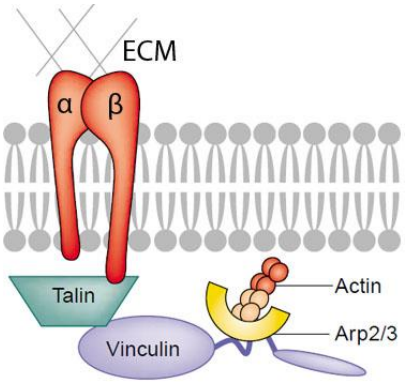

Figure 4: Link between actin polymerization and integrins:

The activated Arp2/3 complex binds directly to vinculin, an adhesion molecule, recruited to integrins by interaction with talin. Binding of the Arp2/3 complex to vinculin localizes polymerization to new sites of integrin adhesion. (modified from DeMali et al., 2003)

The heptameric actin-related protein 2/3 (Arp2/3) complex is one of the best characterized actin nucleators. This complex promotes the branching of new actin filaments out of existing ones and thus forms the branched actin network in lamellopodia. However, the isolated Arp2/3 complex has no endogenous actin nucleating activity and must be activated by the Wiskott-Aldrich Syndrome protein (WASP) family (WASP, N-WASP, WAVE, and WASH proteins) of activator proteins. WASP binding leads to a conformational change in Arp2/3 that allows Arp2/3 to form a template for actin filament elongation. Arp2/3 is recruited to nascent integrin adhesions through interactions with FAK as well as vinculin to promote actin polymerization directly at the site of adhesion. This generates the protrusive force for the lamellopodium (Fig. 4). In the lamellum, the area directly behind the lamellopodium, actin is organized into parallel bundles to establish directional persistence of cell motility. Here actin assembly is mediated by the diaphanous-related formin (DRF) protein family, including mDia or Ena/Vasp. These proteins prevent the binding of ABP named “capping proteins”, which bind to the “barbed ends” of actin and thus inhibit further polymerization(Zigmond et al. 2004).

Rho GTPases (Rho family of small (~21kDa) GTPases) are key regulators of the actin cytoskeleton and its dynamics. They control the processes listed above in a spatiotemporal manner. The Rho family is a subfamily of the Ras (Rat sarcoma) protein family and in mammals consists of 20 signaling proteins. They cycle between an active GTP-bound state and an inactive GDP-bound state and they hydrolyze GTP to GDP (Fig. 5).

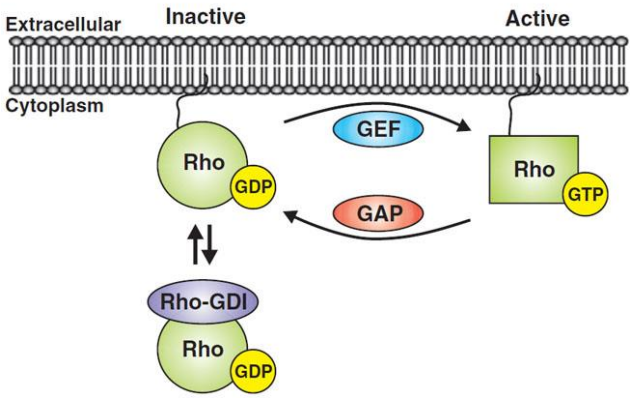

Figure 5: The Rho-GTPase activation cycle.

This model depicts how Rho-GTPases are regulated. Rho-GDP dissociation inhibitors (Rho-GDIs) sequester inactive GDP-bound Rho-GTPases (Rho) in the cytoplasm. After being released Rho-GTPases are targeted to the plasma membrane. Their activation is regulated by GEFs that promote GTP loading, whileinactivation of Rho-GTPases is mediated by GAPs that promote GTP hydrolysis to GDP. (taken from Huveneers et al., 2009)

This cycling is regulated by three sets of proteins, guanine nucleotide exchange factors (GEFs), GTPase-activating proteins (GAPs), and guanine nucleotide dissociation inhibitors (GDIs). GEFs exchange GDP for GTP and thus are required for the activation of Rho GTPases. In contrast, GAPs inactivate Rho GTPases by enhancing their intrinsically inefficient GTPase activity. While in humans a large number of GEFs and GAPs are known (over 70 GEFs and around 80 GAPs), only 3 GDIs are identified. GDIs inhibit the guanine nucleotide exchange and retain Rho GTPases in an inactive state in the cytosol. After dissociation from the inhibitory GDIs, Rho GTPases can relocate to plasma membranes. The best characterized Rho GTPases for the regulation of actin dynamics at FAs are Rac, Cdc42, and RhoA. (Fig. 6).

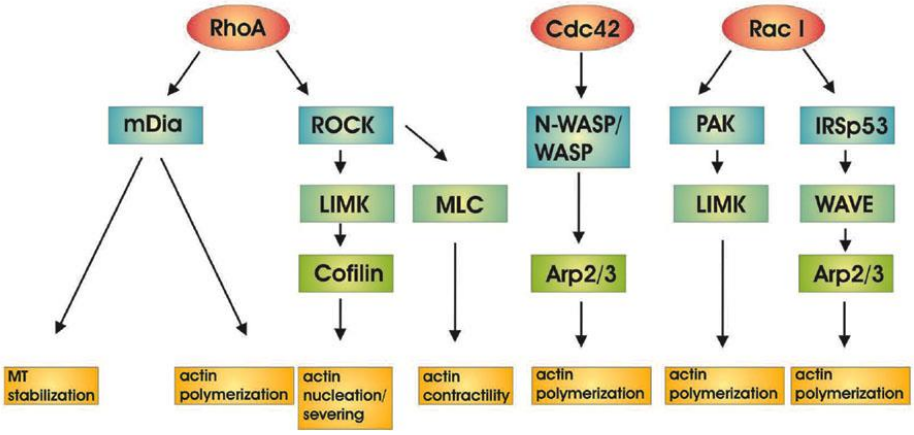

Figure 6. Downstream effector targets of Rho family of GTP ases. (taken from Spiering et al. 2011)

Rac - regulator of lamellopodium formation

Because of their similarity in sequence, RAC1, RAC2, RAC3 and the more distinctly related RhoG form a subfamily within the Rho GTPases. Rac proteins stimulate lamellopodium formation at the leading edge of cells, which was proven experimentally by inhibition of Rac1 or in Rac1 null epiblasts (Ridley et al.

2001). Both approaches led to severe migration defects. The effect of constitutively active Rac1 is not consistent in all cell lines. In macrophages overexpression of constitutively active Rac1 resulted in polarization defects due to lamellopodium formation all around the cell and therefore impaired migration (Allen et al. 1998). In Boyden chamber assays a positive or a negative effect of constitutively active Rac1 on the transmigration rate of cells was observed (Banyard et al. 1999, Leng et al. 1999) . Rac1, the best studied member of this family is ubiquitously expressed, while Rac2 expression restricted to hematopoietic cells and Rac3 is mostly found in brain. RhoG also stimulates lamellopodium formation, probably by activating RacGEFs, which activate Rac (Heasman et al. 2009). It was shown that integrin activation and clustering lead to membrane recruitment of Rac as well as recruitment of several GEFs via signaling modules such as the FAK–p130Cas–CrkII–DOCK180 (Cary et al. 1998, Kiyokawa et al. 1998) pathway, or the paxillin–GIT–PIX pathway (Nayal et al. 2006). The critical importance of integrin-Rac signaling could be demonstrated by knockout studies of either of these proteins in Schwann cells. β1 integrin-deficient Schwann cells display decreased Rac1 activity and are deficient in the extension of lamellopodia. This defect can be partly rescued by expressing constitutively active Rac (Nodari et al. 2007). In the opposite experiment, deletion of Rac1 in Schwann cells, or treating these cells with Rac inhibitor, results in loss of lamellopodia *in vitro* (Benninger et al. 2007). Rac proteins can regulate actin polymerization at lamella in different ways: first, they are able to activate actin nucleating proteins, including the ARP2/3 complex (through Scar/WAVE proteins) and formins like mDia. Second, Rac proteins can remove the barbed end capping proteins of actin. Third, Rac-mediated activation of the Ser/Thr kinase PAK (p21-activated kinase) phosphorylates LIM (Lin11, Isl1, Mec3) kinase (LIMK). The actin depolymerizing protein cofilin is one target of this kinase and the phosphorylation and thereby inactivation of cofilin is resulting in decreased depolymerization of F-actin (Heasman et al. 2009). Cofilin severs actin filaments, leading to an increase in uncapped barbed ends, thus creating new sites for actin polymerization and filament elongation (Ghosh et al. 2004).

Cdc42: regulator of cell polarity and filopodia formation

Cdc42 has a conserved role in regulating cell polarity in many eukaryotic organisms and was first discovered in *Saccharomyces cerevisiae*, where loss of Cdc42 results in budding deficiencies (Etienne-Manneville et al. 2004). The constitutive deletion of Cdc42 in mice results in early embryonic lethality before E7.5 (Chen et al. 2000), but deletion studies in mammalian cell lines have demonstrated a critical role for Cdc42 in the regulation of cell polarity and filopodia formation, like in embryonic stem cells and neurons (Chen et al. 2000, Garvalov et al. 2007). Cdc42 regulates cell polarity by activating Arp2/3 through N-WASP or WASP, which establishes sites for lamellopodium formation and by orienting the microtubule-organizing center and Golgi apparatus in front of the nucleus where the leading edge is forming or maintained (Jaffe et al. 2005). This regulation process CDC42 seems to function via two distinct pathways: first, through PAR6 (polarity-protein-partitioning-defective-6) and thus with PAR3 and/or aPKC (atypical protein kinase C). This complex has been suggested to mediate organization of microtubules at the front of the cell and to orientate the Golgi and MTOC (microtubule organizing centre) during the establishment of cell polarity (Etienne-Manneville et al. 2003). Second, Cdc42 functions through its target, myotonic-dystrophy-kinase-related Cdc42-binding kinase, to move the nucleus behind the MTOC (Gomes et al. 2005). Additionally, Cdc42 can activate PAK1, like it was shown for Rac (Edwards et al. 1999). Activation of PAK1 leads in turn to the activation of LIMK and thereby

inactivation of cofilin. Although both proteins, Rac1 and Cdc42 activate similar downstream pathways to regulate the actin cytoskeleton, they are associated with distinct actin-containing structures. Rac1 is connected to lamellopodia formation, as it was discussed above, and Cdc42 is thought to be the main mediator of the parallel linear actin filaments constituting filopodia. Filopodia are thin cytoplasmic projections that extend beyond the leading edge of lamellopodia in migrating cells. In many cell types, both constitutively active Cdc42 and dominant negative Cdc42 affect the formation of filopodia (Gupton et al. 2007). In mouse embryonic fibroblasts (MEF) deletion of Cdc42 results in the total absence of filopodia while a CDC42GAPnull mouse with increased Cdc42 activity has a strong increase in filopodia formation (Yang et al. 2006). Different cellular processes have been described that require filopodia formation, including the establishment of the neural circuitry during development and the formation of "adhesion zippers" between endothelial cells that lead to the tight linkage between single cells (Gupton et al. 2007).

RhoA: regulator of cell contractility

Rho activity in migrating cells is associated with FA assembly and cell contractility and is responsible for cell body contraction and rear end retraction. RhoA GTPase promotes cell contractility through two key effector pathways: the Rho kinase (ROCK), which promotes contractility by increasing phosphorylation of the regulatory light chain of myosin II (MLC2), and DRFs, which regulate actin bundling and microtubule stability. A recent study discovered that calpain cleavage of β3 integrin at Tyr759 serves as a molecular switch that changes the outcome of the integrin outside-in signals from mediating cell spreading to promoting cell retraction. This switch from cell spreading to retraction is mediated by calpain cleavage of the c-Src binding site at the integrin C-terminus. This relieves the c-Src–dependent inhibition of RhoA, and facilitates integrin-mediated, RhoA-dependent contractile signaling (Flevaris et al. 2007). It is not yet clear, if also other integrin β subunits are able to modulate RhoA activity. There are studies demonstrating that integrins αvβ3 and α5β1 differentially regulate RhoA activity after binding to FN, which suggests, that there are different ways to modulate RhoA activity (Danen et al. 2002). If this process is indeed dependent on c-Src binding, it may be explained with the high ability of β3 tail to bind c-Src, which has not been demonstrated for β1 tails (Arias-Salgado et al. 2005).

ROCK is one of the best characterized Rho effectors, which exists in two isoforms: ROCK1 (also known as ROK*β* or p160ROCK) and ROCK2 (also called ROK*α*), which are both ubiquitously expressed with redundant functions and are both able to bind to RhoA in a GTP-dependent manner (Nakagawa et al. 1996). Since ROCK is a main candidate for regulating contractility and actin reorganization in vascular smooth muscle cells (vSMC), it is often associated to vascular disorders like hypertension, atherosclerosis and stroke. The major regulatory mechanism of cell contraction in smooth muscle and non-muscle cells is not regulated via troponin and tropomyosin but through phosphorylation/dephosphorylation of myosin light chain (MLC). The myosin superfamily consists of more than 25 members. Myosin II is one subfamily which includes skeletal, cardiac, smooth muscle myosin and nonmuslce myosin II and is the only known myosin so far, able to form filaments. Myosin II is a hexameric molecule that can reversibly bind to actin and is composed of a myosin heavy chain (MHC) dimer that also form the actin binding head domains and α-helical coiled-coils at the tail, as well as two pairs of MLC. Actin filaments have a plus end ("barbed end") and a minus end ("pointed end") and like most other myosins, myosin II moves towards the barbed ends of actin. In mammals there are

three different MHC known: A, B and C, that lead to the formation of myosin IIA, IIB and IIC (De La Cruz et al. 2004, Krendel et al. 2005). Interestingly myosin IIA and IIB strongly differ in their duty ratio, which is the proportion of the ATPase cycle that a motor spends strongly attached to its track. While myosin IIB is a high duty ratio motor, that is necessary for continuous movement and most likely the maintenance of cortical tension, myosin IIA is a low duty ratio motor, more suited for rapid contractile movements. The MLCs are non-covalently bound to the MHC and are required for stabilization and regulation of myosin II (Conti et al. 2008). MLC2 can be phosphorylated by the Ca^{2+}-calmodulin–activated MLC kinase (MLCK) specifically at Ser19, which induces the separation of the head domains of myosin II that possess an ATP-binding site as well as an actin-binding site (Walsh 2011). Cell contraction is performed via the "sliding filament" mode of action. Contraction is induced by bipolar myosin II filaments that force two actin filaments of opposing polarity to slide towards each other and thereby shortening the fiber. At the rear of a migrating cell, myosin II is localized to stress fibers (Saitoh et al. 2001) and contraction promotes movement of the cell body and facilitates detachment of the cell rear. Dephosphorylation is mediated only by the Ca_2-independent MLC phosphatase (MLCP) (Murthy 2006). MLCP is a heterotrimer composed of a catalytic subunit of type 1 phosphatase δ isoform and two regulatory subunits: a target/regulatory subunit (myosin phosphatase target subunit 1; MYPT1) containing 7 ankyrin repeats followed by a PP1c-binding motif and a smaller regulatory subunit (M20) (Ito et al. 2004). It was shown, that RhoA/ROCK can modulate the phosphorylation state of MLC2 in two independent ways: by phosphorylation of the regulatory subunit of MLCP (MYPT1), which attenuates binding to pMLC2 and therefore stabilization of pMLC levels, or by directly phosphorylating MLC2 (Kimura 1996). ROCK not only controls MLC phosphorylation, but it also activates LIMK by phosphorylation at Thr508 (Ohashi et al. 2000). LIMK can in turn phosphorylate cofilin at Ser3, which inactivates cofilin and thereby promotes stress fiber stability (Jaffe et al. 2005). RhoA can also directly bind to the formin mDia1 which leads to the exposition of an FH2 domain on mDia that then binds to the barbed end of actin filaments and additionally prevents binding of other capping proteins (Zigmond et al. 2004). The affinity of the FH2 domain for G-actin is low but formin-induced filaments turn over fast, suggesting that other proteins are required for actin polymerization. One of these co-factors is the actin binder profilin, which can bind to the FH1 domain of mDia.The fact that G-actin-profilin complex is present at higher concentrations than G-actin alone makes it very likely the primary substrate for nucleation.

ILK – PINCH – Parvin, the IPP complex

As described above the cytoplasmatic tail of integrins has no intrinsic enzymatic activity and signaling is dependent on the recruitment of intracellular adaptor, linker and signaling proteins. A ternary protein complex consisting of ILK, PINCH and parvin is one key component of this integrin-mediated signaling, at least for β1 and β3 and will here be discussed in more detail (Fig. 7).

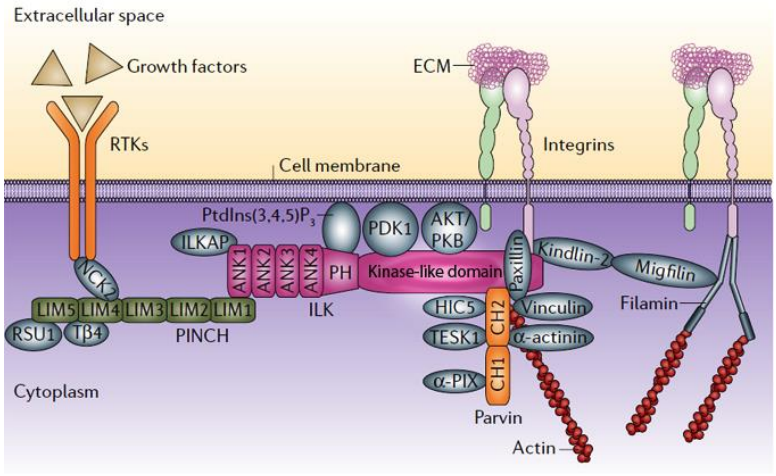

Figure 7: The IPP complex and its binding partners.

The scheme depicts the protein structure of the IPP complex members ILK, PINCH and parvin as well as some of its binding partners. (modified from Legate 2006)

The composition and assembly of the IPP complex

ILK was the first of the three IPP components that was identified. In 1996 ILK was found as a binding partner for β1 integrin tails in a yeast two hybrid (Y2H) screen (Hannigan et al. 1996). Subsequently, ILK binding to β3 integrin was shown (Yamaji et al. 2002). The ubiquitously expressed protein is composed of five N-terminal ankyrin (ANK) repeats and a C-terminal kinase-like domain. Additionally, ILK has a central PH domain, which may bind phosphatidylinositol-3,4,5-trisphosphate (PtdIns(3,4,5)P3). The ANK repeats of ILK mediate the interaction between ILK and PINCH, a family of LIM domain only containing proteins, while the kinase-like domain is serving as binding site for parvin and thus linking ILK to the cytoskeletion. ILK has been mostly shown to function as adaptor protein, but there were studies demonstrating a catalytic activity of ILK. The initial study that identified ILK showed that bacterially expressed recombinant ILK possesses kinase activity and phosphorylates serine and threonine residues in the cytoplasmic tail of β1 integrin (Hannigan et al. 1996). Since then, more and more substrates for ILK, found by in vitro experiments, were published. Among them were the kinase Akt, a regulater of key functions like survival and differentiation of cells and MLC (Legate et al. 2006), which upon phosphorylation is mediating cell contraction. The first evidence, that ILK may have no kinase activity came from *in vivo* studies in *C. elegans* and *D. melanogaster.* The kinase dead ILK mutants used in their assays could fully rescue the severe phenotypes of ILK deletion in both species (Zervas et al. 2001, Mackinnon et al. 2002). They suggested that ILK might be an adaptor and scaffolding protein rather than a kinase. While in later years more and more studies demonstrated an important role for ILK in actin organization, the final evidence for ILK being a kinase was still lacking. Interestingly even opposite functions of ILK were published. The vSMC specific ILK deletion is resulting in hyperphosphorylation of MLC2 rather than decreased phosphorylation, suggesting that ILK may not act as a kinase for MLC in vivo (Kogata et al. 2009). The analysis of knock-in mice with ILK point mutations, which were reported to affect kinase activity, was a breakthrough in this discussion. Mice with mutations in the PH domain (R211A) or in the autophosphorylation site (S343A or S343D) are normal and do not show changes in Akt

or Gsk-3b phosphorylation and actin organization downstream of integrins (Lange et al. 2009). When the potential ATP-binding site (K220A/M) was destroyed mice died shortly after birth from kidney agenesis. But this phenotype is not the result of an impaired kinase activity, since no changes in phospho-levels of reported ILK substrates could be detected. Finally, in 2009 also the crystal structure of ILK bound to α-parvin was solved (Fukuda et al. 2009). The structure revealed a distinct pseudo-active site in ILK thus, defining it as a pseudokinase. A more detailed analysis demonstrated that this kinase-like domain is necessary to recognize α-parvin and for targeting of IPP to FAs.

PINCH1 (*p*articularly *i*nteresting *n*ew *c*ysteine-*h*istidine-rich protein) also known as LIMS1 was originally identified in 1994 as a marker for senescent erythrocytes (Rearden 1994). As a binding partner to ILK it was found in a Y2H screen, using ILK as bait (Tu 1999). PINCH1 is a widely expressed FA protein consisting of five LIM domains, of which the second zinc finger of the most N-terminal LIM domain (LIM1) is binding to the N-terminal ANK domain of ILK. Beside PINCH1 a second highly homologous isoform (92% sequence identity in mice) was identified in vertebrates only and named PINCH2 (Braun et al. 2003). Like PINCH1 also PINCH2 is localizing to FAs. Interestingly both proteins have mostly overlapping expression patterns in different cells and tissues, but only in the adult organism. During embryogenesis, only PINCH1 was detectable until E14.5. Expression of PINCH2 starts shortly after midgestation and is then only partially overlapping with PINCH1 expression. PINCH1 for example is expressed exclusively in spleen and thymus as well as megakaryocytes during fetal liver hematopoiesis.

Parvin was the last identified member of the IPP complex. It was identified in 2000 in a screen for paxillin leucine-rich sequence domain (LD1) binding proteins (Nikolopoulos 2000). It was initially named actopaxin, because of its ability to bind both, actin and paxillin. In 2001 Olski et al. detected a new member of the α-actinin superfamily, while searching for new proteins containing an actin binding domain (ABD) and named it α-parvin While lower organisms like *C.elegans* and *D.melanogaster* only have one parvin-like protein, in vertebrates three different isoforms were identified: α-parvin and the paralogues β- (also known as affixin) and γ-parvin. Like other members of the α-actinin superfamily, α-parvin contains at its C-terminus two in tandem arranged calponin homology (CH) domains. Based on the low sequence similarity to CH-domains of other ABD-containing proteins the parvins built up their own family among the α-actinin superfamily. In α-parvin and β-parvin, but not in γ-parvin, two putative N-terminal nuclear localization signals (NLSs) as well as three potential SH3-binding sites (Src homology 3) were identified. Also in 2001 Tu et al. found a new calponin homology (CH) domain-containing ILK binding protein that is widely expressed and highly conserved among different organisms and named it therefore CH-ILKBP. It was further shown that this protein forms a ternary complex consisting of ILK-PINCH and CH-ILKBP. The binding to ILK is mediated via the second of the two CH-domains of CH-ILKBP. Interestingly, while all three parvin isoforms share a high sequence homology, they display a distinct expression pattern with α-parvin being ubiquitously expressed, β-parvin expression is enriched in heart and skeletal muscle, and γ-Parvin expression is restricted to the haematopoietic system (Korenbaum et al. 2001).

The ILK-PINCH-parvin (IPP) complex is formed prior to cell adhesion, suggesting that IPP complex formation is happening in the cytoplasm and is then recruited to FAs (Zhang et al. 2002b). The stability and also recruitment to FAs of the IPP complex is critically dependent on the presence of all three members of the complex (Fukuda et al. 2003b). If one IPP member is missing, the remaining two

proteins are to a large extend degraded by the proteasome, which makes deletion studies and assigning specific functions to distinct IPP members challenging. But since that degradation is not complete, it may be that there are IPP complex independent functions for ILK, PINCH and parvin. Many cell types express both isoforms of PINCH as well as both, α- and β-parvin. It was shown that binding of PINCH and parvin isoforms to ILK is mutually exclusive (Fukuda et al, 2003; Montanez et al, 2009), allowing cells to form distinct IPP complexes that could compensate for each other. It could be shown that the loss of β-parvin in vSMC could be fully compensated by α-parvin, while compensation by β-parvin in α-parvin null vSMC is not fully working. When α-parvin is deleted from these cells, an upregulation of β-parvin was observed that could compensate protein levels and FA targeting of ILK and PINCH but was unable to functionally rescue the loss of α-parvin (Montanez et al. 2009). Comparable results were obtained for PINCH1 and 2. Fukuda et al. 2003 showed that depletion of PINCH2 can be fully rescued by PINCH1 overexpression in HeLa cells. On the other hand PINCH2 is not rescuing PINCH1 functions, although protein levels of ILK and parvin were stabilized. A different result was obtained for cardiomyocytes, where a cardiac phenotype only arises after deletion of PINCH1 and 2, while the single knockout in both cases showed no overt phenotype in vivo and in vitro (Liang et al. 2005 and 2009.

ILK binding partners

ILK was first identified as a binding partner for β1 integrin, but over the years, a large number of proteins has been shown to bind to ILK apart from parvins and PINCHs (all reviewed in Wickström et al. 2009). Interestingly the evidence of ILK binding directly to the β1 integrin tail is still missing and it is more likely that this interaction is indirectly mediated by kindlins (Montanez et al. 2008, Chen et al. 2008). Since there is no additional ILK isoform all direct ILK binding partners in theory all direct ILK partners could be detected at all IPP complexes, regardless of which subset of parvins and PINCHs are present. But it is more likely that protein binding to ILK is requiring a certain isoform of parvin and PINCH or even simultaneously binding by both proteins, if there are binding sites for more than one IPP complex component. Paxillin for example, can bind directly to ILK, but also simultaneously to α- and γ-parvin but not to β-parvin (Nikolopoulos et al. 2000 and 2001, Yoshimi et al. 2006). Direct ILK binding partners, either shown by Y2H experiments, interaction of recombinant proteins or co-crystallization studies, include β1 and β3 integrins, PINCH and parvin, paxillin, thymosin β4, ELMO-2, EphA1, kAE1 (kidney anion exchanger), the serine/threonine phosphatase ILKAP (ILK-associated phosphatase), PKB (protein kinase B)/Akt, Rictor, Src, the muscle LIM protein (MLP/CRP3) and IQGAP (Wickström et al. 2010). A SILAC-based approach in 2008 revealed further possible binding partners of ILK including RuvB-like 1 and α-tubulin (Dobreva et al. 2008). In 2002 it was additionally shown by immunofluorescence in C.elegans that UNC-112 (Kindlin2) localization to pat3 (β-integrin) requires the presence of pat4 / ILK (Mackinnon et al. 2002). In a Y2H experiment full-length UNC-112 and pat4 strongly interact with each other and further studies with deleted constructs mapped the binding site the kinase-like domain of pat4 / ILK. Moreover ILK localization to FAs failed in mammalian cells in the absence of kindlin2. Further immunoprecipitation assays with fibroblast lysates showed that Kindlin-2 interacts with ILK (Montanez et al. 2008).

PINCH binding partners

Although PINCH is an essential part of the IPP complex and its binding to ILK facilitates the localization of IPP to the FAs, not many direct PINCH binding partners are known so far. Interestingly all binding partners have only been verified for PINCH1 and no specific interactors for PINCH2 have been identified yet.. Besides binding to ILK with the first LIM domain, PINCH1 is also able to bind to Nck-2, a Src homology (SH) adaptor protein (Tu et al. 1998). The PINCH–Nck-2 interactions are mediated through the 4th LIM domain of PINCH and the third SH3 domain of Nck-2. Point mutations of LIM4 residues in the SH3-binding interface disrupted the PINCH-Nck-2 interaction leading to impaired localization of PINCH to FAs (Velyvis et al., 2003). Nck-2 can bind to IRS-1, to growth factor receptors such as PDGFRβ (platelet derived growth factor receptor β) and EGF-receptors, as well as PAK, WASP and DOCK180. This suggests that Nck-2 functions as an adaptor protein that serves as a connection between growth factor receptor-signaling pathways and integrin-signaling pathways. The *in vivo* relevance for this binding was not shown so far. PINCH1 but not PINCH2 can bind to the Ras-suppressor protein RSU1 through the LIM5 domain, which might explain why PINCH2 is unable to rescue PINCH1 deletion (Kadrmas et al. 2004, Dougherty et al. 2005). RSU1 functions as a negative regulator of JNK (Jun N-terminal kinase) activation, inhibits Rho (ROCK) kinase activity and can alter the actin cytoskeleton organization. Additional binding partners of PINCH are the G-actin binding and sequestering protein thymosin-β4 that binds to LIM4 andLIM5 of PINCH1 and is able to simultaniously bind ILK (Bock-Marquette et al. 2004). The formation of a complex between ILK / PINCH1 and thymosin-β4 promotes myocyte survival and motiliy. Another binding partner is the phosphatase PP1α, whose binding depends on the KFVEF-motif in the LIM5-domain of PINCH1 (Eke et al. 2010). Binding of PP1α to PINCH1 inhibits PP1α in dephosphorylation of Akt and thereby PINCH1 acts as a survival factor for cells. This explains why PINCH1 was found to be overexpressed in human tumors and was contributing to radiation cell survival in vitro and in vivo. Since most of the studies mentioned focused only on PINCH1 it was not determined if these binding partners, apart from RSU1 are also capable of binding PINCH2.

Parvin binding partners

The structure of parvin is characterized by two in tandem arranged CH-domains, which serve as ABD also in a variety of other actin binding proteins like α-actinin, filamin and smoothelin. α-parvin binds directly to F-actin through this domain (Olski et al. 2001), but also via the interaction with paxillin. If β- and γ-parvin also directly interact with F-actin has not been shown yet, but indirectly through their interaction with the actin binding protein α-actinin (Yamaji et al., 2004, Yoshimi et al., 2006), to which α-parvin does not bind (Nikolopoulos et al. 2002). Therefore one of parvins most important functions is the linkage of the actin cytoskeleton to FAs and integrins. α-parvin can additionally bind the paxillin-homologue Hic-5 highly expressed in SMC. Hic-5 has many binding partners similar to paxillin but they have a distinct role and distribution in cells. Paxillin regulates cell morphology through Rac1 signaling, while Hic-5 is acting through RhoA signaling (Deakin et al. 2012). For β-parvin an interaction with the GEF αPIX and βPIX (Matsuda et al. 2008) could be shown. While overexpression of β-parvin resulted in high Rac1 levels, this could be counterbalanced by expressing mutant versions of αPIX or βPIX lacking the GEF-activity. This suggests a role for β-parvin in Rac1 mediated signaling. Furthermore, α-parvin was recently shown to also interact with αPIX *in vitro* (Pignatelli et al 2012) Other binding partners are CdGAP, a Cdc42- and Rac-specific GAP that concentrates at the ends of actin stress fibers (LaLonde et al.

2006), and TESK1 (testicular protein kinase 1), a Ser/Thr kinase closely related to LIMK that phosphorylates and activates the actin-regulating protein cofilin (LaLonde et al. 2005). The interaction between α-parvin and TESK1 is negatively regulating TESK1 kinase activity. Normally in cells spreading on FN, this interaction is strongly reduced but cells, expressing a shortend α-parvin construct where α-parvin / TESK1 interaction is not reduced upon binding, display a spreading defect.

***In vivo* functions of the IPP complex**

To understand the *in vivo* function of the IPP complex and the specific role of each protein and its isoforms, several deletion studies have been performed in *C. elegans*, *D. melanogaster* and mice. In general all of these studies confirm a critical role for IPP as an adaptor between actin and the ECM as well as in actin remodelling. However, as not all deletions result in the same phenotype each IPP member also has distinct functions.

Invertebrates represent a relative simple model to study these functions, because of their low number of integrin subunits and single isoforms of ILK, PINCH and parvin. In *C. elegans* deletion of pat-4 (ILK), unc-97 (PINCH), or pat-6 (parvin), as well as βpat-3, the only β-integrin, result in a PAT (paralyzed and arrested elongation at twofold) phenotype (Mackinnon et al. 2002, Norman et al. 2007, Lin et al. 2003). This broad class of lethal mutations affects muscle formation caused by cell attachment defects. Similar observations were made *in D. melanogaster*, where deletions of βPS, the orthologue of β1 integrin, or the orthologues of ILK and PINCH result in abnormal muscle attachments. In βPS null flies, the link between cell and ECM is impaired, whereas loss of ILK or PINCH leads to the detachment of actin filaments from the plasma-membrane (Zervas et al. 2001, Clark et al. 2003). Interestingly, only the deletion of βPS and PINCH, not of ILK, results in dorsal-closure defects (Brown et al. 1994, Kadrmas et al. 2004), hinting at an additional cell migration defect and a specific role for βPS and PINCH in this process. In mice genetic ablations of β1 integrin, ILK, PINCH1 or α-parvin result in embryonic lethality at different stages (Fässler et al. 1995, Sakai et al. 2003, Li et al. 2005, Montanez et al. 2008). In contrast, mice deficient of PINCH2, or β- and/ or γ-parvin (Montanez et. al. 2008, Chu et al. 2006, Stanchi et al. 2005) are without phenotype, most likely due to compensation by PINCH1 or α-parvin. β1 integrin $^{-/-}$, ILK $^{-/-}$ and PINCH $^{-/-}$ embryos arrest their development at the peri-implantation stage, but while β1 integrin$^{-/-}$ and ILK$^{-/-}$ embryos die at E5.5–E6.5, PINCH null mice survive one day longer until E6.5–E7.5. Functional analysis at this early stage is difficult, but could be overcome by generating embryoid bodies (EB) from embryonic stem cells (ES cells), or by creating tissue specific deletions. Studies on EB revealed that β1 integrin is required for LN1 secretion and formation of a BM (Aumailley et al. 2000). While this process was unaffected in ILK- or PINCH1-null EB, their loss led to abnormal epiblast polarity, impaired cavitation and detachment of primitive endoderm from the BM and abnormal actin reorganization (Li et al. 2005a, Sakai et al. 2003). These defects were worse in ILK mutants, but PINCH1 mutants additionally displayed cell-cell adhesion defects and impaired endoderm survival. In contrast to the early lethality described for β1 integin, ILK and PINCH1, constitutive α-parvin knockout mice survive until E10.5 to E14.5 (Montanez et al. 2008). Here, defects are prevalent to the cardiovascular system and were especially severe for vSMC. Additionally, these embryos show kidney agenesis/dysgenesis due to impaired ureteric bud invasion into the metanephric mesenchyme (Lange et al. 2009). It could be observed that in α-parvin-

null cells isolated from these mice β-parvin is upregulated, which suggests a compensatory function of β-parvin during development and explains the longer survival of α-parvin$^{-/-}$ animals. Although β-parvin can stabilize ILK and PINCH protein levels and FA localization, is not able to fully compensate loss of α-parvin in vSMC. These cells display a strong hypercontractility, due to elevated RhoA and ROCK levels, suggesting that this regulation might be a specific function of α-parvin. Comparable results were obtained in the microvasculature of ILK deficient vSMC as shown by Kogota et al. 2009. In contrast Shen et al. showed in 2011 a downregulation of contractility markers in the aorta of mice with a conditional deletion of ILK in SMC. Conditional deletion of β1 integin in vSMC also results in a severe vascular phenotype while no hypercontractility could be detected in these cells (Abraham et al. 2008). Over the past years different conditional deletion studies have been performed on IPP and their corresponding integrins, like in keratinocytes, endothelial cells, Schwann cells, chondrocytes, etc. A detailed list of phenotypes can be found in Wickström et al. 2009.

Extracellular matrix

The extracellular matrix (ECM), which is surrounding most cells, plays an important role during development and tissue homeostasis, but also in disease. The ECM is a heterogeneous meshwork of fibrillar and non-fibrillar components and is assembled in complex structures like BMs: it provides structural support for organs and tissues, serves as substrate for cell motility, and plays a role in signaling to cells through adhesion receptors and growth factor storage and presentation. Thus, ECM proteins and structures play vital roles in the determination, differentiation, proliferation, survival, polarity and migration of cells (Hynes 2009). A major fraction of the ECM is composed of Col, LN and other glycoproteins such as FN, which are secreted by the cells themselves and function as substrates for different adhesion molecules including integrins. Not all integrin heterodimers are able to bind to all glycoproteins as described above, and different integrin/ECM pairings are able to start distinct signaling pathways within the cell. It is therefore easy to understand that changing the ECM environment of a cell, for example in an inflamed tissue, also changes cell behavior.
The following paragraph will shortly introduce the most important ECM components and their function.

Collagens are triple helical proteins that occur in the ECM and at the cell–ECM interface. There are more than 30 Cols and Col-related proteins known so far. Cols can be roughly divided into two classes; the fibril forming Col (Col I, II, III, V and XI) and the more heterogeneous class of non-fibrillar Col, (Col IV, VIII and X). All Col family members are characterized by containing domains with repetitions of the proline-rich tripeptide Gly-X-Y that is important in the formation of the Col triple-helices. Some Cols are almost ubiquitously expressed, while others are found only in distinct tissues. The most abundant and widespread family of Col with about 90% of the total Col is represented by the fibril-forming Col. Col I contributes to the structural backbone of bone, tendons, skin, ligaments, cornea, and many interstitial connective tissues, while Col II and XI contribute to the fibrillar matrix of articular cartilage. Col VI form microfilaments found in almost all connective tissues. Col IV has a more flexible triple helix and its presence in the BM of glomeruli and arteries is important for their proper function. (Gelse et al. 2003 and Kadler et al. 2008)

LNs are heterotrimers constituted by the association of 3 different gene products, the α, β and γ chains. Mammals possess at least 15 LNs formed through the combinations of several α, β, and γ subunits with additional variation resulting from mRNA splicing. LNs polymerize into sheet-like supramolecular structures which interact with the Col network via entactin/nidogen or perlecan and with receptors on the cell surface such as integrins and dystroglycans. LN is a ubiquitous component of BM appearing at a very early developmental stage of mouse embryos, even before Col can be detected. They have a critical function in organ development as well as in organ homeostasis in adult organisms. (Miner et al. 2004)

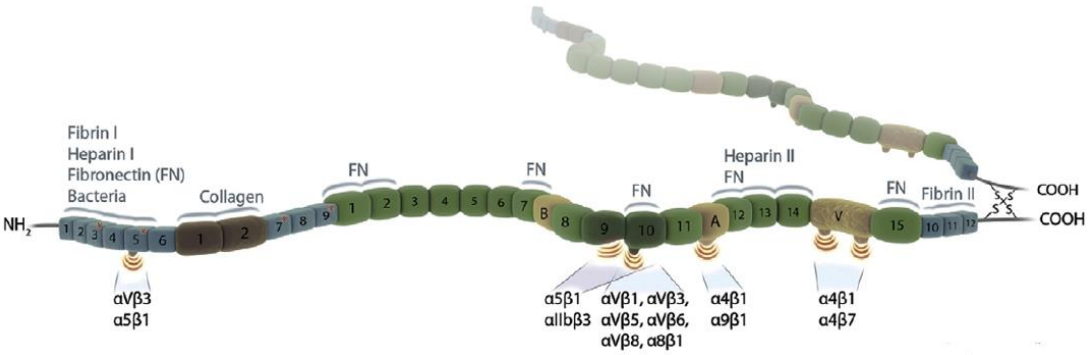

Figure 8: Schematic depiction of the modular structure of FN.

FN consists of three different domains (type I: blue; type II: brown; type III: green). The alternatively spliced extradomains B, A, and variable region (V) are shown in ochre. Two sulfide bonds at the C-terminus are necessary for dimerization.The dimer forms via two disulfide bonds at the C-terminus. Integrin binding sites and binding domains for FN, collagen, fibrin, heparin and bacteria are indicated. (modified from Leiss et al. 2008)

FN is a modular protein, consisting of repetitions of type I, II and III domains. It is secreted as a disulfide-bonded dimer, and the dimerization seems to be required to assemble FN into a fibrillar matrix (Fig. 8). The FN gene can be alternatively spliced which leads to the expression of up to 12 isoforms in mouse, which may result in an even larger variety of FN dimers. FN exists in two versions: one form is cellular FN (cFN), which contains, depending on the tissue, variable proportions of the alternatively spliced exons coding for the extra domains A and B (EDA, EDB). The other form is plasma FN (pFN), which lacks EDA and EDB and is synthesized by hepatocytes and released into the circulation where it remains soluble. Assembly of FN into insoluble and biologically active fibrils critically depends on the interaction with integrins. This is resulting in the unmasking of cryptic FN binding sites, association with other FN proteins and finally crosslinking by tissue transglutaminases into a fibrillar matrix. FN fibrils possess binding sites for multiple ECM components, which are used to orchestrate the assembly of several other ECM proteins like Col and Fibrin. In developing mouse embryos, FN is first expressed in blastocysts and in vitro experiments demonstrated a role for FN in mouse embryo attachment and outgrowth (Armant et al. 1986). Therefore it has been suggested that FN may promote migration of parietal endoderm and trophoblast outgrowth during implantation. Interestingly FN-null mice blastocysts are normal and knockout embryos survive until E 8.5 (George et al. 1993). They show a clear quantitative deficit in mesoderm and it was suggested, that the lack of FN impairs the migration of mesodermal cells.

Vasculature

In vertebrates distribution of gases, liquids, nutrients and signaling molecules into organs and cells is no longer efficient just by diffusion. This important transportation task is performed by the cardiovascular system, the first functional organ that forms during embryonic development. It consists of the heart and two highly branched, tree-like tubular networks: the blood vessels and the lymphatic vessels, which are organized in a hierarchical structure. Both vessels tubes are formed by endothelial cells (EC) and covered by mural cells and ECM. Both endothelial networks are essential for homeostasis in the healthy organism and their malformation or dysfunction contributes to the pathogenesis of many diseases (Carmeliet 2003). Insufficient blood vessel supply can lead to tissue ischaemia in cardiovascular diseases, while abnormal or excessive angiogenesis is often found in tumor tissue or inflammatory diseases.

Development of the vasculature

During embryonic development, the vasculature forms by two processes: vasculogenesis (*de novo* formation of vessels from endothelial precursors) and angiogenesis (sprouting from new vessels out of existing vessels) (Fig. 9). The processes that lead to the formation of a mature vascular network will be closer discussed in the next paragraphs.

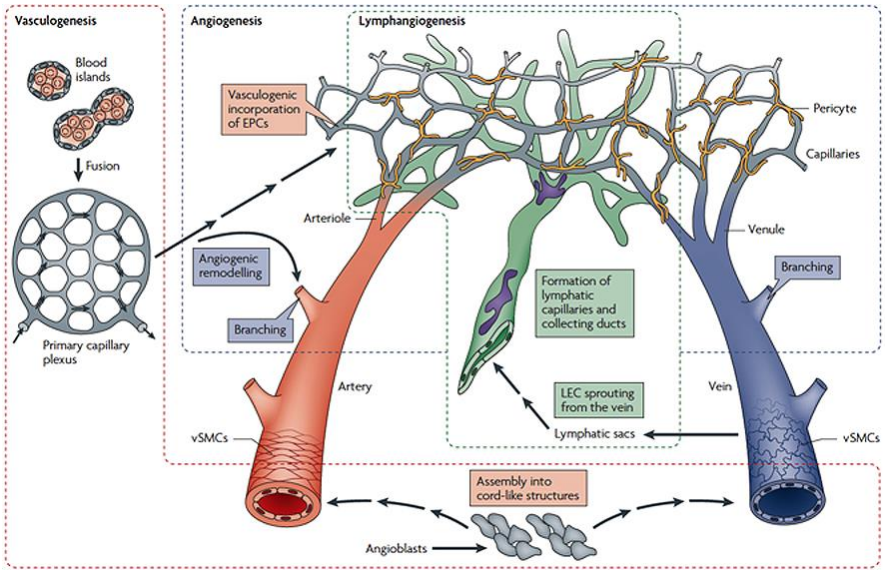

Figure 9: Origin of endothelial cells and assembly of the vasculature.

Vasculogenesis describes the formation of blood islands out of endothelial precursors and the formation of a primary capillary plexus. During Angiogenesis this plexus is highly remodeled and new vessels are formed by sprouting leading to the hierarchical network of arterioles and arteries (red), capillaries (grey), and venules and veins (blue). Vascular smooth-muscle cells (vSMCs) are associated with arteries and veins, whereas capillaries are covered by pericytes (yellow). (taken from Adams et al. 2007)

Vasculogenesis

Vasculogenesis, the de novo formation of blood vessels, occurs at two different locations within the embryo: the extraembryonic yolk sac tissue and the intraembryonic tissue. In both cases, endothelial cells have to differentiate from endothelial precursor cells (angioblasts) from the mesenchyme. Drake et

al. 2003 defines 5 distinct steps necessary in the formation of the first vascular plexus: 1) the formation of angioblasts; 2) angioblast aggregation; 3) angioblast elongation into cord-like structures; 4) the organization of isolated vascular segments into networks; 5) endothelialization and lumen formation. The dorsal aorta, the cardinal vein and the yolk-sac vasculature are generated by this process (Adams et al. 2007).

Angiogenesis

Angiogenesis describes the remodeling process taking place after the formation of the first primitive vascular plexus that finally leads to the hirarchical structuring of major arteries and veins, smaller (pre-capillary) arterioles and (post-capillary) venules, and a branched network of fine capillaries Therefore more ECs are generated to form new vessels by either sprouting out of a preexisting vessel, splitting, or by intussusception (Risau, 1997). Hypoxia is an important stimulus for expansion of the vascular bed. In the beginning the few cells of the embryo are oxygenated by simple diffusion, but when tissues grow beyond the limit of oxygen diffusion, hypoxia triggers vessel growth. This happens through signaling via hypoxia-inducible transcription factors (HIFs). HIFs upregulate many pro-angiogenic genes, especially VEGF (Pugh et al. 2003). How essential VEGF is for sprouting can be observed in heterozygous VEGF null mice, where vessels display a strongly reduced sprouting (Carmeliet et al. 1996). It is important that for the sprouting process only some ECs are selected. These ECs are known as tip cells, which lead the growing sprout and are characterized by the formation of multiple filopodia that enables the cell to sense their environemt and follow attractive cues. To prevent that all ECs become tip cells this process is tightly regulated via Notch receptors and their endothelial specific ligand Delta-like-4 (DLL4). DLL4 is expressed on endothelial tip cells as a response to VEGFR2 signalling and presented at their cell surface. DLL4 will then ligate the Notch receptor expressed by neighbouring cells and induce its activation. Ligand binding to Notch facilitates the proteolytic procession of its intracellular domain, subsequent translocation to the nucleus and transcriptional regulation of target genes. This induces the downregulation of VEGFR2 expression on ECs adjacent to tip cells and abolishes their responsiveness to VEGF-A (Mettouchi 2012). Recent publications have demonstrated that integrins and the BM component LN play a critical role in the selected expression of DLL4 and Notch signalling. Vascular LNs are LN 511 which displays prominent expression in the nascent vascular plexus and LN 411 that shows a restricted expression at the vascular front and even stronger in tip cells. These LNs are bound by differents subsets of integrins, with LN 411 being bound by α2β1, α3β1 and α6β1, while LN 511 is a ligand for α3β1 and α6β1 only. In *in vitro* experiments only ECs cultured on LN 411 showed increased levels of DLL4 expression and studies with LN 111, which can bind to α2β1 and α6β1 integrins as does LN 411, demonstrate a cooperating mechanism by these two integrins is required for DLL4 upregulation. Interestingly this observation was specific for LN 411 and DLL4, since no other endothelial Notch ligand showed an integrin dependent regulation and also no other ECM protein like Col I or FN was able to regulate DLL4 / Notch- signaling (Estrach et al. 2011, Stenzel et al. 2011). These selected ECs have then to flip their apical–basal polarity, dissolve their connection to neighboring cells, induce motile and invasive activity, and start to degrade the local matrix (through matrix metalloproteinase (MMP) 2, 3 and 9 mainly). Tip cells, while migrating, leave a trail of platelet-derived growth factor B (PDGF-B). This promotes the following recruitment of pericytes and smooth muscle cells (SMA), which are necessary

for later vessel stabilization. The tip cells are followed by other ECs – the stalk cells, which migrate behind the leading tip cell and with their high proliferative capacity build up the new vessel lumen. Once they encounter their target, like other sprouts or capillaries, tip cells have to change again into a non-motile resting phenotype and reestablish their strong cell-cell contacts, which prevent leakiness of the vessels. In addition the formation of arteriovenous shunts has to be prevented, most likely by repellant signaling events (Adams et al. 2007). For proper blood flow, these newly formed vessel structures have to establish a lumen. Two different ways of lumen formation have been discussed: cord hollowing and cell hollowing. Cell hollowing is based on the observation of large intracellular vacuoles in ECs, which would build up a vascular lumen out of each central lumen in a single EC. However it is more likely that cord hollowing is the mechanism of lumen formation. In this model the opposing ECs separate from each other, they elongate in parallel and flatten and thus form the new vessel lumen (Axnick et al. 2012).

Vessel maturation

The maturation step is required to transform the immature vascular network, formed by vasculogenesis and / or angiogenesis into the steady hirarchical structure found in higher organism. Maturation of the wall involves according to Jain et al. 2003 the recruitment of mural cells, development of the surrounding matrix and elastic laminae, cell specialization like inter-endothelial junctions, fenestrations, apical-basal polarity and expression of specific surface receptors. Also arteries and veins are formed in a process that is known as arteriovenous differentiation.
Mural cells can be subdivided into two different cell types: SMC and pericytes (Fig. 10).

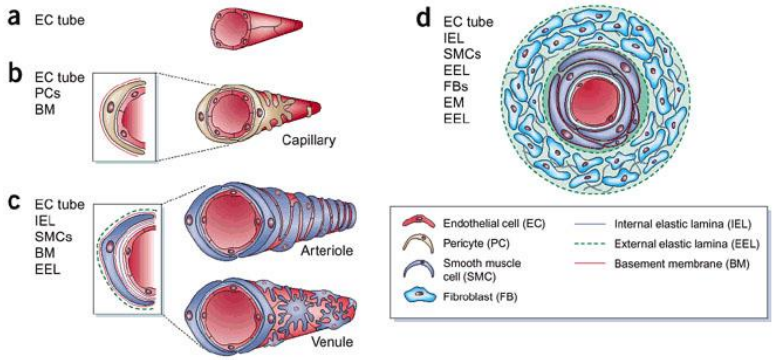

Figure 10: Wall composition of nascent versus mature vessels.

(a) Nascent vessels consist of a tube of ECs. They mature into the specialized structures of capillaries, arteries and veins. (b) Capillaries consist of ECs surrounded by a BM and pericytes which are in direct contact to the EC layer. (c) Arterioles and venules are more strongly covered by mural cells compared with capillaries. (d) The walls of larger vessels consists of three layers: an intima out of EC, a media out of layers of vSMCs, separated by elastic laminae and an adventitia of fibroblasts. ECs and vSMC are separated by a BM. VSMCs and elastic laminae contribute to the vessel tone and mediate the control of vessel diameter and blood flow. (taken from Jain et al. 2003)

Capillaries and immature blood vessels are covered by pericytes, which are embedded in the BM and establish direct connections with ECs through cell-cell contacts. Larger vessels are covered by one or multiple layers of vSMCs, which are separated from the endothelium by the vascular BM and also have an active function in regulating the vascular tone. The origin of these cells is not completely clear and seems to be very heterogeneous. Some mural cells are derived from neural crest cells that delaminate from the neural tube early in embryogenesis, while others are derived from undifferentiated mesenchymal cells or vascular stem cells (Adams et al. 2007). Mural cell recruitment is essentially required for vessel stabilization, which enables them to withstand the increasing blood pressure during development. Additionally, mural cells also keep ECs in a resting state, since a loss of pericytes leads to endothelial hyperplasia, abnormal junctions, and excessive luminal membranefolds (Hellström et al. 2001). It is thought that this recruitment process is depending on 4 different molecular pathways: PDGFB – PDGF receptor β(PDGFRβ); endothelial differentiation sphingolipid G-protein-coupled receptor-1 (EDG1)); Ang1-Tie2; and transforming growth factor β(TGFβ).

Endothelial tip cells secrete PDGF-BB, while mural cells express the corresponing PDGFRβ. Receptor activation is resulting in proliferation and migration of mural cells during vessel maturation. The knockout of PDGF-BB and PDGFRβ in mice leads to similar phenotypes and perinatal death caused by vascular dysfunction (Levéen et al. 1994, Soriano et al. 1994). The primary cause of the phenotype is the lack of pericytes and most likely further endothelial dysfunction due to upregulated VEGF-A levels, observed in these mice.

Sphingosine-1-phosphate (S1P) is a secreted sphingolipid engaged in cell communication through G-protein coupled receptors named as S1P1 (also called edg1). Mice deficient in S1P1 display mid/ late-gestational lethality with vascular abnormalities and defective vSMC/pericyte coverage of vessels (Liu et al. 2000). Interestingly, although S1P1 is expressed on both – mural cells and ECs – only the EC-specific knockout of S1P1 could show the same phenotype than the full knockout (Allende et al. 2003). It was suggested that S1P1 signaling through Rac results in the location of N-cadherin to the plasma membrane in endothelial cells and thereby strengthening their contact with mural cells. (Armulik et al. 2005)

Tie-2 is a tyrosine receptor kinase that binds both angiopoietins (Ang-1 and Ang-2). Unlike Ang-2, which activates Tie-2 on some cells but blocks Tie-2 on others, Ang-1 consistently activates Tie-2. Genetic experiments in mice have shown that binding of Ang-1 (which is expressed by mural cells) to Tie2 promotes angiogenesis and pericyte association to the endothelium, reduces vascular leakage and has anti-inflammatory properties. Ang-2 on the other side can antagonize that signaling. Ang1- or Tie2 knockout mice die at mid-gestation from cardiovascular failure. Angiogenesis is defective and vessels display a badly organized BM as well as reduced mural cell coverage (Armulik et al. 2005). However, Ang2 may also promote angiogenesis depending on the tissue and context.

TGF-β (transforming growth factor β) is a multifunctional cytokine that is critically for *de novo* formation of mural cells by differentiation of mesenchymal cells. The bioavailability of TGF-β is regulated through its storage into the ECM, especially FN, anchored by the latent TGFβ-binding protein (LTBP). Knockout studies in mice of TGF-β as well as its receptors TGFβ receptor-2 (Tgfbr2) or activin-receptor-like kinase-1 and -5 (Alk1 and Alk5) and also deletion of the downstream target SMAD5 have demonstrated severe vascular defects and embryonic lethality (Adams et al. 2007).

Cell – ECM interaction in the vasculature

Vascular development as well as vessel homeostasis requires correct interactions between different cell types (EC-EC and EC-pericyte) and between these cell types and their BM. Interactions of EC and pericytes / SMC with their ECM involve various ECM molecules, which differ to some degree among vessels, and are dependent on the state of the vessel (quiescent or angiogenic). In quiescent vessels ECs and pericytes are adhering to a BM consisting of mostly of LN (mainly laminin-8/ laminin411 and laminin-10/ laminin511), Col IV, perlecan, nidogens, Col XVIII and vWFA (Hynes 2007b). Likewise the BM of contractile vSMC, which are unlike perycites separated from the EC layer, is mostly containing LN and Col IV. This structure changes dramatically in angiogenesis or wound healing, when cells, ECs as well as pericytes / SMC have to proliferate and migrate again. FN is one of these ECM proteins predominantly found in vessels during development, diseased vessels and tumor vasculature and it is believed that FN triggers an active phenotype of ECs and pericytes / SMC. This was further strengthened by knockout studies in mice of FN or its receptors which lead to severe vascular defects and reduced somite formation during embryonic development (George et al. 1993, Francis et al. 2002).

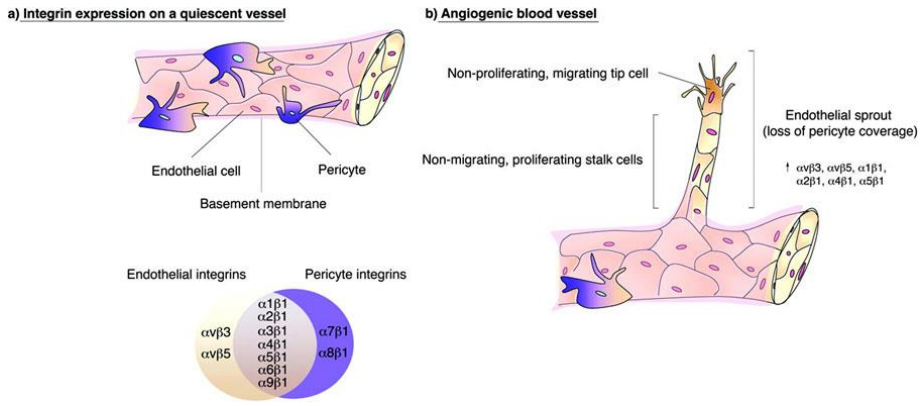

Figure 11: Integrins involved in angiogenesis.

(a) A quiescent capillary comprises ECs,pericytes and a shared BM. These cell types express partly overlapping integrin profiles. (b) In sprouting angiogenesis a proliferating endothelial stalk with a single guiding migratory tip cell at its end is formed. This process requires changes in cell adhesion and therefore changes in the integrin profile, including the upregulation of , αvβ3, αvβ5, α1β1, α2β1, α4β1, and α5β1, whose expression appears to be upregulated during this process. (taken from Silva et al. 2008)

ECs and pericytes both express a broad range of different integrin receptors (Fig. 11): the FN receptors α4β1, α5β1; the Col receptors, α1β1, α2β1; the LN receptors, α3β1, α6β1, and α6β4; and the osteopontin receptor, α9β1. ECs additionally express αvβ3 and αvβ5, two VN binding integrins. Pericytes and vSMC exclusively express integrin α7β1, which is a LN receptor and α8β1, an osteopontin receptor (Silva et al. 2008). αvβ8 on glial cells also regulates brain blood vessel development (Avraamides et. al. 2008). Most insight into the specific function of the different integrins in vascular development and disease has been gained by constitutive or conditional gene deletions in mice.

FN as one of the key proteins in vessel development is bound by α5β1, αvβ5 and αvβ3 integrin on its RGD site, or by integrins α4β1 and α9β1 that bind to the alternatively spliced EDA, EDB and IIICS

domains. The β1 integrin subunit builds three of the most important integrins required for angiogenesis: α5β1, α4β1 and α9β1. Genetic ablation of β1 results in impaired EC proliferation and defective branching of blood vessels in EBs. Similar, only host derived blood vessels are forming in β1-deficient teratomas (Bloch et al. 1997). Furthermore, the EC specific deletion of β1 integrin leads to severe angiogenic sprouting defects at E9.5 and death of homozygous mice before E10.5 (Tanjore et al. 2008). Whereas the large vessels develop normally, branching and sprouting is strongly reduced, resulting in hypoxia in the embryos. Absence of β1 integrin on mural cells also results in a lethal phenotype in mice, but later than for EC (Abraham et al. 2008). Vessels of these mice were often dilated; the mural cells had a severe spreading phenotype and could not support the vasculature sufficiently. Interestingly an almost similar phenotype was observed for the mural cell specific loss of α-parvin and ILK, two downstream proteins of integrin signaling. Here the defects in spreading and polarity of mural cells was explained by overactive RhoA / ROCK signaling and hypercontractility, that could not be seen when β1 integrin was deleted (Kogata et al. 2009, Montanez et al. 2009). Instead, the proliferation of mural cells was increased along with a loss of differentiation in the absence of β1 integrin. Genetic ablation of α5 integrin results embryonic lethality at E10 to E11 and showed severe neural tube and mesodermal defects in the posterior trunk region (Yang et al. 1993). At E9.5 defects in blood vessel formation and leaking of vessels in the embryo and extraembyonic tissue were visible along with a reduced number of blood cells within vessels and heart. As a properly assembled FN matrix was detectable it was suggested that other FN binding integrins could partly rescue the phenotype and thus explain the longer survival of embryos compared to FN null and also β1 integrin null mice. The α4 null embryos show defects in two cell-cell adhesion events; allantois-chorion fusion during placental development (death at E11) or epicardium-myocardium attachment during cardiac development (death at E13.5 to E14.5) (Yang et al. 1996). Importantly, α4β1 is not only binding to FN but additionally to VCAM1. α4 integrin is expressed in the chorion, whereas VCAM1 is expressed in the allantois, suggesting that the phenotype is a result of the lost interaction between these two proteins. This is further supported by the VCAM1 knockout, which leads to comparable defects to the α4 knockout (Gurtner et al. 1995). A second study with α4 knockout mice could demonstrate the exclusive expression of α4β1 integrin on mural cells but not on EC (Grazioli et al. 2006). Pericytes on cranial microvessels were severely reduced in number as well as mislocalized and their migration speed impaired. Integrin α9β1 can bind to FN but also to a number of other ligands. α9β1 null mice die P8 to P12 due to defects in development of the lymphatic system, but they do not show any obvious defects in the cardiovascular system (Huang et al. 2000). However it was shown that α9β1 binds to VEGF-A and thrombospondin and thus promotes angiogenesis (Avraamides et al. 2008).

The genetic ablation of the two Col binding integrins expressed on ECs α1β1 and α2β1 leads to opposing results. Deletion of α1 did not affect embryonic development but tumor angiogenesis is reduced in mice lacking α1β1 (Pozzi et al. 2000). In the absence of α2β1, tumor angiogenesis was increased in melanomas and in Lewis lung carcinomas (LLC), although only upon PLGF (placental growth factor) treatment (Zhang et al. 2008b). This shows that both integrins are dispensable for vascular development, they can modulate pathological angiogenesis, but in different directions.

α3β1, α6β1, and α6β4 integrin all bind to LN. For α3β1 also thrombospondin is acting as a ligand and is able to interact with tetraspanin, CD151, the metalloproteinase inhibitor TIMP2 and the α3-noncollagenous (α3NC1) domain of Col IV, all of which have been implicated in either promoting or inhibiting angiogenesis (Silva et al. 2008). The knockout of α3, although lethal hours after birth due to several defects, does not display any signs of vascular malfunctions (Kreidberg et al. 1996). Also the ablation of α6, which can dimerize with β1 or β4, is lethal and shows a skin blistering phenotype, but no cardiovascular defects are reported. Different *in vitro* and *in vivo* studies propose a role for this integrin subunit in tumor angiogenesis but with opposing findings (Silva et al. 2008).

ECs express two different VN binding integrins: αvβ3 and αvβ5 while glial cells express αvβ8. Deletion of αv in mice leads to embryonic lethality in most animals around E11.5 due to vascular defects and pericardial edema formation. Interestingly around 20% of homozygous mutants survive this stage, but then die shortly after birth because of intracranial and intestinal hemorrhages (Bader et al. 1998). In mice lacking αv specifically at ECs these bleedings in the brain vasculature could not be detected. In contrast specific deletion αv in neuronal cells or total loss β8 displays a similar phenotype to the constitutive deletion of αv integrin subunit (McCarty et al. 2005, Zhu et al. 2002). This proposes that the observed defect in αv knockout mice was due to the loss of αvβ8 on glial cells not because of lacking αvβ3 and αvβ5 on EC. Unlike αv integrin knockout mouse, the β3 and β5 integrin–null mice are viable and fertile and their vasculature is without visible defect (Reynolds et al. 2002). While β3 integrin is not detectable in quiescent vessels its expression is apparently upregulated on tumor biopsies and therefore implicates a role for β3 in tumor angiogenesis (Silva et al. 2008). Its expression on endothelial cells is stimulated by angiogenic growth factors such as bFGF, TNFα, and IL-8 (Brooks et al. 1994). Because of these findings antibodies blocking αvβ3 like Vitaxin and the RGD-mimetic Cilengitide are used to suppress neovascularization and tumor growth. However studies in mice lacking β3 integrins or both β3 and β5 integrins showed that tumorigenesis is not only supported, but tumor growth was even enhanced (Reynolds et al. 2002). Tumors displayed enhanced angiogenesis, strongly suggesting that neither β3 nor β5 integrins are essential for neovascularization.

α7β1 is a LN receptor only expressed on vSMC and not detectable on ECs. While most studies focused on the role of α7β1 on skeletal muscle development, the deletion of α7 also results in partial embryonic lethality (Flintoff-Dye et al. 2005). Around 70% of the embryos die between E10.5 and E14.5 and displayed vascular hemorrhaging and reduced vasculogenesis. *In vitro* studies have suggested a possible crosstalk between α7β1 and PDGF signaling (Chao et al. 2005). VSMC treated with PDGF showed increased adhesion to LN, which could be partially abrogated by blocking α7β1.

Atherosclerosis

Atherosclerosis is a progressive inflammatory disease characterized by the accumulation of lipids and ECM in the large arteries, especially the aorta. As the disease can result in severe health complications like stroke, heart attack and thrombosis it is the major cause of death in the western world.

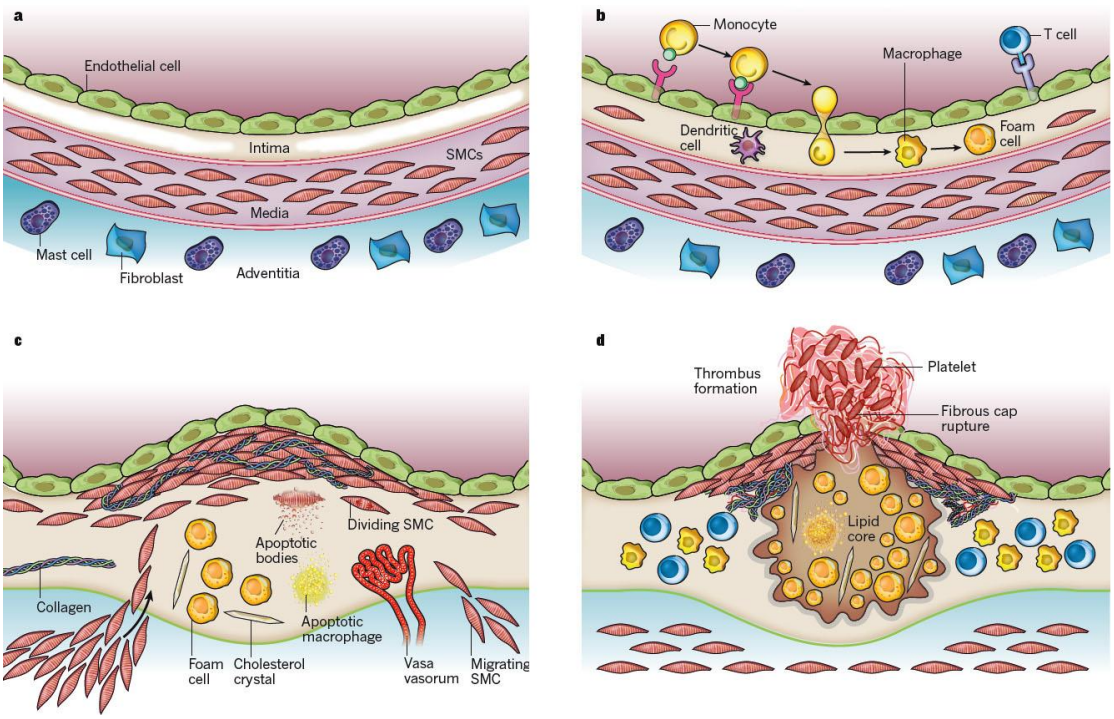

Figure 12: Stages in the development of atherosclerotic lesions.

(a) The inner layer of the aorta, the tunica intima, is formed by a EC monolayer. The middle layer, the tunica media, contains layers of vSMCs separated by elastic laminae. The adventitia, the outer layer of arteries, contains fibroblasts, nerve endings and microvessels. (b) The initial steps of atherosclerosis include adhesion and transmigration of leukocytes across the injured endothelial monolayer, maturation of monocytes into macrophages, and their uptake of lipid that transforms them into foam cells. (c) Lesion progression involves the proliferation of vSMC and their migration from the media to the intima along with increased expression of Col that leads to the formation of a fibrous cap. Foam cells and vSMCs can die in advancing lesions and form together with free lipids the so-called lipid- / necrotic core. (d) Plaque rupture is the result of a thinning fibrous cap and leads to thrombus formation. (modified from Libby et al. 2011)

Atherosclerosis begins with an endothelial injury caused by many different stimuli including diabetes mellitus, hypertension, and dyslipidemia (Fig. 12) and weakens the monolayer of EC. This is followed by the subendothelial deposition of lipids, especially LDL and VLDL, and the induction of inflammatory signaling by EC. This includes the expression of ICAM1 and VCAM1 at the cell surface of ECs and promotes the adhesion of monocytes to the EC layer. They subsequently transmigrate to the subendothelial space, start to proliferate and differentiate into macrophages. Their scavenger-receptors enable them to take up the cell-activating oxidized LDL (oxLDL) and transform into lipid-filled “foam cells”. These small lesions, named “fatty streaks” can already be observed during the first decade of life (Lusis 2000). They form preferentially at areas with turbulent blood flow in the aorta, found at

curvatures and bifurcations. The changes in signaling by ECs as well as signals derived from the accumulated immune cells can start a switching in the underlying vSMC layer from a resting and contractile phenotype to a proliferative and migrative phenotype. They migrate from the tunica media and form a so called fibrous cap out of vSMC and a Col-rich matrix. This cap shields the core region of the plaque, which becomes necrotic during progression of atherosclerosis, from the blood stream. In most patients, myocardial infarctions occur as a result of erosion or thinning and subsequent rupture of the fibrous cap. That often happens at the shoulder regions of the plaque. This event can be the result of cell apoptosis in this area or also of elevated MMP expression and matrix degradation by macrophages (Gough et al 2005). The consequence of plaque rupture is an immediate platelet activation and aggregation due to the contact with cell debris of the necrotic core and a subsequent thrombus formation (Lusis 2000, Rudijanto et al. 2007). Over the years on atherosclerosis research most findings were derived from patient studies, blood analysis and biopsies but a great breakthrough was the development of animal models to study atherosclerosis. These models allowed a new perspective on how atherosclerosis develops and that there is more to it, than the accumulation of lipids due to high cholesterol levels observed in the patient's blood. Although mice normally do not develop atherosclerosis, there is a large variety of genetically modified mouse models and diets available that can induce the disease in mice (Maganto-Garcia et al. 2012). The most commonly used model is the $ApoE^{-/-}$ mice which develop lesions resembling all phases of atherosclerosis throughout the arterial tree after being fed a high-fat / high-cholesterol containing diet (Nakashima et al. 1994). Unfortunately the final stage of atherosclerosis – the rupture of plaques – cannot be studied in this model, but it allows the detailed analysis of all preceding stages, especially what modulates the immune response leading to leukocyte adhesion to atheroprone areas. It was thereby shown, that VCAM1 is significantly upregulated in $ApoE^{-/-}$ mice even before leukocyte recruitment started. Additionally, experiments with hypomorphic variants of VCAM1 introduced into $ApoE^{-/-}$ mice show reduced lesion formation. Also deleting other proteins mediating leukocyte adhesion like E-selectin and P-selectin appear to play quantitative roles in monocyte accumulation based on a 40% to 60% decrease in atherosclerosis in ApoE–deficient mice lacking both genes. Similarly, gene deletion of ICAM1 resulted in small but significant reductions in monocyte recruitment to atherosclerotic lesions in ApoE–deficient mice. Also the absence of proteins required for monocyte transmigration into the vascular wall reduces lesion formation. This was shown by the disruption of the MCP-1 (monocyte chemotactic protein 1) or CCR2 genes, which markedly reduces the development of atherosclerosis in $ApoE^{-/-}$ mice (Glass et al. 2001, Libby 2002). *In vitro* experiments have demonstrated that upregulation of inflammatory mediators is highly dependent on the type of blood flow the ECs experience in the vessel. While high shear force seems to be protective against atherosclerosis, turbulent flow results in the activation of NF-κB, c-Jun NH2-terminal kinases (JNKs) and p21-activated kinase (PAK) (Funk et al. 2010, Hahn & Schwartz 2008, Hahn et al. 2009, Orr et al. 2005, 2007, 2008). These inflammatory mediators induce endothelial permeability, sustain an inflammatory state and thereby enforce the consequences of the turbulent blood flow during atherogenesis (Hahn et al. 2009, Orr et al. 2005, 2007). Also the composition of the ECM around ECs and vSMC modulates initiation and progression of atherosclerosis. It was already shown over 20 years ago, that FN expression is higher in atherosclerotic areas, which suggested an involvement of FN in the course of atherosclerosis (Glukhova et al. 1989). While binding of fibrillar Col to α2β1 integrin prevents pro-inflammatory signals, *in vitro* experiments found that FN depositions at atheroprone areas leads to a

sustained inflammatory response by the EC and thus further stimulating monocyte attraction (Feaver et al. 2010). In line with this observation, genetic deletion of the alternatively spliced EDA domain in atherosclerosis-prone mice was reported to reduce the number and size of atherosclerotic lesions (Babaev et al. 2008). Additionally FN also promotes the synthetic phenotype of vSMC, which is crucial for the migration of vSMC through the plaque in order to form the fibrous cap and can act as a chemoattractant for vSMC. Interesting results were also obtained for Col in atherosclerosis. The normal BM of vSMC consists of LN and Col IV which is important for a contractile phenotype of vSMC. During atherogenesis vSMC begin to deposit soluble, non-polymerized Col I and III, elastin and FN. The accumulation of collagen is very high and it is estimated that collagens comprise 60% of the protein in the plaque. These non-fibrillar forms of Col I promote proliferation and migration (Adiguzel et al.2009).

Aim of the thesis

Adhesion and migration are two key events during vessel development and vessel homeostasis. Integrins, as the main receptors for cell adhesion and their binding partners are well known for their critical function during this process. Changes in protein content of this adhesion complexes, mostly done by knockout studies in mice, often result in embryonic lethality due to severe malformations in vasculogenesis or angiogenesis. Inducible knockout strategies demonstrated an equally important role for the integrin adhesome in the adult organism, where protein deletions resulted frequently in pathological conditions like tumor angiogenesis or other cardiovascular diseases.

Aim 1

Fibronectin depositions in these areas of the aorta, where atherosclerotic plaques develop were already discovered 20 years ago. They form preferentially at sites of turbulent blood flow like branchings and bifurcations. Also *in vitro* studies demonstrated a critical role for FN in initiating and sustaining the inflammatory signaling of the endothelium that leads to leukocyte adhesion. It was not clear however, what the source of these FN deposits is. FN is an ECM molecule either secreted and assembled by cells into fibrils (cFN) or secreted by hepatocytes in a soluble form into the circulation (pFN). It has been shown, that pFN can also be assembled into fibrils after being bound by integrins or after diffusing into tissues. Previous studies demonstrated a role for the alternatively spliced EDA and EDB domain of FN in formation and progression of atherosclerosis. In some other studies elevated pFN levels were observed in patients with atherosclerotic plaques. We therefore wanted to investigate the role of pFN in initiation and progression of atherosclerosis in ApoE $^{-/-}$ mice. MxCre mediated deletion of FN was used to overcome the problem of early embryonic lethality in FN null mice. Because MxCre also targets hematopoietic cells, a second Cre-line (VavCre) was used to distinguish between effects of pFN and hematopoietic derived FN in our results.

Aim 2

β1 integrin and the members of the IPP complex have been shown to be essential for proper vSMC alignment on vessels during vessel maturation. vSMC specific deletion of β1 integrin and ILK lead to vessels that are poorly covered by vSMC leading to edemas and aneurysms. Isolated cells are unable to spread, polarize and, in the case of ILK, are hypercontractility due to upregulated RhoA/ROCK signaling. The constitutive deletion of α-parvin also results in lethality due to severe cardiovascular defects. vSMC remain round and are unable to support the vasculature sufficiently. Consistent with findings in vSMC lacking ILK, αpv null vSMC are highly contractile with elevated pMLC2 levels and upregulated active RhoA. In a next step we wanted to investigate the specific function of α-parvin in vSMC by performing Cre-mediated deletion of αpv in SMC only. This should abolish any possible contributions to the phenotype by other αpv deleted cell types in the constitutive knockout model. An cell tape-specific and inducible Cre-line were used to investigate the function of α-parvin in late development and in adult SMC, where the cells have properly attached to vessels and other SMC containing organs.

Short summary of publications

Publication 1: Plasma fibronectin deficiency impedes atherosclerosis progression and fibrous cap formation

Atherosclerosis is an inflammatory disease of the artery wall that can lead to vascular occlusion representing the most common cause of death in the Western world. It is characterized by the formation of atherosclerotic plaques which are filled with lipids, leukocytes and ECM and covered by a thick layer of vSMC. This cap erodes over time, which then leads to the life threatening condition of plaque rupture and subsequent thrombus formation. Plaques do not form randomly in the aorta but rather at places of turbulent blood flow like branchings and bifurcations. FN is one of the earliest ECM proteins deposited at these atherosclerosis-prone sites, even before leukocyte adhesion is visible. Additionally *in vitro* studies demonstrated enhanced inflammatory signaling of ECs when plated on FN. Therefore it was suggested that FN promotes atherosclerotic lesion formation. Until now the source of the FN detected at atherosclerosis prone sites was unknown. Here, we report that atherosclerosis-prone apolipoprotein E-null mice lacking hepatocyte-derived pFN fed with a pro-atherogenic diet display strongly reduced FN depositions at atheroprone sites, which results in significantly smaller and fewer atherosclerotic lesions. We show that FN indeed enhances signaling events at the endothelium that result in enhanced adhesion of leukocytes and bigger lesions. However, the atherosclerotic lesions from pFN-deficient mice displayed an insufficient covering by vSMC. We could show that FN acts as a chemoattractant to vSMC in culture, which suggests that FN also promotes vSMC migration towards the cap. Thus, our results demonstrate that FN acts in two ways in atherosclerosis. It promotes initiation of atherosclerosis by enhancing inflammatory signaling of ECs and leukocyte adhesion. FN also acts as a migration stimulus for vSMC and secures fibrous cap formation. Absence of pFN results in smaller and fewer plaques but also more vulnerable lesions.

Publication 2: α-Parvin controls contraction and actin organization in smooth muscle cells

α-parvin (αpv) is a focal adhesion (FA) protein that has been shown to be essential for blood vessel maturation during mouse development by regulating RhoA/ROCK signaling in vascular smooth muscle cells (vSMC). Here we report that a conditional deletion of the *αPv* gene in SMCs leads to lethality in mice around 4 weeks of age. The vasculature of mutant mice displays severe defects in the organization of the smooth muscle layer and spreading of single vSMC leading to dilations and aneurysm development in the aorta. Vessels are insufficiently covered by vSMCs and elastic fibers are degraded. In addition, the mutant mice suffer from intestinal pseudoobstruction and glomerulosclerosis in their kidneys. Deleting αpv from adult mice with an inducible knockout strategy leads to the death of homozygous mice 4-6 weeks after Cre induction, due to intestinal defects after the loss of αpv in the intestinal smooth muscle cell (iSMC) layer. Isolated primary vSMC and iSMC display a hypercontractile phenotype and fail to spread and polarize their cytoskeleton. We show that the loss of αpv in vSMC leads to higher activation of Myosin II, as well as elevated levels of MMP expression and matrix

degradation. Our findings identify αpv as a key component for vessel integrity and a regulator of vSMC organization and contractility.

References

Abraham S, Kogata N, Fässler R, Adams RH.; Integrin beta1 subunit controls mural cell adhesion, spreading, and blood vessel wall stability.; Circ Res. 2008 Mar 14;102(5):562-70. doi: 10.1161/CIRCRESAHA.107.167908. Epub 2008 Jan 17.

Adams RH, Alitalo K.; Molecular regulation of angiogenesis and lymphangiogenesis.; Nat Rev Mol Cell Biol. 2007 Jun;8(6):464-78.

Adiguzel E, Ahmad PJ, Franco C, Bendeck MP.; Collagens in the progression and complications of atherosclerosis.; Vasc Med. 2009 Feb;14(1):73-89. doi: 10.1177/1358863X08094801.

Allen WE, Zicha D, Ridley AJ, Jones GE.; A role for Cdc42 in macrophage chemotaxis.; J Cell Biol. 1998 Jun 1;141(5):1147-57.

Allende ML, Yamashita T, Proia RL.; G-protein-coupled receptor S1P1 acts within endothelial cells to regulate vascular maturation.; Blood. 2003 Nov 15;102(10):3665-7. Epub 2003 Jul 17.

Arias-Salgado EG, Lizano S, Shattil SJ, Ginsberg MH.; Specification of the direction of adhesive signaling by the integrin beta cytoplasmic domain.; J Biol Chem. 2005 Aug 19;280(33):29699-707. Epub 2005 Jun 3.

Armant DR, Kaplan HA, Lennarz WJ.; Fibronectin and laminin promote in vitro attachment and outgrowth of mouse blastocysts.; Dev Biol. 1986 Aug;116(2):519-23.

Armulik A, Abramsson A, Betsholtz C.; Endothelial/pericyte interactions.; Circ Res. 2005 Sep 16;97(6):512-23.

Aumailley M, Pesch M, Tunggal L, Gaill F, Fässler R.; Altered synthesis of laminin 1 and absence of basement membrane component deposition in (beta)1 integrin-deficient embryoid bodies.; J Cell Sci. 2000 Jan;113 Pt 2:259-68.

Avraamides CJ, Garmy-Susini B, Varner JA.; Integrins in angiogenesis and lymphangiogenesis.; Nat Rev Cancer. 2008 Aug;8(8):604-17. doi: 10.1038/nrc2353. Epub 2008 May 22.

Axnick J, Lammert E.; Vascular lumen formation.; Curr Opin Hematol. 2012 May;19(3):192-8. doi: 10.1097/MOH.0b013e3283523ebc.

Babaev VR, Porro F, Linton MF, Fazio S, Baralle FE, Muro AF. Absence of regulated splicing of fibronectin EDA exon reduces atherosclerosis in mice. Atherosclerosis. 2008;197:534–540.

Bader BL, Rayburn H, Crowley D, Hynes RO.; Extensive vasculogenesis, angiogenesis, and organogenesis precede lethality in mice lacking all alpha v integrins.; Cell. 1998 Nov 13;95(4):507-19.

Banyard J, Anand-Apte B, Symons M, Zetter BR; Motility and invasion are differentially modulated by Rho family GTPases.; Oncogene. 2000 Jan 27;19(4):580-91.

Benninger Y, Thurnherr T, Pereira JA, Krause S, Wu X, Chrostek-Grashoff A, Herzog D, Nave KA, Franklin RJ, Meijer D, Brakebusch C, Suter U, Relvas JB; Essential and distinct roles for cdc42 and rac1 in the regulation of Schwann cell biology during peripheral nervous system development.; J Cell Biol. 2007 Jun 18;177(6):1051-61.

Bloch W, Forsberg E, Lentini S, Brakebusch C, Martin K, Krell HW, Weidle UH, Addicks K, Fässler R.; Beta 1 integrin is essential for teratoma growth and angiogenesis.; J Cell Biol. 1997 Oct 6;139(1):265-78.

Bock-Marquette I, Saxena A, White MD, Dimaio JM, Srivastava D.; Thymosin beta4 activates integrin-linked kinase and promotes cardiac cell migration, survival and cardiac repair.; Nature. 2004 Nov 25;432(7016):466-72.

Braun A, Bordoy R, Stanchi F, Moser M, Kostka G G, Ehler E, Brandau O, Fässler R.; PINCH2 is a new five LIM domain protein, homologous to PINCH and localized to focal adhesions.; Exp Cell Res. 2003 Apr 1;284(2):239-50.

Brooks PC, Clark RA, Cheresh DA.; Requirement of vascular integrin alpha v beta 3 for angiogenesis.; Science. 1994 Apr 22;264(5158):569-71.

Brown NH.; Null mutations in the alpha PS2 and beta PS integrin subunit genes have distinct phenotypes.; Development. 1994 May;120(5):1221-31.

Carmeliet P, Ferreira V, Breier G, Pollefeyt S, Kieckens L, Gertsenstein M, Fahrig M, Vandenhoeck A, Harpal K, Eberhardt C, Declercq C, Pawling J, Moons L, Collen D, Risau W, Nagy A.; Abnormal blood vessel development and lethality in embryos lacking a single VEGF allele.; Nature. 1996 Apr 4;380(6573):435-9.

Carmeliet P.; Angiogenesis in health and disease.; Nat Med. 2003 Jun;9(6):653-60.

Cary LA, Han DC, Polte TR, Hanks SK, Guan JL.; Identification of p130Cas as a mediator of focal adhesion kinase-promoted cell migration.; J Cell Biol. 1998 Jan 12;140(1):211-21.

Chao JT, Martinez-Lemus LA, Kaufman SJ, Meininger GA, Ramos KS, Wilson E.; Modulation of alpha7-integrin-mediated adhesion and expression by platelet-derived growth factor in vascular smooth muscle cells.; Am J Physiol Cell Physiol. 2006 Apr;290(4):C972-80. Epub 2005 Nov 9.

Chen F, Ma L, Parrini MC, Mao X, Lopez M, Wu C, Marks PW, Davidson L, Kwiatkowski DJ, Kirchhausen T, Orkin SH, Rosen FS, Mayer BJ, Kirschner MW, Alt FW.; Cdc42 is required for PIP(2)-induced actin polymerization and early development but not for cell viability.; Curr Biol. 2000 Jun 29;10(13):758-65.

Chen K, Tu Y, Zhang Y, Blair HC, Zhang L, Wu C.; PINCH-1 regulates the ERK-Bim pathway and contributes to apoptosis resistance in cancer cells.; J Biol Chem. 2008 Feb 1;283(5):2508-17. Epub 2007 Dec 6.

Choi CK, Zareno J, Digman MA, Gratton E, Horwitz AR.; Cross-correlated fluctuation analysis reveals phosphorylation-regulated paxillin-FAK complexes in nascent adhesions.; Biophys J. 2011 Feb 2;100(3):583-92. doi: 10.1016/j.bpj.2010.12.3719.

Chu H, Thievessen I, Sixt M, Lämmermann T, Waisman A, Braun A, Noegel AA, Fässler R.; gamma-Parvin is dispensable for hematopoiesis, leukocyte trafficking, and T-cell-dependent antibody response.; Mol Cell Biol. 2006 Mar;26(5):1817-25.

Clark KA, McGrail M, Beckerle MC.; Analysis of PINCH function in Drosophila demonstrates its requirement in integrin-dependent cellular processes.; Development. 2003 Jun;130(12):2611-21.

Conti MA, Adelstein RS.; Nonmuscle myosin II moves in new directions.; J Cell Sci. 2008 Jan 1;121(Pt 1):11-8.

Danen EH, Sonneveld P, Brakebusch C, Fassler R, Sonnenberg A.; The fibronectin-binding integrins alpha5beta1 and alphavbeta3 differentially modulate RhoA-GTP loading, organization of cell matrix adhesions, and fibronectin fibrillogenesis.; J Cell Biol. 2002 Dec 23;159(6):1071-86. Epub 2002 Dec 16.

Deakin NO, Turner CE.; Distinct roles for paxillin and Hic-5 in regulating breast cancer cell morphology, invasion, and metastasis.; Mol Biol Cell. 2011 Feb 1;22(3):327-41. doi: 10.1091/mbc.E10-09-0790.

De La Cruz EM, Ostap EM; Relating biochemistry and function in the myosin superfamily.; Curr Opin Cell Biol. 2004 Feb;16(1):61-7.

del Pozo MA, Alderson NB, Kiosses WB, Chiang HH, Anderson RG, Schwartz MA.; Integrins regulate Rac targeting by internalization of membrane domains.; Science. 2004 Feb 6;303(5659):839-42.

DeMali KA, Wennerberg K, Burridge K.; Integrin signaling to the actin cytoskeleton.; Curr Opin Cell Biol. 2003 Oct;15(5):572-82.

Dobreva I, Fielding A, Foster LJ, Dedhar S.; Mapping the integrin-linked kinase interactome using SILAC.; J Proteome Res. 2008 Apr;7(4):1740-9. doi: 10.1021/pr700852r. Epub 2008 Mar 10.

Dougherty GW, Chopp T, Qi SM, Cutler ML.; The Ras suppressor Rsu-1 binds to the LIM 5 domain of the adaptor protein PINCH1 and participates in adhesion-related functions.; Exp Cell Res. 2005 May 15;306(1):168-79.

Drake CJ.; Embryonic and adult vasculogenesis.; Birth Defects Res C Embryo Today. 2003 Feb;69(1):73-82.

Edwards DC, Sanders LC, Bokoch GM, Gill GN.; Activation of LIM-kinase by Pak1 couples Rac/Cdc42 GTPase signalling to actin cytoskeletal dynamics.; Nat Cell Biol. 1999 Sep;1(5):253-9.

Eke I, Koch U, Hehlgans S, Sandfort V, Stanchi F, Zips D, Baumann M, Shevchenko A, Pilarsky C, Haase M, Baretton GB, Calleja V, Larijani B, Fässler R, Cordes N.; PINCH1 regulates Akt1 activation and enhances radioresistance by inhibiting PP1alpha.; 2010 Jul;120(7):2516-27. doi: 10.1172/JCI41078. Epub 2010 Jun 7.

Estrach S, Cailleteau L, Franco CA, Gerhardt H, Stefani C, Lemichez E, Gagnoux-Palacios L, Meneguzzi G, Mettouchi A.; Laminin-binding integrins induce Dll4 expression and Notch signaling in endothelial cells.; Circ Res. 2011 Jul 8;109(2):172-82. doi: 10.1161/CIRCRESAHA.111.240622. Epub 2011 Apr 7.

Etienne-Manneville S, Hall A; Rho GTPases in cell biology.; Nature. 2002 Dec 12;420(6916):629-35.

Etienne-Manneville S, Hall A.; Cdc42 regulates GSK-3beta and adenomatous polyposis coli to control cell polarity.; Nature. 2003 Feb 13;421(6924):753-6. Epub 2003 Jan 29.

Etienne-Manneville S.; Cdc42--the centre of polarity.; J Cell Sci. 2004 Mar 15;117(Pt 8):1291-300.

Evans R, Patzak I, Svensson L, De Filippo K, Jones K, McDowall A, Hogg N.; Integrins in immunity.; J Cell Sci. 2009 Jan 15;122(Pt 2):215-25. doi: 10.1242/jcs.019117.

Fässler R, Meyer M.; Consequences of lack of beta 1 integrin gene expression in mice.; Genes Dev. 1995 Aug 1;9(15):1896-908.

Feaver RE, Gelfand BD, Wang C, Schwartz MA, Blackman BR. Atheroprone hemodynamics regulate fibronectin deposition to create positive feedback that sustains endothelial inflammation. Circ. Res. 2010;106:1703–1711

Flevaris P, Stojanovic A, Gong H, Chishti A, Welch E, Du X.; A molecular switch that controls cell spreading and retraction.; J Cell Biol. 2007 Nov 5;179(3):553-65. Epub 2007 Oct 29.

Flintoff-Dye NL, Welser J, Rooney J, Scowen P, Tamowski S, Hatton W, Burkin DJ.; Role for the alpha7beta1 integrin in vascular development and integrity.; Dev Dyn. 2005 Sep;234(1):11-21.

Francis SE, Goh KL, Hodivala-Dilke K, Bader BL, Stark M, Davidson D, Hynes RO.; Central roles of alpha5beta1 integrin and fibronectin in vascular development in mouse embryos and embryoid bodies.; Arterioscler Thromb Vasc Biol. 2002 Jun 1;22(6):927-33

Fukata M, Nakagawa M, Kaibuchi K.; Roles of Rho-family GTPases in cell polarisation and directional migration.; Curr Opin Cell Biol. 2003 Oct;15(5):590-7.

Fukuda K, Gupta S, Chen K, Wu C, Qin J.; The pseudoactive site of ILK is essential for its binding to alpha-Parvin and localization to focal adhesions.; 2009 Dec 11;36(5):819-30. doi: 10.1016/j.molcel.2009.11.028.

Fukuda T, Chen K, Shi X, Wu C.; PINCH-1 is an obligate partner of integrin-linked kinase (ILK) functioning in cell shape modulation, motility, and survival.; J Biol Chem. 2003 Dec 19;278(51):51324-33. Epub 2003 Oct 8.

Funk SD, Yurdagul A Jr, Green JM, Jhaveri KA, Schwartz MA, Orr AW.; Matrix-specific protein kinase A signaling regulates p21-activated kinase activation by flow in endothelial cells.; Circ Res. 2010 Apr 30;106(8):1394-403. doi: 10.1161/CIRCRESAHA.109.210286. Epub 2010 Mar 11.

Garvalov BK, Flynn KC, Neukirchen D, Meyn L, Teusch N, Wu X, Brakebusch C, Bamburg JR, Bradke F.; Cdc42 regulates cofilin during the establishment of neuronal polarity.; J Neurosci. 2007 Nov 28;27(48):13117-29.

Geiger B, Bershadsky A, Pankov R, Yamada KM.; Transmembrane crosstalk between the extracellular matrix--cytoskeleton crosstalk; Nat Rev Mol Cell Biol. 2001 Nov;2(11):793-805.

Gelse K, Pöschl E, Aigner T.; Collagens--structure, function, and biosynthesis.;Adv Drug Deliv Rev. 2003 Nov 28;55(12):1531-46.

George EL, Georges-Labouesse EN, Patel-King RS, Rayburn H, Hynes RO; Defects in mesoderm, neural tube and vascular development in mouse embryos lacking fibronectin.; Development. 1993 Dec;119(4):1079-91.

Stenzel D, Franco CA, Estrach S, Mettouchi A, Sauvaget D, Rosewell I, Schertel A, Armer H, Domogatskaya A, Rodin S, Tryggvason K, Collinson L, Sorokin L, Gerhardt H.; Endothelial basement membrane limits tip cell formation by inducing Dll4/Notch signalling in vivo.; EMBO Rep. 2011 Oct 28;12(11):1135-43. doi: 10.1038/embor.2011.194.

Ghosh M, Song X, Mouneimne G, Sidani M, Lawrence DS, Condeelis JS.; Cofilin promotes actin polymerization and defines the direction of cell motility.; Science. 2004 Apr 30;304(5671):743-6.

Gimona M, Djinovic-Carugo K, Kranewitter WJ, Winder SJ.; Functional plasticity of CH domains.; FEBS Lett. 2002 Feb 20;513(1):98-106.

Glass CK, Witztum JL; Atherosclerosis. the road ahead.; Cell. 2001 Feb 23;104(4):503-16.

Glukhova MA, Frid MG, Shekhonin BV, Vasilevskaya TD, Grunwald J, Saginati M, Koteliansky VE. Expression of extra domain A fibronectin sequence in vascular smooth muscle cells is phenotype dependent. J. Cell Biol. 1989;109:357–366

Gomes ER, Jani S, Gundersen GG.; Nuclear movement regulated by Cdc42, MRCK, myosin, and actin flow establishes MTOC polarization in migrating cells.; Cell. 2005 May 6;121(3):451-63.

Gough PJ, Gomez IG, Wille PT, Raines EW.; Macrophage expression of active MMP-9 induces acute plaque disruption in apoE-deficient mice.; J Clin Invest. 2006 Jan;116(1):59-69. Epub 2005 Dec 22.

Grazioli A, Alves CS, Konstantopoulos K, Yang JT.; Defective blood vessel development and pericyte/pvSMC distribution in alpha 4 integrin-deficient mouse embryos.; Dev Biol. 2006 May 1;293(1):165-77. Epub 2006 Mar 10.

Gupton SL, Gertler FB.; Filopodia: the fingers that do the walking.; Sci STKE. 2007 Aug 21;2007(400):re5.

Gurtner GC, Davis V, Li H, McCoy MJ, Sharpe A, Cybulsky MI.; Targeted disruption of the murine VCAM1 gene: essential role of VCAM-1 in chorioallantoic fusion and placentation.; Genes Dev. 1995 Jan 1;9(1):1-14.

Hahn C, Schwartz MA.; The role of cellular adaptation to mechanical forces in atherosclerosis.; Arterioscler Thromb Vasc Biol. 2008 Dec;28(12):2101-7. doi: 10.1161/ATVBAHA.108.165951. Epub 2008 Sep 11.

Hahn C, Schwartz MA.; Mechanotransduction in vascular physiology and atherogenesis.; Nat Rev Mol Cell Biol. 2009 Jan;10(1):53-62. doi: 10.1038/nrm2596.

Hannigan GE, Leung-Hagesteijn C, Fitz-Gibbon L, Coppolino MG, Radeva G, Filmus J, Bell JC, Dedhar S.; Regulation of cell adhesion and anchorage-dependent growth by a new beta 1-integrin-linked protein kinase.; Nature. 1996 Jan 4;379(6560):91-6.

Hansson GK, Libby P.; The immune response in atherosclerosis: a double-edged sword.; Nat Rev Immunol. 2006 Jul;6(7):508-19. Epub 2006 Jun 16.

Heasman SJ, Ridley AJ.; Mammalian Rho GTPases: new insights into their functions from in vivo studies.; Nat Rev Mol Cell Biol. 2008 Sep;9(9):690-701. doi: 10.1038/nrm2476.

Hellström M, Kalén M, Lindahl P, Abramsson A, Betsholtz C.; Role of PDGF-B and PDGFR-beta in recruitment of vascular smooth muscle cells and pericytes during embryonic blood vessel formation in the mouse.;Development. 1999 Jun;126(14):3047-55.

Hellström M, Gerhardt H, Kalén M, Li X, Eriksson U, Wolburg H, Betsholtz C.; Lack of pericytes leads to endothelial hyperplasia and abnormal vascular morphogenesis.; J Cell Biol. 2001 Apr 30;153(3):543-53.

Huang XZ, Wu JF, Ferrando R, Lee JH, Wang YL, Farese RV Jr, Sheppard D; Fatal bilateral chylothorax in mice lacking the integrin alpha9beta1.; Mol Cell Biol. 2000 Jul;20(14):5208-15.

Humphries JD, Byron A, Humphries MJ.; Integrin ligands at a glance.; J Cell Sci. 2006 Oct 1;119(Pt 19):3901-3.

Huveneers S, Danen EH.; Adhesion signaling - crosstalk between integrins, Src and Rho.;J Cell Sci. 2009 Apr 15;122(Pt 8):1059-69. doi: 10.1242/jcs.039446.

Hynes RO.; Integrins: a family of cell surface receptors.; Cell. 1987 Feb 27;48(4):549-54.

Hynes RO, Zhao Q.; The evolution of cell adhesion.; J Cell Biol. 2000 Jul 24;150(2):F89-96.

Hynes RO.; Integrins: bidirectional, allosteric signaling machines; Cell. 2002 Sep 20;110(6):673-87.

Hynes RO.; Cell-matrix adhesion in vascular development.; J Thromb Haemost. 2007b Jul;5 Suppl 1:32-40.

Hynes RO.; The extracellular matrix: not just pretty fibrils.; Science. 2009 Nov 27;326(5957):1216-9. doi: 10.1126/science.1176009.

Ito M, Nakano T, Erdodi F, Hartshorne DJ.; Myosin phosphatase: structure, regulation and function.; Mol Cell Biochem. 2004 Apr;259(1-2):197-209.

Jaffe AB, Hall A.; Rho GTPases: biochemistry and biology.; Annu Rev Cell Dev Biol. 2005;21:247-69.

Jain RK.; Molecular regulation of vessel maturation.; Nat Med. 2003 Jun;9(6):685-93.

Jiang G, Giannone G, Critchley DR, Fukumoto E, Sheetz MP.; Two-piconewton slip bond between fibronectin and the cytoskeleton depends on talin.; Nature. 2003 Jul 17;424(6946):334-7.

Kadler KE, Hill A, Canty-Laird EG.; Collagen fibrillogenesis: fibronectin, integrins, and minor collagens as organizers and nucleators.; Curr Opin Cell Biol. 2008 Oct;20(5):495-501. doi: 10.1016/j.ceb.2008.06.008. Epub 2008 Jul 30.

Kadrmas JL, Smith MA, Clark KA, Pronovost SM, Muster N, Yates JR 3rd, Beckerle MC.; The integrin effector PINCH regulates JNK activity and epithelial migration in concert with Ras suppressor 1.; J Cell Biol. 2004 Dec 20;167(6):1019-24. Epub 2004 Dec 13.

Kano Y, Katoh K, Masuda M, Fujiwara K.; Macromolecular composition of stress fiber-plasma membrane attachment sites in endothelial cells in situ.; Circ Res. 1996 Nov;79(5):1000-6.

Kim M, Carman CV, Springer TA; Bidirectional transmembrane signaling by cytoplasmic domain separation in integrins.; Science. 2003 Sep 19;301(5640):1720-5.

Kimura K, Ito M, Amano M, Chihara K, Fukata Y, Nakafuku M, Yamamori B, Feng J, Nakano T, Okawa K, Iwamatsu A, Kaibuchi K.; Regulation of myosin phosphatase by Rho and Rho-associated kinase (Rho-kinase); Science. 1996 Jul 12;273(5272):245-8.

Kiyokawa E, Hashimoto Y, Kobayashi S, Sugimura H, Kurata T, Matsuda M.; Activation of Rac1 by a Crk SH3-binding protein, DOCK180.; Genes Dev. 1998 Nov 1;12(21):3331-6.

Kogata N, Tribe RM, Fässler R, Way M, Adams RH.; Integrin-linked kinase controls vascular wall formation by negatively regulating Rho/ROCK-mediated vascular smooth muscle cell contraction.; Genes Dev. 2009 Oct 1;23(19):2278-83. doi: 10.1101/gad.535409.

Korenbaum E, Olski TM, Noegel AA.; Genomic organization and expression profile of the parvin family of focal adhesion proteins in mice and humans.; Gene. 2001 Nov 14;279(1):69-79.

Kos CH, Le TC, Sinha S, Henderson JM, Kim SH, Sugimoto H, Kalluri R, Gerszten RE, Pollak MR.; Mice deficient in alpha-actinin-4 have severe glomerular disease.; J Clin Invest. 2003 Jun;111(11):1683-90.

Kreidberg JA, Donovan MJ, Goldstein SL, Rennke H, Shepherd K, Jones RC, Jaenisch R.; Alpha 3 beta 1 integrin has a crucial role in kidney and lung organogenesis.; Development. 1996 Nov;122(11):3537-47.

Krendel M, Mooseker MS.; Myosins: tails (and heads) of functional diversity.; Physiology (Bethesda). 2005 Aug;20:239-51.

Kuijpers TW, van de Vijver E, Weterman MA, de Boer M, Tool AT, van den Berg TK, Moser M, Jakobs ME, Seeger K, Sanal O, Unal S, Cetin M, Roos D, Verhoeven AJ, Baas F.; LAD-1/variant syndrome is caused by mutations in FERMT3.; Blood. 2009 May 7;113(19):4740-6. doi: 10.1182/blood-2008-10-182154. Epub 2008 Dec 8.

LaLonde DP, Grubinger M, Lamarche-Vane N, Turner CE; CdGAP associates with actopaxin to regulate integrin-dependent changes in cell morphology and motility.; Curr Biol. 2006 Jul 25;16(14):1375-85.

LaLonde DP, Brown MC, Bouverat BP, Turner CE; Actopaxin interacts with TESK1 to regulate cell spreading on fibronectin.; J Biol Chem. 2005 Jun 3;280(22):21680-8. Epub 2005 Apr 6.

Lange A, Wickström SA, Jakobson M, Zent R, Sainio K, Fässler R.; Integrin-linked kinase is an adaptor with essential functions during mouse development.; Nature. 2009 Oct 15;461(7266):1002-6. doi: 10.1038/nature08468.

Laukaitis CM, Webb DJ, Donais K, Horwitz AF.; Differential dynamics of alpha 5 integrin, paxillin, and alpha-actinin during formation and disassembly of adhesions in migrating cells.; J Cell Biol. 2001 Jun 25;153(7):1427-40.

Legate KR, Montañez E, Kudlacek O, Fässler R.; ILK, PINCH and parvin: the tIPP of integrin signaling.; Nat Rev Mol Cell Biol. 2006 Jan;7(1):20-31.

Legate KR, Fässler R.; Mechanisms that regulate adaptor binding to beta-integrin cytoplasmic tails.; J Cell Sci. 2009 Jan 15;122(Pt 2):187-98. doi: 10.1242/jcs.041624.

Legate KR, Wickström SA, Fässler R.; Genetic and cell biological analysis of integrin outside-in signaling.; Genes Dev. 2009 Feb 15;23(4):397-418. doi: 10.1101/gad.1758709.

Leiss M, Beckmann K, Girós A, Costell M, Fässler R.; The role of integrin binding sites in fibronectin matrix assembly in vivo.; Curr Opin Cell Biol. 2008 Oct;20(5):502-7. doi: 10.1016/j.ceb.2008.06.001. Epub 2008 Jul 21.

Leng J, Klemke RL, Reddy AC, Cheresh DA; Potentiation of cell migration by adhesion-dependent cooperative signals from the GTPase Rac and Raf kinase.; J Biol Chem. 1999 Dec 31;274(53):37855-61.

Levéen P, Pekny M, Gebre-Medhin S, Swolin B, Larsson E, Betsholtz C.; Mice deficient for PDGF B show renal, cardiovascular, and hematological abnormalities.; Genes Dev. 1994 Aug 15;8(16):1875-87

Li S, Bordoy R, Stanchi F, Moser M, Braun A, Kudlacek O, Wewer UM, Yurchenco PD, Fässler R.; PINCH1 regulates cell-matrix and cell-cell adhesions, cell polarity and cell survival during the peri-implantation stage.; J Cell Sci. 2005 Jul 1;118(Pt 13):2913-21.

Liang X, Sun Y, Ye M, Scimia MC, Cheng H, Martin J, Wang G, Rearden A, Wu C, Peterson KL, Powell HC, Evans SM, Chen J.; Targeted ablation of PINCH1 and PINCH2 from murine myocardium results in dilated cardiomyopathy and early postnatal lethality.; Circulation. 2009 Aug 18;120(7):568-76. doi: 10.1161/CIRCULATIONAHA.109.864686. Epub 2009 Aug 3.

Liang X, Zhou Q, Li X, Sun Y, Lu M, Dalton N, Ross J Jr, Chen J.; PINCH1 plays an essential role in early murine embryonic development but is dispensable in ventricular cardiomyocytes.; Mol Cell Biol. 2005 Apr;25(8):3056-62.

Libby P.; Inflammation in atherosclerosis.; Nature. 2002 Dec 19-26;420(6917):868-74.

Libby P, Ridker PM, Hansson GK.; Progress and challenges in translating the biology of atherosclerosis.; Nature. 2011 May 19;473(7347):317-25. doi: 10.1038/nature10146.

Lin X, Qadota H, Moerman DG, Williams BD.; C. elegans PAT-6/actopaxin plays a critical role in the assembly of integrin adhesion complexes in vivo.; Curr Biol. 2003 May 27;13(11):922-32.

Lindahl P, Johansson BR, Levéen P, Betsholtz C.; Pericyte loss and microaneurysm formation in PDGF-B-deficient mice.; Science. 1997 Jul 11;277(5323):242-5.

Liu Y, Wada R, Yamashita T, Mi Y, Deng CX, Hobson JP, Rosenfeldt HM, Nava VE, Chae SS, Lee MJ, Liu CH, Hla T, Spiegel S, Proia RL.; Edg-1, the G protein-coupled receptor for sphingosine-1-phosphate, is essential for vascular maturation.; J Clin Invest. 2000 Oct;106(8):951-61.

Lu C, Takagi J, Springer TA.; Association of the membrane proximal regions of the alpha and beta subunit cytoplasmic domains constrains an integrin in the inactive state.; J Biol Chem. 2001 May 4;276(18):14642-8. Epub 2001 Jan 30.

Luo BH, Springer TA.; Integrin structures and conformational signaling.; Curr Opin Cell Biol. 2006 Oct;18(5):579-86. Epub 2006 Aug 14.

Luo BH, Carman CV, Springer TA.; Structural basis of integrin regulation and signaling.; Annu Rev Immunol. 2007;25:619-47.

Lusis AJ.; Atherosclerosis.; Nature. 2000 Sep 14;407(6801):233-41.

Ma YQ, Yang J, Pesho MM, Vinogradova O, Qin J, Plow EF.; Regulation of integrin alphaIIbbeta3 activation by distinct regions of its cytoplasmic tails.; Biochemistry. 2006 May 30;45(21):6656-62.

Ma YQ, Qin J, Wu C, Plow EF.; Kindlin-2 (Mig-2): a co-activator of beta3 integrins.; J Cell Biol. 2008 May 5;181(3):439-46. doi: 10.1083/jcb.200710196.

MacArthur DG, Seto JT, Raftery JM, Quinlan KG, Huttley GA, Hook JW, Lemckert FA, Kee AJ, Edwards MR, Berman Y, Hardeman EC, Gunning PW, Easteal S, Yang N, North KN.; Loss of ACTN3 gene function alters mouse muscle metabolism and shows evidence of positive selection in humans.; Nat Genet. 2007 Oct;39(10):1261-5. Epub 2007 Sep 9.

Mackinnon AC, Qadota H, Norman KR, Moerman DG, Williams BD.; C. elegans PAT-4/ILK functions as an adaptor protein within integrin adhesion complexes.; Curr Biol. 2002 May 14;12(10):787-97.

Maganto-Garcia E, Tarrio M, Lichtman AH.; Mouse models of atherosclerosis.; Curr Protoc Immunol. 2012 Feb;Chapter 15:Unit 15.24.1-23. doi: 10.1002/0471142735.im1524s96.

Matsuda C, Kameyama K, Suzuki A, Mishima W, Yamaji S, Okamoto H, Nishino I, Hayashi YK.; Affixin activates Rac1 via betaPIX in C2C12 myoblast.; FEBS Lett. 2008 Apr 9;582(8):1189-96. doi: 10.1016/j.febslet.2008.01.064. Epub 2008 Mar 4.

McCarty JH, Lacy-Hulbert A, Charest A, Bronson RT, Crowley D, Housman D, Savill J, Roes J, Hynes RO.; Selective ablation of alphav integrins in the central nervous system leads to cerebral hemorrhage, seizures, axonal degeneration and premature death.; Development. 2005 Jan;132(1):165-76. Epub 2004 Dec 2.

Mettouchi A.; The role of extracellular matrix in vascular branching morphogenesis.; Cell Adh Migr. 2012 Nov-Dec;6(6):528-34. doi: 10.4161/cam.22862. Epub 2012 Nov 1.

Miner JH, Yurchenco PD.; Laminin functions in tissue morphogenesis.; Annu Rev Cell Dev Biol. 2004;20:255-84.

Monkley SJ, Zhou XH, Kinston SJ, Giblett SM, Hemmings L, Priddle H, Brown JE, Pritchard CA, Critchley DR, Fässler R.; Disruption of the talin gene arrests mouse development at the gastrulation stage.; Dev Dyn. 2000 Dec;219(4):560-74.

Montanez E, Ussar S, Schifferer M, Bösl M, Zent R, Moser M, Fässler R.; Kindlin-2 controls bidirectional signaling of integrins.; Genes Dev. 2008 May 15;22(10):1325-30. doi: 10.1101/gad.469408.

Montanez E, Wickström SA, Altstätter J, Chu H, Fässler R.; Alpha-parvin controls vascular mural cell recruitment to vessel wall by regulating RhoA/ROCK signaling.; 2009 Oct 21;28(20):3132-44. doi: 10.1038/emboj.2009.295. Epub 2009 Oct 1.

Moser M, Bauer M, Schmid S, Ruppert R, Schmidt S, Sixt M, Wang HV, Sperandio M, Fässler R.; Kindlin-3 is required for beta2 integrin-mediated leukocyte adhesion to endothelial cells.; Nat Med. 2009 Mar;15(3):300-5. doi: 10.1038/nm.1921. Epub 2009 Feb 22.

Moser M, Legate KR, Zent R, Fässler R.; The tail of integrins, talin, and kindlins.; Science. 2009 May 15;324(5929):895-9. doi: 10.1126/science.1163865.

Murthy KS.; Signaling for contraction and relaxation in smooth muscle of the gut.; Annu Rev Physiol. 2006;68:345-74.

Nakagawa O, Fujisawa K, Ishizaki T, Saito Y, Nakao K, Narumiya S.; ROCK-I and ROCK-II, two isoforms of Rho-associated coiled-coil forming protein serine/threonine kinase in mice.; FEBS Lett. 1996 Aug 26;392(2):189-93.

Nakashima Y, Plump AS, Raines EW, Breslow JL, Ross R.; ApoE-deficient mice develop lesions of all phases of atherosclerosis throughout the arterial tree.; Arterioscler Thromb. 1994 Jan;14(1):133-40.

Nayal A, Webb DJ, Brown CM, Schaefer EM, Vicente-Manzanares M, Horwitz AR.; Paxillin phosphorylation at Ser273 localizes a GIT1-PIX-PAK complex and regulates adhesion and protrusion dynamics.; J Cell Biol. 2006 May 22;173(4):587-9.

Nikolopoulos SN, Turner CE.; Actopaxin, a new focal adhesion protein that binds paxillin LD motifs and actin and regulates cell adhesion.; J Cell Biol. 2000 Dec 25;151(7):1435-48.

Nikolopoulos SN, Turner CE.; Integrin-linked kinase (ILK) binding to paxillin LD1 motif regulates ILK localization to focal adhesions; J Biol Chem. 2001 Jun 29;276(26):23499-505. Epub 2001 Apr 13.

Nishiuchi R, Takagi J, Hayashi M, Ido H, Yagi Y, Sanzen N, Tsuji T, Yamada M, Sekiguchi K.; Matrix Biol. 2006 Apr;25(3):189-97. Epub 2006 Jan 18.; Ligand-binding specificities of laminin-binding integrins: a comprehensive survey of laminin-integrin interactions using recombinant alpha3beta1, alpha6beta1, alpha7beta1 and alpha6beta4 integrins.

Nodari A, Zambroni D, Quattrini A, Court FA, D'Urso A, Recchia A, Tybulewicz VL, Wrabetz L, Feltri ML.; Beta1 integrin activates Rac1 in Schwann cells to generate radial lamellae during axonal sorting and myelination.; J Cell Biol. 2007 Jun 18;177(6):1063-75.

Norman KR, Cordes S, Qadota H, Rahmani P, Moerman DG; UNC-97/PINCH is involved in the assembly of integrin cell adhesion complexes in Caenorhabditis elegans body wall muscle.; Dev Biol. 2007 Sep 1;309(1):45-55. Epub 2007 Jun 22.

Ohashi K, Nagata K, Maekawa M, Ishizaki T, Narumiya S, Mizuno K.; Rho-associated kinase ROCK activates LIM-kinase 1 by phosphorylation at threonine 508 within the activation loop.; J Biol Chem. 2000 Feb 4;275(5):3577-82.

Olski TM, Noegel AA, Korenbaum E.; Parvin, a 42 kDa focal adhesion protein, related to the alpha-actinin superfamily.; J Cell Sci. 2001 Feb;114(Pt 3):525-38.

Orr AW, Sanders JM, Bevard M, Coleman E, Sarembock IJ, Schwartz MA. The subendothelial extracellular matrix modulates NF-kappaB activation by flow: a potential role in atherosclerosis. J. Cell Biol. 2005;169:191–202

Orr AW, Stockton R, Simmers MB, Sanders JM, Sarembock IJ, Blackman BR, Schwartz MA. Matrix-specific p21-activated kinase activation regulates vascular permeability in atherogenesis. J. Cell Biol. 2007;176:719–727

Orr AW, Hahn C, Blackman BR, Schwartz MA. p21-activated kinase signaling regulates oxidant-dependent NF-kappa B activation by flow. Circ. Res. 2008;103:671–679.

O'Toole TE, Katagiri Y, Faull RJ, Peter K, Tamura R, Quaranta V, Loftus JC, Shattil SJ, Ginsberg MH.; Integrin cytoplasmic domains mediate inside-out signal transduction.; J Cell Biol. 1994 Mar;124(6):1047-59.

Pignatelli J, LaLonde SE, LaLonde DP, Clarke D, Turner CE.; Actopaxin (α-parvin) phosphorylation is required for matrix degradation and cancer cell invasion.; J Biol Chem. 2012 Oct 26;287(44):37309-20. doi: 10.1074/jbc.M112.385229. Epub 2012 Sep 6.

Pozzi A, Moberg PE, Miles LA, Wagner S, Soloway P, Gardner HA; Elevated matrix metalloprotease and angiostatin levels in integrin alpha 1 knockout mice cause reduced tumor vascularization; Proc Natl Acad Sci U S A. 2000 Feb 29;97(5):2202-7.

Pugh CW, Ratcliffe PJ.; Regulation of angiogenesis by hypoxia: role of the HIF system.; Nat Med. 2003 Jun;9(6):677-84.

Raftopoulou M, Hall A.; Cell migration: Rho GTPases lead the way.; Dev Biol. 2004 Jan 1;265(1):23-32.

Rearden A.; A new LIM protein containing an autoepitope homologous to "senescent cell antigen".; Biochem Biophys Res Commun. 1994 Jun 30;201(3):1124-31.

Rees DJ, Ades SE, Singer SJ, Hynes RO.; Sequence and domain structure of talin.; Nature. 1990 Oct 18;347(6294):685-9.

Reynolds LE, Wyder L, Lively JC, Taverna D, Robinson SD, Huang X, Sheppard D, Hynes RO, Hodivala-Dilke KM.; Enhanced pathological angiogenesis in mice lacking beta3 integrin or beta3 and beta5 integrins.; Nat Med. 2002 Jan;8(1):27-34.

Ridley AJ.; Rho GTPases and cell migration.; J Cell Sci. 2001 Aug;114(Pt 15):2713-22.

Risau W.; Mechanisms of angiogenesis.; Nature. 1997 Apr 17;386(6626):671-4.

Rohwedder I, Montanez E, Beckmann K, Bengtsson E, Dunér P, Nilsson J, Soehnlein O, Fässler R.; Plasma fibronectin deficiency impedes atherosclerosis progression and fibrous cap formation.; EMBO Mol Med. 2012 Jul;4(7):564-76. doi: 10.1002/emmm.201200237. Epub 2012 Apr 19.

Rudijanto A.; The role of vascular smooth muscle cells on the pathogenesis of atherosclerosis.; Acta Med Indones. 2007 Apr-Jun;39(2):86-93.

Saitoh T, Takemura S, Ueda K, Hosoya H, Nagayama M, Haga H, Kawabata K, Yamagishi A, Takahashi M; Differential localization of non-muscle myosin II isoforms and phosphorylated regulatory light chains in human MRC-5 fibroblasts.; FEBS Lett. 2001 Dec 14;509(3):365-9.

Sakai T, Li S, Docheva D, Grashoff C, Sakai K, Kostka G, Braun A, Pfeifer A, Yurchenco PD, Fässler R.; Integrin-linked kinase (ILK) is required for polarizing the epiblast, cell adhesion, and controlling actin accumulation.; Genes Dev. 2003 Apr 1;17(7):926-40.

Schiller HB, Friedel CC, Boulegue C, Fässler R.; Quantitative proteomics of the integrin adhesome show a myosin II-dependent recruitment of LIM domain proteins.; EMBO Rep. 2011 Mar;12(3):259-66. doi: 10.1038/embor.2011.5. Epub 2011 Feb 11.

Shen D, Li J, Lepore JJ, Anderson TJ, Sinha S, Lin AY, Cheng L, Cohen ED, Roberts JD Jr, Dedhar S, Parmacek MS, Gerszten RE.; Aortic aneurysm generation in mice with targeted deletion of integrin-linked kinase in vascular smooth muscle cells.; Circ Res. 2011 Sep 2;109(6):616-28. doi: 10.1161/CIRCRESAHA.110.239343. Epub 2011 Jul 21.

Silva R, D'Amico G, Hodivala-Dilke KM, Reynolds LE; Integrins: the keys to unlocking angiogenesis.; Arterioscler Thromb Vasc Biol. 2008 Oct;28(10):1703-13. doi: 10.1161/ATVBAHA.108.172015. Epub 2008 Jul 24.

Spiering D, Hodgson L.; Dynamics of the Rho-family small GTPases in actin regulation and motility.; Cell Adh Migr. 2011 Mar-Apr;5(2):170-80. Epub 2011 Mar 1.

Soriano P.; Abnormal kidney development and hematological disorders in PDGF beta-receptor mutant mice.; Genes Dev. 1994 Aug 15;8(16):1888-96.

Stanchi F, Bordoy R, Kudlacek O, Braun A, Pfeifer A, Moser M, Fässler R.; Consequences of loss of PINCH2 expression in mice.; J Cell Sci. 2005 Dec 15;118(Pt 24):5899-910. Epub 2005 Nov 29.

Svensson L, Howarth K, McDowall A, Patzak I, Evans R, Ussar S, Moser M, Metin A, Fried M, Tomlinson I, Hogg N.; Leukocyte adhesion deficiency-III is caused by mutations in KINDLIN3 affecting integrin activation.; Nat Med. 2009 Mar;15(3):306-12. doi: 10.1038/nm.1931. Epub 2009 Feb 22.

Takada Y, Ye X, Simon S.; The integrins.; Genome Biol. 2007;8(5):215.

Tanjore H, Zeisberg EM, Gerami-Naini B, Kalluri R.; Beta1 integrin expression on endothelial cells is required for angiogenesis but not for vasculogenesis.; Dev Dyn. 2008 Jan;237(1):75-82.

Tu Y, Li F, Wu C.; Nck-2, a novel Src homology2/3-containing adaptor protein that interacts with the LIM-only protein PINCH and components of growth factor receptor kinase-signaling pathways.; 1998 Dec;9(12):3367-82.

Tu Y, Li F, Goicoechea S, Wu C.; The LIM-only protein PINCH directly interacts with integrin-linked kinase and is recruited to integrin-rich sites in spreading cells.; Mol Cell Biol. 1999 Mar;19(3):2425-34.

Tu Y, Huang Y, Zhang Y, Hua Y, Wu C.; A new focal adhesion protein that interacts with integrin-linked kinase and regulates cell adhesion and spreading.; J Cell Biol. 2001 Apr 30;153(3):585-98.

Turner CE, Kramarcy N, Sealock R, Burridge K.; Localization of paxillin, a focal adhesion protein, to smooth muscle dense plaques, and the myotendinous and neuromuscular junctions of skeletal muscle.; Exp Cell Res. 1991 Feb;192(2):651-5.

Ussar S, Moser M, Widmaier M, Rognoni E, Harrer C, Genzel-Boroviczeny O, Fässler R.; Loss of Kindlin-1 causes skin atrophy and lethal neonatal intestinal epithelial dysfunction.; PLoS Genet. 2008 Dec;4(12):e1000289. doi: 10.1371/journal.pgen.1000289. Epub 2008 Dec 5.

Velyvis A, Vaynberg J, Yang Y, Vinogradova O, Zhang Y, Wu C, Qin J.; Structural and functional insights into PINCH LIM4 domain-mediated integrin signaling.; Nat Struct Biol. 2003 Jul;10(7):558-64.

Walsh MP.; Vascular smooth muscle myosin light chain diphosphorylation: mechanism, function, and pathological implications.; IUBMB Life. 2011 Nov;63(11):987-1000. doi: 10.1002/iub.527. Epub 2011 Oct 12.

Wickström SA, Lange A, Montanez E, Fässler R.; The ILK/PINCH/parvin complex: the kinase is dead, long live the pseudokinase!; EMBO J. 2010 Jan 20;29(2):281-91. doi: 10.1038/emboj.2009.376. Epub 2009 Dec 24.

Wickström SA, Lange A, Hess MW, Polleux J, Spatz JP, Krüger M, Pfaller K, Lambacher A, Bloch W, Mann M, Huber LA, Fässler R.; Integrin-linked kinase controls microtubule dynamics required for plasma membrane targeting of caveolae.; Dev Cell. 2010 Oct 19;19(4):574-88. doi: 10.1016/j.devcel.2010.09.007.

Wu C.; Integrin-linked kinase and PINCH: partners in regulation of cell-extracellular matrix interaction and signal transduction.; J Cell Sci. 1999 Dec;112 (Pt 24):4485-9.

Wu C.; PINCH, N(i)ck and the ILK: network wiring at cell-matrix adhesions.; Trends Cell Biol. 2005 Sep;15(9):460-6.

Yamaji S, Suzuki A, Kanamori H, Mishima W, Takabayashi M, Fujimaki K, Tomita N, Fujisawa S, Ohno S, Ishigatsubo Y.; Possible role of ILK-affixin complex in integrin-cytoskeleton linkage during platelet aggregation.; Biochem Biophys Res Commun. 2002 Oct 11;297(5):1324-31.

Yamaji S, Suzuki A, Kanamori H, Mishima W, Yoshimi R, Takasaki H, Takabayashi M, Fujimaki K, Fujisawa S, Ohno S, Ishigatsubo Y; Affixin interacts with alpha-actinin and mediates integrin signaling for reorganization of F-actin induced by initial cell-substrate interaction.; J Cell Biol. 2004 May 24;165(4):539-51.

Yang JT, Rayburn H, Hynes RO.; Embryonic mesodermal defects in alpha 5 integrin-deficient mice.; Development. 1993 Dec;119(4):1093-105.

Yang JT, Rayburn H, Hynes RO.; Development. 1995 Feb;121(2):549-60.; Cell adhesion events mediated by alpha 4 integrins are essential in placental and cardiac development

Yang L, Wang L, Zheng Y.; Gene targeting of Cdc42 and Cdc42GAP affirms the critical involvement of Cdc42 in filopodia induction, directed migration, and proliferation in primary mouse embryonic fibroblasts.; Mol Biol Cell. 2006 Nov;17(11):4675-85. Epub 2006 Aug 16.

Yoshimi R, Yamaji S, Suzuki A, Mishima W, Okamura M, Obana T, Matsuda C, Miwa Y, Ohno S, Ishigatsubo Y.; The gamma-parvin-integrin-linked kinase complex is critically involved in leukocyte-substrate interaction.; J Immunol. 2006 Mar 15;176(6):3611-24.

Zaidel-Bar R, Geiger B.; The switchable integrin adhesome.; J Cell Sci. 2010 May 1;123(Pt 9):1385-8. doi: 10.1242/jcs.066183.

Zaidel-Bar R, Itzkovitz S, Ma'ayan A, Iyengar R, Geiger B.; Functional atlas of the integrin adhesome.; Nat Cell Biol. 2007 Aug;9(8):858-67.

Zamir E, Katz BZ, Aota S, Yamada KM, Geiger B, Kam Z.; Molecular diversity of cell-matrix adhesions.; J Cell Sci. 1999 Jun;112 (Pt 11):1655-69.

Zervas CG, Gregory SL, Brown NH.; Drosophila integrin-linked kinase is required at sites of integrin adhesion to link the cytoskeleton to the plasma membrane.; J Cell Biol. 2001 Mar 5;152(5):1007-18.

Zhang X, Jiang G, Cai Y, Monkley SJ, Critchley DR, Sheetz MP.; Talin depletion reveals independence of initial cell spreading from integrin activation and traction.; Nat Cell Biol. 2008a Sep;10(9):1062-8. doi: 10.1038/ncb1765.

Zhang Y, Chen K, Guo L, Wu C.; Characterization of PINCH-2, a new focal adhesion protein that regulates the PINCH-1-ILK interaction, cell spreading, and migration.; J Biol Chem. 2002a Oct 11;277(41):38328-38. Epub 2002 Aug 6.

Zhang Y, Chen K, Tu Y, Velyvis A, Yang Y, Qin J, Wu C.; Assembly of the PINCH-ILK-CH-ILKBP complex precedes and is essential for localization of each component to cell-matrix adhesion sites.; J Cell Sci. 2002b Dec 15;115(Pt 24):4777-86.

Zhang Z, Ramirez NE, Yankeelov TE, Li Z, Ford LE, Qi Y, Pozzi A, Zutter MM; alpha2beta1 integrin expression in the tumor microenvironment enhances tumor angiogenesis in a tumor cell-specific manner. Blood. 2008b Feb 15;111(4):1980-8. Epub 2007 Nov 27.

Zhu J, Motejlek K, Wang D, Zang K, Schmidt A, Reichardt LF.; beta8 integrins are required for vascular morphogenesis in mouse embryos.; Development. 2002 Jun;129(12):2891-903.

Zhu J, Carman CV, Kim M, Shimaoka M, Springer TA, Luo BH; Requirement of alpha and beta subunit transmembrane helix separation for integrin outside-in signaling.; Blood. 2007 Oct 1;110(7):2475-83. Epub 2007 Jul 5.

Zigmond SH.; Formin-induced nucleation of actin filaments.; Curr Opin Cell Biol. 2004 Feb;16(1):99-105.

Acknowledgements

This thesis would not have been possible without the help and support of many people.

I would like to express my sincere gratitude to:

Prof. Dr. Reinhard Fässler, for giving me the opportunity to work on these two exciting research topic and for his continuous support, encouragement and the great working conditions that he offered me during these years.

Prof. Dr. Christian Wahl-Schott, who agreed to be the second referee of my thesis and Prof. Dr. Martin Biel, Prof. Dr. Karl-Peter Hopfner, PD Dr. Stefan Zahler and Prof. Dr. Angelika Vollmar, the members of my thesis committee for taking the time to evaluate my work.

Dr. Karsten Beckmann for helping me getting started and Dr. Eloi Montanez for his great help in finishing the atherosclerosis study and introducing me to the parvins.

Dr. Ondrej Tolde, my successor in the parvin-contractility mystery, for his help and the nice discussions.

All current and former members of the Department of Molecular Medicine for creating a good working atmosphere, giving advice and helping me in practical things. In particular I would like to thank Katja, Rosi, Moritz and Emanuel for your help and support in good and bad times, for always cheering me up and for making our retreats unforgettable!

Dr. Walter Göhring, Dr. Armin Lambacher and Klaus Weber for their technical and administrative support and Carmen Schmitz and Ines Lach-Kusevic for the administrative work.

The people from the animal facility, especially Jens Pässler for their often underappreciated but extremely valuable work.

I would like to thank Sebastian for his love and encouragement and for being at my side for all those years.

My very special thanks go to my parents, for their love and support and for always believing in me.

Curriculum vitae

■ Personal Information

Name:	Ina Rohwedder
Adresse:	
Phone:	
Date of birth:	

■ School Education

1989 – 1994	Grundschule
1994 – 2002	Gymnasium

■ University Education

2002 – 2008	Studies in Biology at the Ludwig-Maximilians-Universität in Munich (diploma) - Cell biology (Main subject) - Human genetics (minor subject) - Pharmacology / Toxicology (minor subject)

■ University Degree

11/2008	Diploma in Biology Titel of diploma thesis: *„Nachweis der in vivo Interaktion zwischen LST1 und der potentiellen E3-Ligase KIAA1333“*

■ PhD-Thesis

01/2009 – 02/2013	Doctoral studies at the Max-Planck-Institut of Biochemistry in the department of Molecular Medicine “*Integrin mediated regulation of vascular maturation and atherogenesis”*

Appendix

Publication 1

Plasma fibronectin deficiency impedes atherosclerosis progression and fibrous cap formation

published as

Rohwedder I, Montanez E, Beckmann K, Bengtsson E, Dunér P, Nilsson J, Soehnlein O, Fässler R: ***Plasma fibronectin deficiency impedes atherosclerosis progression and fibrous cap formation***. EMBO Mol Med. 2012 Jul;4(7):564-76.

Plasma fibronectin deficiency impedes atherosclerosis progression and fibrous cap formation

Ina Rohwedder[1†], Eloi Montanez[1,2†], Karsten Beckmann[1,‡], Eva Bengtsson[3], Pontus Dunér[3], Jan Nilsson[3], Oliver Soehnlein[4], Reinhard Fässler[1]*

Keywords: atherosclerosis; fibronectin; fibrous cap; inflammation; migration

DOI 10.1002/emmm.201200237

Received September 23, 2011
Revised February 29, 2012
Accepted March 01, 2012

→See accompanying article
http://dx.doi.org/10.1002/emmm.201200238

Atherosclerotic lesions are asymmetric focal thickenings of the intima of arteries that consist of lipids, various cell types and extracellular matrix (ECM). These lesions lead to vascular occlusion representing the most common cause of death in the Western world. The main cause of vascular occlusion is rupture of atheromatous lesions followed by thrombus formation. Fibronectin (FN) is one of the earliest ECM proteins deposited at atherosclerosis-prone sites and was suggested to promote atherosclerotic lesion formation. Here, we report that atherosclerosis-prone apolipoprotein E-null mice lacking hepatocyte-derived plasma FN (pFN) fed with a pro-atherogenic diet display dramatically reduced FN depositions at atherosclerosis-prone areas, which results in significantly smaller and fewer atherosclerotic plaques. However, the atherosclerotic lesions from pFN-deficient mice lacked vascular smooth muscle cells and failed to develop a fibrous cap. Thus, our results demonstrate that while FN worsens the course of atherosclerosis by increasing the atherogenic plaque area, it promotes the formation of the protective fibrous cap, which in humans prevents plaques rupture and vascular occlusion.

INTRODUCTION

Atherosclerosis is a progressive inflammatory disease of large arteries characterized by an accumulation of lipids and extracellular matrix (ECM) proteins in the affected vessel wall (Lusis, 2000). Atherosclerosis commences with the deposition of lipoprotein particles into the subendothelial matrix and the recruitment of monocytes to the luminal surface of the endothelium. Next, monocytes transmigrate across the endothelial monolayer into the intima, where they proliferate and differentiate into macrophages that take up the lipoprotein particles and form foam cells (Woollard & Geissmann, 2010). Finally, macrophage-derived chemoattractants induce the migration of vascular smooth muscle cells (vSMC) from the vessel wall into the lesion, where they secrete ECM proteins resulting in lesion growth and the formation of the 'fibrous cap' that encloses the lipid-rich core (Newby & Zaltsman, 1999). The rupture of fibrous caps represents an injured vessel surface and triggers adhesion and activation of platelets, which can culminate in thrombus formation and eventually myocardial infarction or stroke (Lusis, 2000). Therefore, the rupture of an atherosclerotic plaque always represents a life-threatening event. Plaque rupture depends on many factors including the composition and vulnerability of plaques (Lusis, 2000). Vulnerable plaques have thin fibrous caps and contain elevated numbers of inflammatory cells (Newby, 2007; Newby et al, 2009).

(1) Department for Molecular Medicine, Max Planck Institute of Biochemistry, Martinsried, Germany
(2) Walter-Brendel-Centre of Experimental Medicine, Ludwig-Maximilians University Munich, Munich, Germany
(3) Department of Clinical Sciences Malmö, Skåne University Hospital, Lund University, Malmö, Sweden
(4) Institute for Cardiovascular Prevention (IPEK), Ludwig-Maximilians University Munich, Munich, Germany
***Corresponding author:** Tel: +49 89 85782424; Fax: +49 89 85782422; E-mail: Faessler@biochem.mpg.de

†These authors contributed equally to this work.
‡Present address: U3 Pharma GmbH, Martinsried, Germany

Despite the systemic nature of atherosclerotic risk factors, which comprise hypercholesterolemia, hyperglycemia, obesity and smoking, atherosclerotic lesions develop preferentially at vessel curvatures, branching points and bifurcations, where the blood flow is highly turbulent (Hahn & Schwartz, 2009). *In vitro* studies suggested that the turbulent blood flow at these atherosclerotic-prone sites exerts mechanical forces on endothelial cells (EC) leading to the activation of EC integrins, the secretion and deposition of fibronectin (FN) (Feaver et al, 2010) and the activation of inflammatory mediators such as NF-κB, the c-Jun NH2-terminal kinases (JNKs) and p21-activated kinase (PAK) (Funk et al, 2010; Hahn & Schwartz, 2008; Hahn et al, 2009; Orr et al, 2005, 2007, 2008). These mediators induce endothelial permeability, sustain an inflammatory state and thereby enforce the consequences of the turbulent blood flow during atherogenesis (Hahn et al, 2009; Orr et al, 2005, 2007).

FNs are a family of large ECM proteins that are generated by alternative splicing from a single gene. FN is found in all vertebrates where it exists in two different forms; one form is cellular FN (cFN), which contains, depending on the tissue, variable proportions of the alternatively spliced exons coding for the extra domains A and B (EDA, EDB). cFN is synthesized and secreted by many cells and assembled into an insoluble fibrillar matrix. The other form is plasma FN (pFN), which lacks EDA and EDB. pFN is synthesized by hepatocytes and released into the circulation where it remains soluble (Leiss et al, 2008; White et al, 2009). Assembly of FN into insoluble and biologically active fibrils critically depends on the interaction with integrins resulting in the unmasking of cryptic FN binding sites, association with other FN proteins and finally crosslinking by tissue transglutaminases into a fibrillar matrix (Hynes, 2002; Leiss et al, 2008). Soluble pFN can also be assembled into fibrils, however, only after it is bound by integrins, *e.g.* on platelets or after transfer into tissues (Moretti et al, 2007; Oh et al, 1981). Studies published more than 20 years ago showed that the expression of FN is elevated in vessel walls of atherosclerotic regions and, therefore, suggested a role for FN during the course of atherosclerosis (Glukhova et al, 1989). Deletion of the *FN* gene in mice leads to early embryonic lethality (George et al, 1993), which precludes the analysis of atherosclerosis. However, a specific ablation of the exon encoding the alternatively spliced EDA domain in atherosclerosis-prone mice was reported to reduce the number and size of atherosclerotic lesions, suggesting that the EDA domain in cFN supports atherogenesis (Babaev et al, 2008; Tan et al, 2004). In line with this observation, the expression of FN-EDA is high during atherosclerosis (Astrof & Hynes, 2009). A correlation between elevated pFN levels and increased incidence for atherosclerosis in human patients has been shown in some studies but also refuted in others (Orem et al, 2003; Ozcelik et al, 2009; Tzanatos et al, 2009; Vavalle et al, 2007; Zhang et al, 2006).

To elucidate the functions of pFN and monocyte/macrophage-derived FN in atherosclerosis, we used the Cre recombinase-loxP sites (*Cre-loxP*) system to delete the *FN* gene in either hepatocytes and/or haematopoietic cells of atherosclerosis-prone (ApoE)-null mice. While deleting *FN* in haematopoietic cells did not affect plaque formation, loss of pFN reduced FN deposits in the subendothelial space of atherosclerosis-prone regions and diminished the number and size of atherosclerotic lesions. Importantly, it also blocked the invasion of vSMCs and the formation of fibrous caps. Thus, pFN plays a dichotomous role in atherosclerosis: it promotes disease by supporting initiation and progression of atherosclerotic lesions but may prevent potential thrombotic events by promoting fibrous cap formation.

RESULTS

FN is deposited at atherosclerosis-prone sites

There are conflicting observations on a correlation of elevated pFN levels with an increased incidence for atherosclerosis in human patients (Orem et al, 2003; Ozcelik et al, 2009; Tzanatos et al, 2009; Vavalle et al, 2007; Zhang et al, 2006). To determine whether pFN plays a role during the course of the disease, we manipulated pFN expression in atherosclerosis-prone $ApoE^{-/-}$ mice using the *Cre-loxP* system. $ApoE^{-/-}$ mice subjected to a high-fat diet develop atherosclerotic lesions over the course of their lifespan (Nakashima et al, 1994). To first test whether FN accumulates at sites of disturbed flow in our model system, we induced atherosclerosis in 3-week-old $ApoE^{-/-}$ mice by feeding them for 12 weeks with a high-fat diet. Oil Red O staining of aortas and the vessels branching from the aortic arch (the innominate, the left common carotid and the left subclavian arteries) confirmed the formation of large, lipid-rich plaques at areas of disturbed blood flow in the innominate and subclavian arteries, and the lesser curvature of the aortic arch (Fig 1A). The Oil Red O-positive plaques were absent before subjecting $ApoE^{-/-}$ mice to the high-fat diet (Fig 1A). Furthermore, cross-sections revealed FN depositions in atherosclerosis-prone regions of aortic arches and innominate arteries, while cross-sections of regions of the aorta and the carotids protected from atherosclerosis did not show FN accumulations (Fig 1B).

Mx-Cre-mediated *FN* gene deletion reduced atherosclerotic plaque formation *in vivo*

Since FN depositions are particularly prominent in the subendothelial space and at the luminal surface of atherosclerosis-prone regions (Fig 1B), we hypothesized that soluble pFN is deposited at these sites and thus might play an important role in atherosclerosis. To test this hypothesis, we intercrossed $ApoE^{-/-}$ mice carrying a *loxP*-flanked *FN* gene ($ApoE^{-/-}FN^{fl/fl}$) with mice expressing the *Cre* recombinase under the control of the interferon- and polyinosinic-polycytidylic acid (poly-IC)-inducible *Mx* promoter (*Mx-Cre*) to produce $ApoE^{-/-}FN^{MxCre}$ mice. Deletion of the *FN* gene was induced in 2-week-old $ApoE^{-/-}FN^{MxCre}$ mice by a single intraperitoneal injection of poly-IC. Western blot (WB) analysis confirmed loss of pFN 1 week after the poly-IC injection (Fig 2A). Elimination of pFN was stable for at least 6 months. WB analysis of cell lysates from $ApoE^{-/-}FN^{MxCre}$ mice showed loss of FN expression in haematopoietic cells but neither in ECs nor in vSMCs from the aorta (Fig 2A and Supporting Information Fig 1A). Together, these results show that *Mx-Cre*-mediated deletion of the *FN* gene

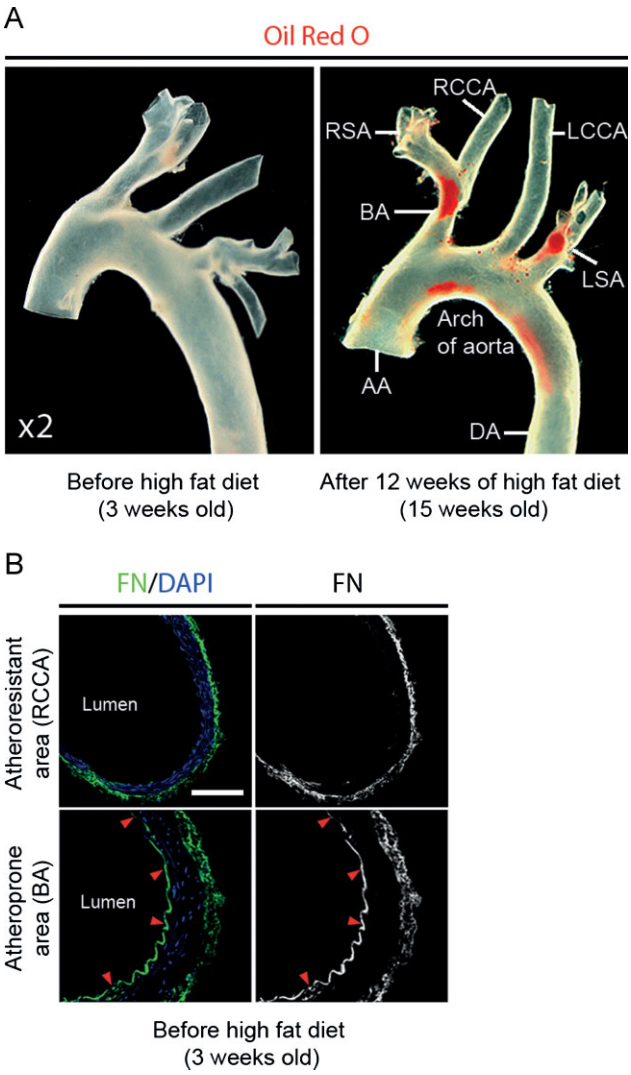

Figure 1. Fatty streaks and FN depositions at atherosclerosis-prone sites.

A. Whole-mount staining of Oil Red O of an aortic arch from ApoE$^{-/-}$ mice before and after feeding a high fat diet. AA, ascending aorta; BA, brachiocephalic artery; RSA, right subclavian artery; RCCA, right common carotid artery; LCCA, left common carotid artery; LSA, left subclavian artery; DA, descending aorta.

B. Immunostaining of FN of the aortic arch from ApoE$^{-/-}$ mice before the high fat diet. FN stains at the luminal side (arrow heads). Nuclei are visualized with DAPI. Scale bars represent 75 μm.

was efficient in hepatocytes and haematopoietic cells resulting in a complete and stable elimination of pFN in ApoE$^{-/-}$FN^{MxCre} mice.

To test whether loss of pFN affects development and/or progression of atherosclerosis, we subjected ApoE$^{-/-}$FN^{MxCre} and their control (ApoE$^{-/-}$FN$^{fl/fl}$) littermates to high-fat diet and performed whole-mount staining of longitudinally opened aortas with Oil Red O to visualize the lipid-rich atherosclerotic plaques. To avoid possible confounding effects of gender differences (Goldbourt & Neufeld, 1986), all experiments were performed with males. After 1 week of high-fat diet, none of the test groups displayed signs of atherosclerotic plaque formation. After 12 weeks of high fat diet, all mice developed atherosclerotic lesions with highest incidence at aortic arches and in the abdominal regions of the aorta (Fig 2B and Supporting Information Fig 1B). However, ApoE$^{-/-}$FN^{MxCre} mice showed significantly fewer atherosclerotic lesions when compared to ApoE$^{-/-}$FN$^{fl/fl}$ control littermates (Fig 2B–E). Quantitative analysis of Oil Red O-stained whole mount aortas revealed that ApoE$^{-/-}$FN^{MxCre} aortas displayed a 50% reduction of lesion areas (Fig 2C), which was due to significantly fewer (Fig 2D) as well as smaller lesions (Fig 2E). Altogether, these results indicate that *Mx-Cre*-mediated deletion of the *FN* gene protects against atherosclerosis.

Vav-Cre-mediated *FN* gene deletion in haematopoietic cells does not affect atherosclerosis

The *Mx-Cre* transgene is known to efficiently disrupt floxed genes in hepatocytes and haematopoietic cells. To determine whether ablation of the *FN* gene in haematopoietic cells including monocytes/macrophages affects the course of atherosclerosis, we intercrossed ApoE$^{-/-}$FN$^{fl/fl}$ mice with mice expressing the *Cre* recombinase under the control of the *Vav* promoter (*Vav-Cre*) to generate ApoE$^{-/-}$FN^{VavCre} mice. WB analysis of cell lysates from ApoE$^{-/-}$FN^{VavCre} mice showed loss of FN expression in haematopoietic cells but neither in hepatocytes nor in ECs and vSMCs from aorta (Fig 3A and unpublished observation). Consistent with normal *FN* gene activity in hepatocytes, ApoE$^{-/-}$FN^{VavCre} mice showed similar pFN levels as ApoE$^{-/-}$FN$^{fl/fl}$ control littermates (Fig 3A and Supporting Information Fig 1C).

Similar to ApoE$^{-/-}$FN$^{fl/fl}$ and ApoE$^{-/-}$FN^{MxCre} mice, ApoE$^{-/-}$FN^{VavCre} mice did not develop atherosclerotic lesions after 1 week of high-fat diet. However, after 12 weeks of a high-fat diet, ApoE$^{-/-}$FN^{VavCre} mice displayed atherosclerotic plaques at atherosclerosis-prone regions (Fig 3B). The overall areas covered with lesions as well as the atherosclerotic plaque sizes and numbers did not differ from those observed in ApoE$^{-/-}$FN$^{fl/fl}$ control littermates (Fig 3C–E). These findings indicate that FN derived from haematopoietic cells does not exert a major impact on the development of atherosclerosis.

Loss of pFN reduced FN deposition at atherosclerosis-prone areas

Lack of pFN significantly reduced the size and number of atherosclerotic lesions. It has been postulated and confirmed in this study (Fig 1B) that FN is deposited at atherosclerosis-prone areas before lesions become visible (Hahn et al, 2009; Orr et al, 2005). To this end, we treated ApoE$^{-/-}$FN$^{fl/fl}$, ApoE$^{-/-}$FN^{VavCre} and ApoE$^{-/-}$FN^{MxCre} mice for 1 week with a high-fat diet and subsequently compared the extent of FN depositions in cross-sections of the atherosclerosis-prone lesser curvature of aortic arches.

Neither mouse strain showed evidence of atherosclerotic plaques after 1 week of high-fat diet. ApoE$^{-/-}$FN$^{fl/fl}$ and ApoE$^{-/-}$FN^{VavCre} mice showed continuous FN deposits at atherosclerosis-prone areas (Fig 4A). In contrast, ApoE$^{-/-}$FN^{MxCre} mice displayed significantly less and often

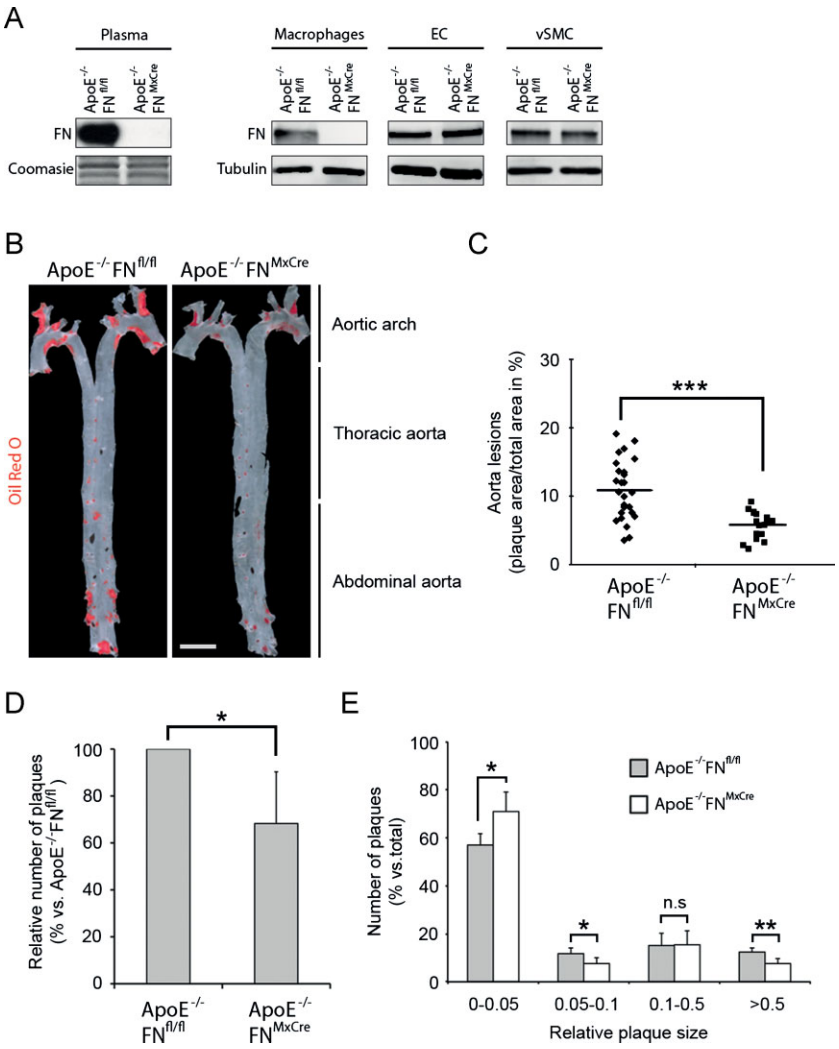

Figure 2. Reduced incidence of atherosclerosis in ApoE$^{-/-}$FN^{MxCre} mice.

A. FN levels in macrophage, EC and vSMC lysates and plasma from ApoE$^{-/-}$FN$^{fl/fl}$ and ApoE$^{-/-}$FN^{MxCre} mice, respectively. Tubulin levels served as loading control.

B. Whole-mount of longitudinally opened aortas from ApoE$^{-/-}$FN$^{fl/fl}$ and ApoE$^{-/-}$FN^{MxCre} mice stained with Oil Red O after 12 weeks on a high-fat diet. Scale bar represents 0.5 cm.

C. Quantification of atherosclerotic lesions in aortas from ApoE$^{-/-}$FN$^{fl/fl}$ ($n = 26$) and ApoE$^{-/-}$FN^{MxCre} ($n = 18$) mice after 12 weeks on a high-fat diet. Data is presented as a mean of atherosclerotic plaque area per total aorta area. Values are mean ± SD; $p = 0.000007$. n.s. = not significant.

D. Quantification of plaque number per aorta. Data is presented as mean of number of plaques per aorta from ApoE$^{-/-}$FN$^{fl/fl}$ ($n = 26$) and ApoE$^{-/-}$FN^{MxCre} ($n = 18$) mice. Values are percentage ± SD; $^{*}p = 0.03$.

E. Quantification of relative size of single lesions. Values are mean ± SD; $p = 0.024$, 0.035, 0.49 and 0.0014. n.s. = not significant.

discontinuous FN staining at the corresponding sites (Fig 4A). These results indicate that pFN, but not haematopoietic cell-derived FN, is deposited at atherosclerosis-prone sites prior to the development of atherosclerotic lesions.

Obesity and hypercholesterolemia are major risk factors for developing atherosclerosis (Lusis, 2000). Since hepatocytes play an important role in cholesterol homeostasis and FN is deleted in these cells, we determined total cholesterol, high-density lipoprotein (HDL) cholesterol and glucose levels and body weight in ApoE$^{-/-}$FN$^{fl/fl}$ and ApoE$^{-/-}$FN^{MxCre} mice treated for 12 weeks with a high-fat diet. We found no differences in either cholesterol, HDL (Fig 4B) and glucose levels (Fig 4C) or in body weight (Fig 4D) between ApoE$^{-/-}$FN$^{fl/fl}$ and ApoE$^{-/-}$FN^{MxCre} mice. These results exclude an involvement of risk factors in the differential development of atherosclerosis in ApoE$^{-/-}$FN$^{fl/fl}$ and ApoE$^{-/-}$FN^{MxCre} mice.

Expression of inflammatory mediators and recruitment of monocytes are reduced in ApoE$^{-/-}$FN^{MxCre} mice

Integrin-FN interactions are believed to promote monocyte/macrophage recruitment and to maintain an inflammatory milieu at atherosclerosis-prone sites by sustaining shear stress-induced NF-κB and PAK activation in ECs, which in turn leads to the expression of downstream genes such as ICAM-1 (Orr et al, 2007) or the activation of signalling molecules such as JNK (Hahn et al, 2009). To analyze whether pFN modulates NF-κB, PAK and JNK activity *in vivo*, we compared the levels of the phosphorylated NF-κB subunit p65, phospho-PAK, phospho-JNK and ICAM-1 on cross-sections of the atherosclerosis-prone lesser curvatures of aortic arches from ApoE$^{-/-}$FN$^{fl/fl}$ and ApoE$^{-/-}$FN^{MxCre} mice fed for 1 week with a high-fat diet. ApoE$^{-/-}$FN$^{fl/fl}$ mice had abundant phospho-NF-κB/p65, phospho-PAK throughout ECs, phospho-JNK enriched in nuclei and ICAM-1 on the luminal surface of the ECs (Fig 5A). In contrast, ApoE$^{-/-}$FN^{MxCre} mice displayed lower levels of phospho-NF-κBp65, phospho-PAK, phospho-JNK and ICAM-1 in corresponding areas (Fig 5A). Interestingly, atherosclerotic plaques of ApoE$^{-/-}$FN$^{fl/fl}$ and ApoE$^{-/-}$FN^{MxCre} mice fed for 10 weeks with a high-fat diet showed similar expression of all tested inflammatory markers (Supporting Information Fig 2A). These results indicate that depositions of pFN facilitate activation of inflammatory mediators at atherosclerosis-prone sites *in vivo*.

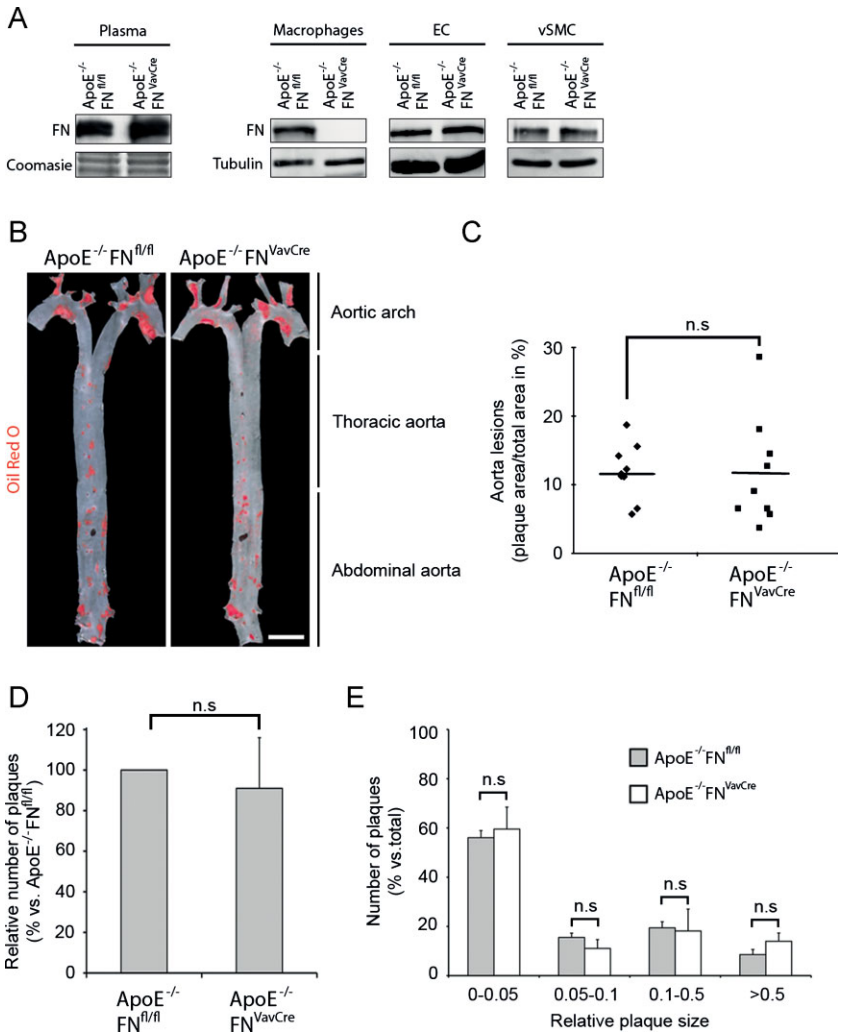

Figure 3. Normal incidence of atherosclerosis in ApoE$^{-/-}$FN^{VavCre} mice.

A. FN levels in macrophage, EC and vSMC lysates and plasma from ApoE$^{-/-}$FN$^{fl/fl}$ and ApoE$^{-/-}$FN^{VavCre} mice, respectively. Tubulin levels served as loading control.

B. Whole-mount of longitudinally opened aortas from ApoE$^{-/-}$FN$^{fl/fl}$ and ApoE$^{-/-}$FN^{VavCre} mice stained with Oil Red O after 12 weeks on a high-fat diet. Scale bar represents 0.5 cm.

C. Quantification of atherosclerotic lesions in aortas from ApoE$^{-/-}$FN$^{fl/fl}$ ($n = 9$) and ApoE$^{-/-}$FN^{VavCre} ($n = 9$) mice after 12 weeks on a high-fat diet. Data is presented as a mean of atherosclerotic plaque area per total aorta area. Values are mean ± SD; $p = 0.96$. n.s. = not significant.

D. Quantification of plaque numbers per aorta. Data is presented as mean of number of plaques per aorta from ApoE$^{-/-}$FN$^{fl/fl}$ ($n = 9$) and ApoE$^{-/-}$FN^{VavCre} ($n = 9$) mice. Values are percentage ± SD; $p = 0.78$. n.s. = not significant.

E. Quantification of the relative size of single lesions. Values are mean ± SD; $p = 0.27$, 0.08, 0.41 and 0.055. n.s. = not significant.

To further confirm these results, we cultured ECs in the presence and absence of pFN and monitored the expression of ICAM-1 by WB. In line with our *in vivo* results, ICAM-1 levels were reduced in ECs when they were cultured in the absence of pFN (Fig 5B).

Adhesion of monocytes to the endothelium is required for the initiation of atherosclerosis (Woollard & Geissmann, 2010). To analyze whether pFN depositions modulate adhesion of monocytes to ECs, we analyzed leukocyte adhesion on the endothelium in atherosclerosis-prone regions of the carotid artery of ApoE$^{-/-}$FN$^{fl/fl}$ and ApoE$^{-/-}$FN^{MxCre} mice using intravital microscopy and found that the number of adherent leukocytes was reduced in ApoE$^{-/-}$FN^{MxCre} mice when compared to ApoE$^{-/-}$FN$^{fl/fl}$ control littermates (Fig 5C and D). Since the number of circulating leukocytes is influencing their adhesion to the endothelium, we determined their numbers and found that they were similar in ApoE$^{-/-}$FN$^{fl/fl}$ and ApoE$^{-/-}$FN^{MxCre} mice (unpublished observation). The adhesion of leukocytes to the endothelium is mediated by the interaction of α4β1 integrins to VCAM-1 (Barringhaus et al, 2004). Immunostaining of cross-sections of aortic arches with anti-VCAM-1 antibodies and FACS analyses of leukocytes to quantify α4β1 integrin surface levels revealed normal levels of both adhesion molecules in ApoE$^{-/-}$FN$^{fl/fl}$ and ApoE$^{-/-}$FN^{MxCre} mice fed for 1 week with a high-fat diet (Supporting Information Fig 2B and 2C).

Next, we measured cell adhesion of Mac-1-positive cells to monolayers of ECs under static and laminar flow conditions, both in the presence and absence of pFN. We used bEnd5 endothelioma cells to test adhesion, since they were shown to promote adhesion of haematopoietic cells equally well as primary ECs (Steiner et al, 2010). Mac-1-positive cells cultured in absence of pFN were suspended in pFN-free medium or pFN-complemented medium (10 μg/ml) and then seeded onto a bEnd5 monolayer. Quantification of adherent cells revealed that twofold more Mac-1-positive cells adhered to the bEnd5 monolayer when they were cultured in pFN-complemented medium as compared to pFN-free medium (Fig 5E), indicating that soluble pFN promotes adhesion of Mac-1-positive cells to ECs.

During atherosclerosis, low-density lipoprotein (LDL) particles aggregate and become oxidized in the vascular ECM. Oxidized LDL will be taken up by macrophages resulting in the

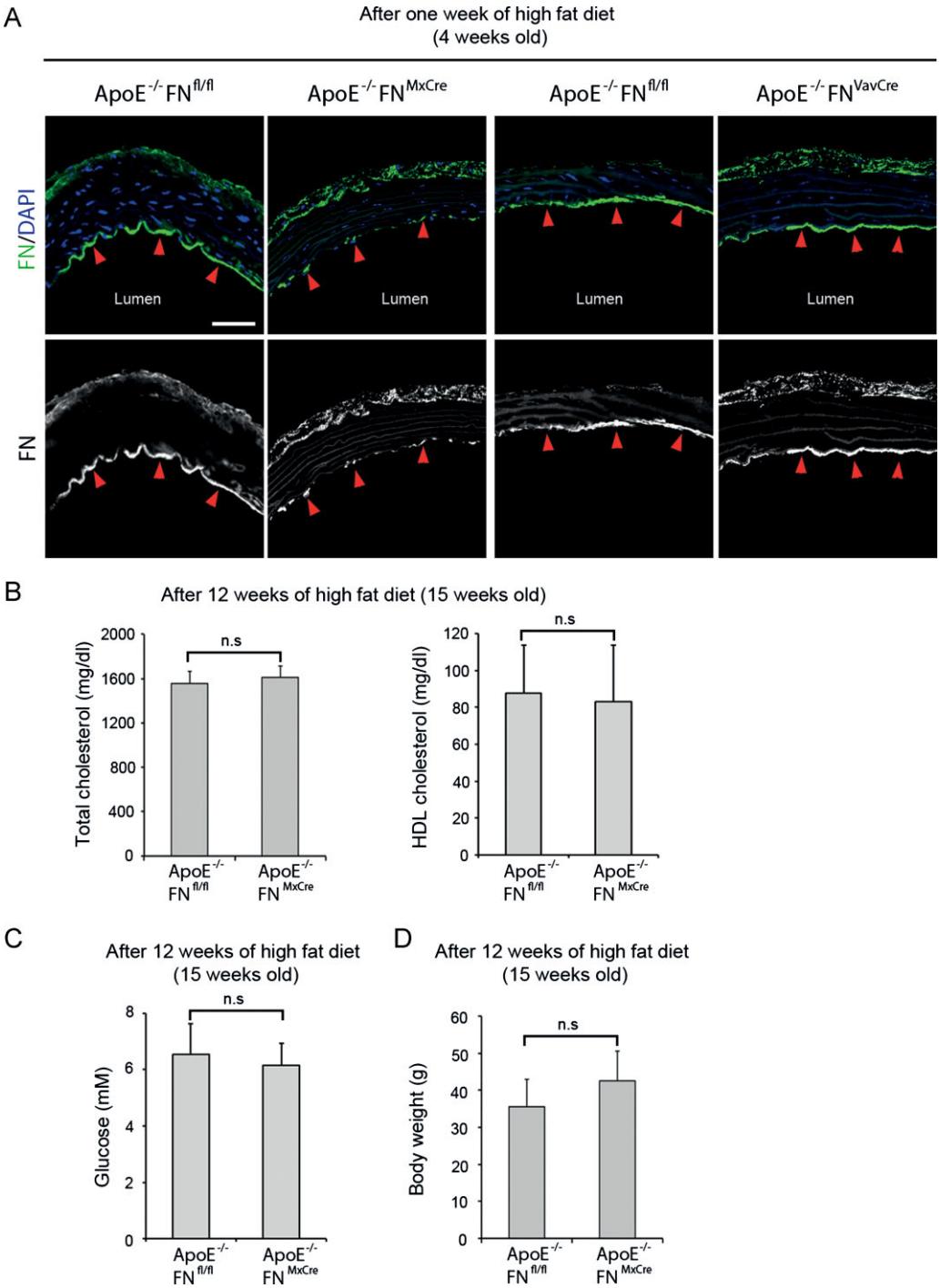

Figure 4. Reduced FN depositions in the aortic arch of ApoE$^{-/-}$FN^{MxCre} mice.

A. Immunostaining of FN in the lesser curvature of the aortic arch from ApoE$^{-/-}$FN^{MxCre}, ApoE$^{-/-}$FN^{VavCre} mice and their respective ApoE$^{-/-}$FN$^{fl/fl}$ mice. Arrowheads point to FN signals at the luminal side of the arch. Nuclei are visualized with DAPI. Scale bar represents 75 μm in all images.

B. Fasting cholesterol and HDL cholesterol levels of ApoE$^{-/-}$FN$^{fl/fl}$ ($n = 13$) and ApoE$^{-/-}$FN^{MxCre} ($n = 13$) mice after 12 weeks on a high-fat diet. Values are mean ± SD; $p = 0.33$. n.s. = not significant.

C. Fasting glucose levels of ApoE$^{-/-}$FN$^{fl/fl}$ ($n = 13$) and ApoE$^{-/-}$FN^{MxCre} ($n = 13$) mice after 12 weeks on a high-fat diet. Values are mean ± SD; $p = 0.15$. n.s. = not significant.

D. Body weight of ApoE$^{-/-}$FN$^{fl/fl}$ ($n = 28$) and ApoE$^{-/-}$FN^{MxCre} ($n = 16$) mice after 12 weeks on a high fat-diet. Values are mean ± SD; $p = 0.11$. n.s. = not significant.

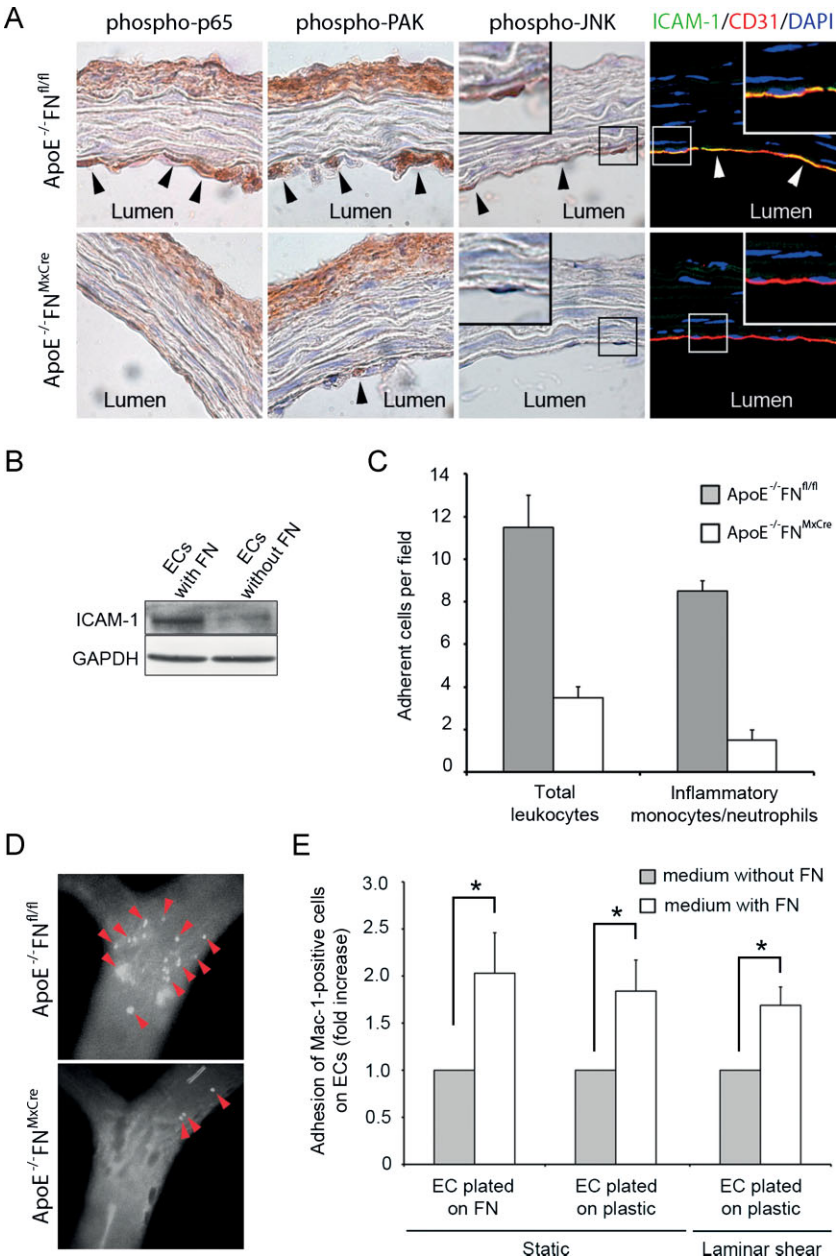

Figure 5. Reduced NF-κB and PAK activation and macrophage recruitment into atheroprone areas of ApoE$^{-/-}$FN^{MxCre} mice.

A. Immunostaining of phosho-NFκB/p65, phospho-PAK, phospho-JNK and ICAM-1 in the lesser curvature of the aortic arch from ApoE$^{-/-}$FN$^{fl/fl}$ and ApoE$^{-/-}$FN^{MxCre} mice. Arrowheads point to immunosignals in ECs.

B. Western blot for ICAM-1 in lysates from ECs cultured for 36 h in the presence or absence of pFN.

C. Adhesion of leukocytes and inflammatory monocytes/neutrophils to carotid arteries of ApoE$^{-/-}$FN$^{fl/fl}$ and ApoE$^{-/-}$FN^{MxCre} mice fed with high-fat diet for 4.5 weeks. Values are mean ± SD.

D. Representative images of inflammatory monocytes/neutrophils adhering (arrowheads) to the luminal side of the external carotid artery in ApoE$^{-/-}$FN$^{fl/fl}$ and ApoE$^{-/-}$FN^{MxCre} mice.

E. Quantification of adhesion of Mac-1-positive cells on a monolayer of ECs under static condition and laminar shear (2.5 dyne/cm^2). Values are mean ± SD and normalized to adherent cells in the presence of FN in the culture medium; $p = 0.025$, 0.023 and 0.029.

formation of aggregated and oxidized LDL foam cells (Woollard & Geissmann, 2010). To test whether pFN modulates lipid accumulation in plaques, we stained cross-sections of atherosclerotic plaques from ApoE$^{-/-}$FN$^{fl/fl}$ and ApoE$^{-/-}$FN^{MxCre} mice with Oil Red O. Lipids were detected in the core region of the plaques and a similar lipid accumulation was found in ApoE$^{-/-}$FN$^{fl/fl}$ and ApoE$^{-/-}$FN^{MxCre} mice (Fig 6A).

To determine whether FN affects macrophage uptake of modified LDL, we incubated freshly isolated macrophages from ApoE$^{-/-}$FN$^{fl/fl}$ and ApoE$^{-/-}$FN^{MxCre} mice (Supporting Information Fig 3) with LDL and acLDL and then stained them with Oil Red O. The intracellular lipid accumulation was similar in macrophages from ApoE$^{-/-}$FN$^{fl/fl}$ and ApoE$^{-/-}$FN^{MxCre} mice (Fig 6B). Finally, we quantified the acLDL uptake by macrophages from ApoE$^{-/-}$FN$^{fl/fl}$ and ApoE$^{-/-}$FN^{MxCre} mice after incubating them for 4 and 24 h with acLDL and found that also the acLDL uptake was normal (Fig 6C). Collectively, these results indicate that FN is dispensable for foam cell formation.

Atherosclerotic lesions in ApoE$^{-/-}$FN^{MxCre} mice lack the fibrous cap

Advanced atherosclerotic lesions are characterized by a subendothelial accumulation of vSMCs, which synthesize and deposit a collagen- and FN-rich matrix into the fibrous cap (Newby & Zaltsman, 1999). To test whether loss of pFN alters fibrous cap formation, we immunostained cross-sections of similarly sized atherosclerotic plaques from ApoE$^{-/-}$FN$^{fl/fl}$ and ApoE$^{-/-}$FN^{MxCre} mice for Mac-1 to visualize monocyte/

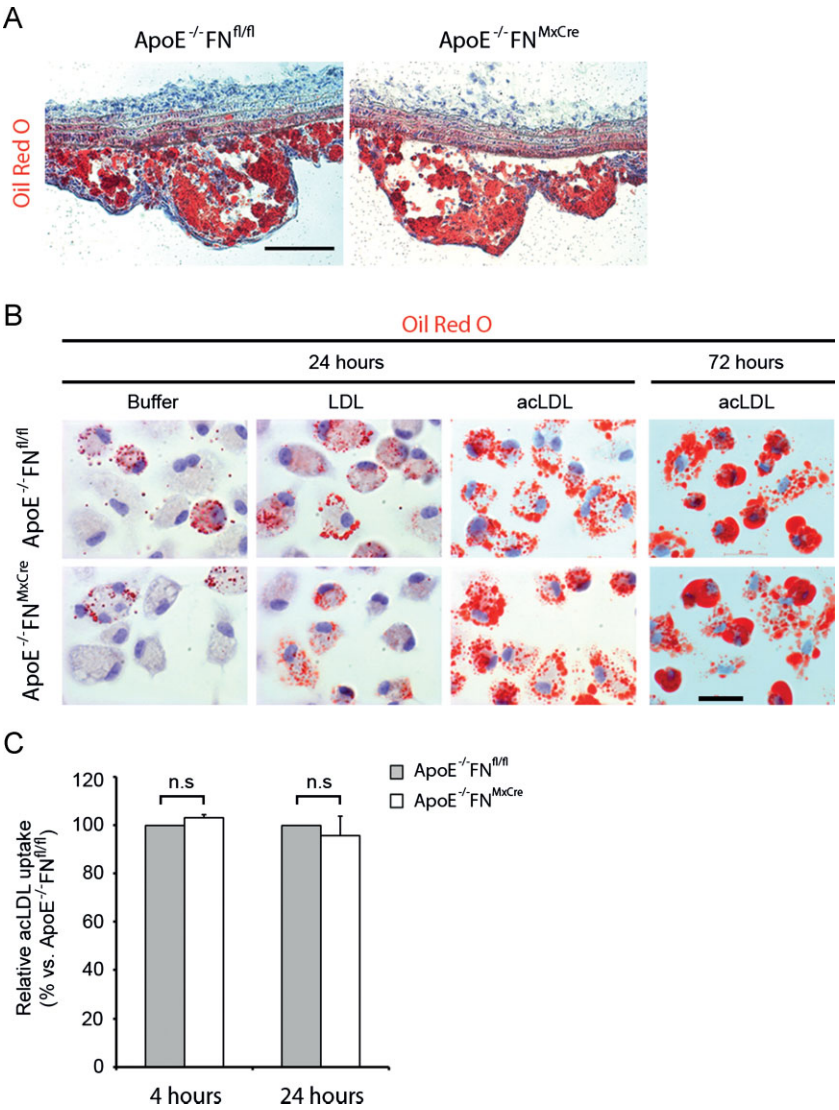

Figure 6. Normal foam cell formation in ApoE$^{-/-}$FN^{MxCre} mice.

A. Staining atherosclerotic plaques from ApoE$^{-/-}$FN$^{fl/fl}$ and ApoE$^{-/-}$FN^{MxCre} mice 12 weeks after a high fat diet with Oil Red O and haematoxylin. Scale bar represents 100 μm.

B. Staining of macrophages from ApoE$^{-/-}$FN$^{fl/fl}$ and ApoE$^{-/-}$FN^{MxCre} mice with Oil Red O and haematoxylin 24-h after incubating them with LDL or AcLDL, respectively. Scale bar represents 20 μm.

C. Quantification of acLDL uptake by macrophages from ApoE$^{-/-}$FN$^{fl/fl}$ and ApoE$^{-/-}$FN^{MxCre} mice. Values are mean ± SD; $p = 0.36$ and 0.29. n.s. = not significant.

macrophages, Thy-1.2/CD3 to visualize T cells, alpha-smooth muscle actin (αSMA) to visualize vSMCs and the ECM proteins FN and collagen type I (Col-I). After 12 weeks of high-fat diet, atherosclerotic plaques from ApoE$^{-/-}$FN$^{fl/fl}$ mice consisted of macrophage-derived foam cells that were covered at the luminal side with a FN- and collagen-rich matrix and a continuous layer of vSMCs (Fig 7A and B and Supporting Information Fig 4A). A few T cells were detected, mainly at the edges of a few plaques (Supporting Information Fig 4B). In sharp contrast, atherosclerotic plaques from ApoE$^{-/-}$FN^{MxCre} mice lacked vSMCs and a collagen matrix and consisted mainly of macrophage-derived foam cells (Fig 7 A and B and Supporting Information Fig 4A). Similarly, atherosclerotic plaques of ApoE$^{-/-}$FN^{MxCre} mice fed for 6 months with a high-fat diet also lacked vSMCs and a collagen matrix. Distribution and number of T cells were unaffected in ApoE$^{-/-}$FN^{MxCre} mice (Supporting Information Fig 4B).

To determine whether monocyte/macrophage-derived FN contributes to vSMCs recruitment and fibrous cap formation, we analyzed lesions from ApoE$^{-/-}$FN^{VavCre} mice and found that the cellular composition of their lesions and the FN deposits in their fibrous caps were similar to ApoE$^{-/-}$FN$^{fl/fl}$ control littermates (Supporting Information Fig 4C). Together, these results indicate that pFN plays an important role in promoting the formation of the fibrous cap.

pFN stimulates vSMC migration

Why do vSMCs fail to colonize the fibrous caps in ApoE$^{-/-}$FN^{MxCre} mice? Successful accumulation of vSMCs in atherosclerotic lesions and subsequent formation of the fibrous cap depends on a number of factors including vSMC proliferation and survival rates as well as their ability to migrate into the lesions (Newby & Zaltsman, 1999). We found no apparent defects in vSMCs proliferation nor did we observe increased apoptosis in lesions from ApoE$^{-/-}$FN^{MxCre} mice subjected to high-fat diet. To test whether pFN modulates migration of vSMCs, we isolated primary vSMCs and performed chemotaxis assays using transwell motility chambers using pFN as a

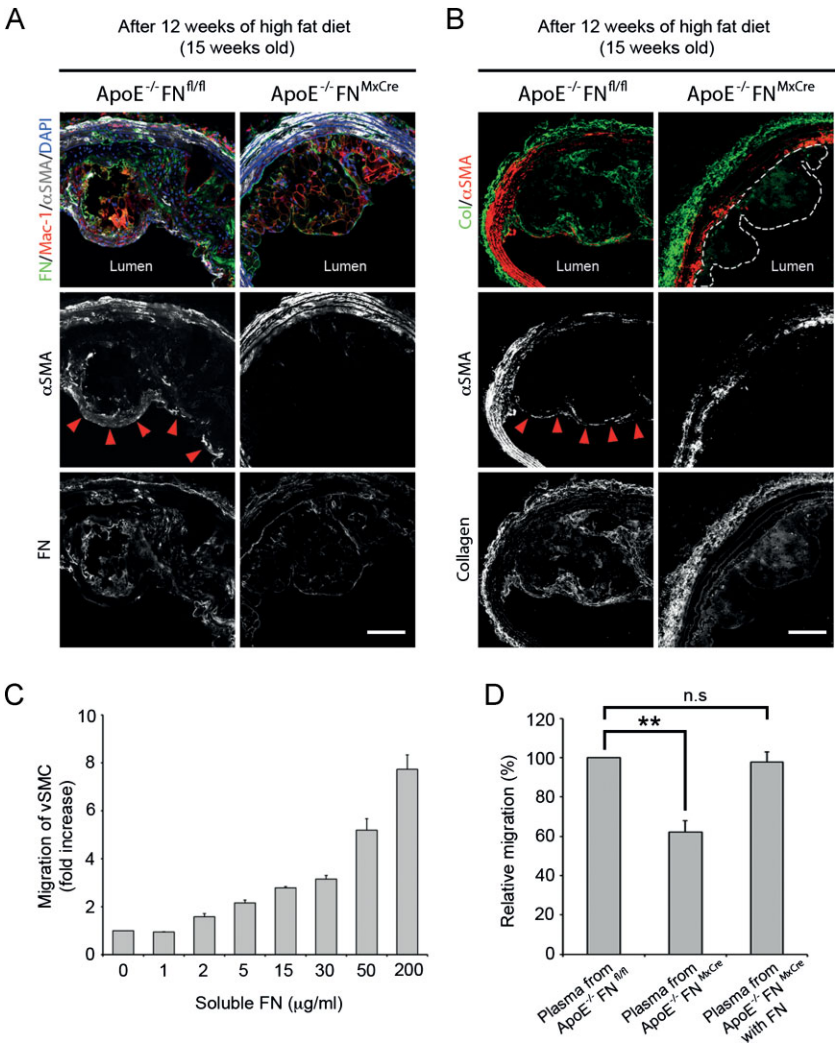

Figure 7. Atherosclerotic lesions from ApoE$^{-/-}$FN^{MxCre} mice lack fibrous caps.

A. Immunostaining of atherosclerotic plaques from ApoE$^{-/-}$FN$^{fl/fl}$ and ApoE$^{-/-}$FN^{MxCre} mice after 12 weeks of high fat diet for FN, macrophage antigen-1 (Mac-1) and αSMA. Arrowheads point to αSMA immunosignals in the fibrous cap. Nuclei are visualized with DAPI. Scale bar represents 75 μm.

B. Immunostaining of atherosclerotic plaques from ApoE$^{-/-}$FN$^{fl/fl}$ and ApoE$^{-/-}$FN^{MxCre} mice after 12 weeks of high fat diet with antibodies against collagen I and αSMA. White dotted line displays plaque surface. αSMA stains the luminal side (arrowheads). Nuclei are visualized with DAPI. Scale bar represents 75 μm.

C. Quantification of vSMC migration against FN in the lower part of Transwell chambers. Control medium lacking FN (0) was used to assess baseline migration.

D. Quantification of vSMC migration against plasma from ApoE$^{-/-}$FN$^{fl/fl}$, ApoE$^{-/-}$FN^{MxCre} mice with and without supplementation of FN (12 μg/ml). Values are percentage of migrating cells ± SD; $p = 0.0045$ and 0.1. n.s. = not significant.

chemoattractant in the lower part of the chambers. We observed that pFN increased the migration of vSMCs in a concentration-dependent manner (Fig 7C). When we added plasma samples from ApoE$^{-/-}$FN$^{fl/fl}$ and ApoE$^{-/-}$FN^{MxCre} mice to the lower part of the migration chamber, we found that plasma from ApoE$^{-/-}$FN$^{fl/fl}$ mice induced twofold higher migration rates of vSMCs than plasma from ApoE$^{-/-}$FN^{MxCre} mice (Fig 7D). Importantly, the decreased migration rates of vSMCs towards plasma derived from ApoE$^{-/-}$FN^{MxCre} mice could be rescued by supplementing the plasma with FN (Fig 7D). These results clearly indicate that pFN is a motility factor for vSMCs.

DISCUSSION

FN deposits and atherosclerotic lesions preferentially form at sites of disturbed blood flow (Hahn & Schwartz, 2009). *In vitro* studies with shear-stressed ECs cultured on FN suggest that the FN deposits enforce and maintain a pro-atherogenic milieu through integrin binding and signalling (Feaver et al, 2010). It is not known, however, whether FN serves a similar function *in vivo* and whether the FN depositions are derived from the circulation or from infiltrating monocytes and/or resident ECs. To address these questions, we generated mice lacking the *FN* gene either in hepatocytes and/or haematopoietic cells and crossed them with atherosclerosis-prone ApoE-null mice and fed them a high-fat diet. Loss of FN expression in blood cells modulated neither the development nor progression of atherosclerosis in mice. In contrast, loss of pFN abrogated FN depositions at atherosclerosis-prone sites resulting in the formation of smaller and fewer atherosclerotic lesions. However, they were covered only with a thin layer of matrix proteins, which is usually a sign of fragility and increased susceptibility for ruptures in human atherosclerotic plaques. These findings suggest a dual function for pFN during atherosclerosis: it supports plaque initiation by providing an adhesive matrix for monocytes and at late stages, it protects the lesions by controlling the formation of the fibrous cap. Thus, targeting atheroma initiation and growth by modulating FN production might have the unforeseen consequences of promoting plaque rupture and arterial occlusions resulting in a significant increase in vascular morbidity and mortality.

The subendothelial matrix of the healthy vasculature is mainly composed of basement membrane (BM) components including collagen IV and laminins. During pathological situations such as inflammation, wound healing or atherosclerosis transitional matrix proteins such as FN or fibrinogen are deposited into the subendothelial matrix (Hahn & Schwartz, 2009). In atherosclerosis, FN is deposited at sites of disturbed flow before fatty streaks are formed (Hahn & Schwartz, 2009; Hahn et al, 2009; Orr et al, 2005) but the source of the FN deposits is not known. *In vitro* studies have shown that disturbed flow induces the expression and deposition of FN by ECs (Feaver et al, 2010) suggesting that shear-stressed ECs deposit FN into the vessel wall. We confirmed these findings showing that FN is indeed deposited into the subendothelial space at sites of disturbed blood flow. Since pFN can be transferred from the plasma into tissues (Moretti et al, 2007; Oh et al, 1981), we next tested whether pFN contributes to the FN depositions. To this end, we ablated a conditional *FN*-null allele in ApoE-null mice with the *Mx-Cre* transgene ($ApoE^{-/-}FN^{MxCre}$) that deletes efficiently in hepatocytes and haematopoietic cells, and fed the offspring a high fat diet. The *Mx-Cre* transgene can also delete genes at low efficiency in other tissues than liver and blood cells, which is, however, efficiently compensated by diffusion of FN from non-deleted neighbouring cells (Sakai et al, 2001). The $ApoE^{-/-}FN^{MxCre}$ offspring showed very little FN at atheroprone areas suggesting that pFN represents a major source for FN depositions at the atherosclerosis-prone areas of the vasculature. The presence of residual FN in vessel walls of $ApoE^{-/-}FN^{MxCre}$ mice indicates that small contributions from ECs and/or vSMCs may add to the FN depositions at atherosclerosis-prone areas. Previous reports associating increased pFN levels with atherosclerosis (Orem et al, 2003) and ischemic heart disease (Ozcelik et al, 2009; Song et al, 2001; Taznatos et al, 2009) support a role of pFN as atherosclerosis promoting factor. On the other hand, however, it has also been shown that pFN levels were unchanged or even decreased in cohorts of atherosclerosis patients (Vavalle et al, 2007; Zhang et al, 2006). It is thus possible that other risk factors, which probably depend on the patient population, are able to either attenuate or aggravate the effect of pFN on the course of atherosclerosis. Unfortunately, the nature of these risk factors is not known.

In atherosclerosis, it is believed that binding of fibrillar collagens to α2β1 prevents pro-inflammatory signals, while FN sustains a shear-stressed induced inflammatory environment and therefore is thought to aggravate the course of the disease. Mechanistically, FN mediates its pro-inflammatory role through β1-containing integrins, most likely α5β1 (Orr et al, 2006), which in turn induces phosphorylation of NF-κB through the activation of the small GTPase Rac1 (Tzima et al, 2002). In line with these findings we found that ECs of $ApoE^{-/-}FN^{MxCre}$ mice contain significantly less of the phosphorylated NF-κB subunit p65 and less phosphorylated PAK, and develop smaller plaques than control mice. In line with reduced NF-κB activity we also observed reduced expression of the downstream gene *ICAM-1* on ECs. Consequently, the adhesion of monocytes to the endothelium at atherosclerosis-prone regions in $ApoE^{-/-}FN^{MxCre}$ mice was also reduced when compared to control littermates, providing a good explanation for the reduced recruitment of monocytes to atherosclerosis-prone sites. Interestingly, we found that the levels of inflammatory markers in developed lesions of $ApoE^{-/-}FN^{MxCre}$ mice were comparable with those of control mice, indicating that pFN is required for inflammation during plaque initiation, but not anymore once the plaques have formed. Since the deletion of the *FN* gene in monocytes by Vav-Cre did not affect the course of atherosclerosis, we expected normal monocyte recruitment to plaques in these mice, although we did not confirm this by intravital microscopy. In summary, we collected several lines of evidence suggesting that monocyte recruitment is indeed impaired in pFN-deficient mice: the expression of ICAM-1 on ECs was markedly reduced, the adhesion of monocytes to the endothelium was reduced in pFN-deficient mice, and the number and size of atherosclerotic plaques was significantly diminished in $ApoE^{-/-}FN^{MxCre}$ mice.

The reduced number and size of atherosclerotic plaques in $ApoE^{-/-}FN^{MxCre}$ mice corroborate previous observations made using *in vitro* systems. In addition, our findings revealed a previously unknown function for FN in atherosclerosis. Almost all atherosclerotic lesions in $ApoE^{-/-}FN^{MxCre}$ mice were devoid of vSMC, contained reduced levels of collagen I and lacked a fibrous cap, which points to a role for FN in the reinforcement of atherosclerotic plaques. Atherosclerotic plaques that are not stabilized with fibrous caps in humans lead to an increased likelihood of rupture and subsequent thrombus-mediated vascular occlusion leading to myocardial infarction, stroke and sudden death (Lusis, 2000). Unfortunately, plaque ruptures with thrombosis do not occur in mouse models and therefore, the consequences could not be tested (Glass & Witztum, 2001; Libby et al, 2011). The formation of a fibrous cap critically depends on the activation and proliferation of vSMCs in the intima of the affected vessel and their subsequent migration into the plaque area where they deposit a collagen-rich matrix. Since we found normal proliferation and survival rates of vSMCs in $ApoE^{-/-}FN^{MxCre}$ mice, we conclude that the vascular FN deposits represent a trigger for the recruitment of vSMCs. This notion is supported by our *in vitro* experiments demonstrating that vSMCs were less efficient at migrating towards plasma lacking pFN.

These new findings strongly argue against the use of inhibitors designed to treat atherosclerosis by blocking the function of FN, such as by using peptides derived from FN. This type of treatment would inhibit pro-inflammatory signalling and thus reduce the number and size of atherosclerotic plaques but would also at the same time destabilize these plaques and increase the danger of thrombus formation and thrombotic diseases. Furthermore, reducing pFN levels would also destabilize thrombi and trigger the shedding of platelet clumps into the circulation (Ni et al, 2003) resulting in chronic embolism.

MATERIALS AND METHODS

Animal procedures

$ApoE^{-/-}$ (Jackson Laboratory) and $FN^{fl/fl}$ mice (Sakai et al, 2001) were intercrossed with Mx-Cre transgenic mice (Kuhn et al, 1995; Schneider

The paper explained

PROBLEM:

Vascular occlusion of atheromatous arteries is the commonest cause of death in the western world. The main cause of vascular occlusions is the rupture of atherosclerotic plaques followed by thrombus formation. Atherosclerotic plaques are asymmetric focal thickenings of the artery consisting of lipids, various cell types and ECM including FN. Expression of FN is elevated in vessel walls of atherosclerotic regions, however, the source and functions of FN in atherosclerosis are not clear.

RESULTS:

In our study, we show that atherosclerosis-prone mice lacking hepatocyte-derived pFN and fed with a pro-atherogenic diet lack FN deposits and show reduced pro-inflammatory signals at atherosclerosis-prone areas resulting in significantly smaller and fewer atherosclerotic plaques. Unexpectedly, the atherosclerotic lesions were devoid of fibrous caps, which play an important role for plaque stability and to prevent plaque rupture.

IMPACT:

Our results demonstrate that FN plays a dichotomous role in atherosclerosis: while FN worsens the course of atherosclerosis by increasing the atherogenic plaque area, it stabilizes the plaques with fibrous caps and protects from secondary damage and vascular occlusion.

et al, 2003) to produce ApoE$^{-/-}$FN^{MxCre} mice, or with Vav-Cre transgenic mice (Georgiades et al, 2002) to produce ApoE$^{-/-}$FN^{VavCre} mice. Deletion of the floxed *FN* alleles was induced in 2-week-old mice by a single intraperitoneal injection of 175 μg poly-IC (Sigma).
Atherosclerosis was accelerated by feeding the mice for 12 weeks with a high fat diet (provided by Altromin, Lage/Lippe, Germany) containing 21% fat, 0.15% cholesterol but lacking cholate (composition according to Harlan Teklad TD88137 diet). All experiments with mice were performed in accordance to German guidelines and regulations.

Atherosclerotic lesion analysis

Mice were anesthetized with Avertin, hearts were perfused with 15 ml of phosphate-buffered saline (PBS) containing 5 mM ethylenediaminetetracetic acid (EDTA) and then with PBS containing 2% paraformaldehyde (PFA), 7.5% sucrose. The adventitia was thoroughly cleaned under a dissecting microscope, and the aorta was cut open longitudinally and pinned on to a silicone plate. After 5 min equilibration in 60% isopropanol, aortas were stained with Oil Red O (Sigma, Germany), plaques were analyzed under the Leica MZ16FA stereomicroscope, and quantified with Metamorph® software. The aortic lesions of each animal are presented as percentage of the total aortic luminal surface area.

Plasma cholesterol

Total and HDL cholesterol levels in plasma were quantified as previously described (Dunér et al, 2011; Fredrikson et al, 2003).

Plasma glucose measurement

Plasma glucose was measured using a commercial kit (Abcam).

Antibodies

The following antibodies were used: biotinylated rat anti-Mac-1 monoclonal antibody (Pharmingen), CD3-PE, Thy-1.2 CD90.2, GM-130, ICAM-1, PECAM-1 (CD31) (all from Pharmingen), Cy3-coupled mouse anti-αSMA antibody (Sigma), rabbit anti-FN polyclonal antibody (Millipore), rabbit anti-Col-I antibody (Millipore), phospho-NFκB p65 (Santa Cruz), phospho-PAK1/2 (Cell Signaling), phosphor-JNK (Cell Signaling). Secondary antibodies were purchased from Jackson Immuno Research Laboratories, Molecular Probes or Invitrogen.

Histology and immunostaining

Heart and aorta tissues were embedded into a cryo-matrix (Thermo) and 10 or 12 μm sections were prepared using a cryotome. Sections were blocked with 3% bovine serum albumin (BSA) 0.2% Triton-X in PBS and incubated with antibodies.

Intravital microscopy

Intravital microscopy of the left carotid artery was performed as described previously (Drechsler et al, 2010). The left jugular vein was cannulated with polyethylene tubing (PE50) for the intravenous administration of anti-Gr1 antibodies (RB6-8C5, 2.5 μg/mouse) for visualizing inflammatory monocytes and neutrophils and rhodamine 6G to visualize total leukocytes. Intravital microscopy was performed with an Olympus BX51 microscope equipped with a Hamamatsu 9100-02 EMCCD camera and a 10× saline-immersion objective. For image acquisition and analysis Olympus cell^{R} software was used.

Isolation of smooth muscle cells

Aortas were dissected, longitudinally opened, washed with PBS, cut and digested with digestion buffer (2 mg/ml collagenase type II and 0.5 mg/ml elastase in Dulbecco's modified Eagle medium (DMEM)) for 30 min at 37°C. Digestion was terminated with 10% foetal bovine serum (FBS) in DMEM. Released cells were centrifuged and re-suspended in DMEM containing 10% FBS, transferred to 6-well dishes and further expanded for analysis.

Isolation of aortic endothelial cells

Cells were isolated as previously described (Kobayashi et al, 2005).

In vitro foam cell formation assay

Thioglycolate-elicited peritoneal macrophages were plated on 12-well plates in macrophage serum-free medium (Macrophage-SFM, Invitrogen). After 24 h, non-adherent cells were washed off, and macro-

phages were incubated in fresh serum-free medium complemented with 50 μg/ml native, acetylated human LDL (acLDL) or buffer control for 24–72 h. Cells were stained for 60 min with Oil Red O and counterstained with haematoxylin.

Modified LDL uptake

Thioglycolate-elicited peritoneal macrophages were plated on coverslips in macrophage serum-free medium (Invitrogen). After 24 h, non-adherent cells were washed off and adherent macrophages were incubated in serum-free medium complemented with 10 μg/ml native, acLDL:Dil for 4 or 24 h. Afterwards cells were washed with PBS, fixed with 4% PFA and nuclei were stained with 4,6-diamidino-2-phenylindole (DAPI). Fluorescence was analyzed with ImageJ software. Five microscopic fields were counted per experiment.

SDS–PAGE and immunoblotting

Plasma samples and cells were incubated in lysis buffer (150 mM NaCl, 50 mM Tris pH 7.4, 1 mM EDTA, 1% Triton X-100 supplemented with protease inhibitors (Roche)), homogenized in Laemmli sample buffer and boiled for 5 min. Proteins were resolved by SDS–polyacrylamide gel electrophoresis (SDS–PAGE) gels and then electrophoretically transferred from the gels onto nitrocellulose membranes, which were subsequently incubation with antibodies. Bound antibodies were detected using enhanced chemiluminescence (Millipore Corporation, Billerica, USA).

Migration assay

Migration assays were performed in 8 μm pore size chamber inserts (BD Falcon). 4×10^4 vSMCs were seeded into the chambers, which were then transferred into 24-well plates containing serum-free medium supplemented with dilutions of pFN or plasma from control and $ApoE^{-/-}FN^{MxCre}$ mice, respectively.

After an overnight incubation, the cells in the bottom part of the chamber were fixed in 4% PFA and stained with 0.2% crystal violet. Five microscopic fields per chamber were counted. Data are represented as percentage of reference cell number/field. Three independent experiments were performed, each of them in triplicate.

Adhesion assays

Adhesion assays of primary peritoneal macrophages to the endothelioma cell line bEnd5 were carried out as follows. bEnd5 cells were cultured in serum-free medium in 4-well NUNC chamber slides until confluence, either on 1 μg/ml FN or on plastic. Macrophages were isolated and co-cultured with bEnd5 cells for 6 h, either with additional FN (10 μg/ml) or without in the medium. Cells were washed with PBS, fixed with 4% PFA and stained for Mac-1. Six microscopic fields were counted per experiment.

Adhesion assays of primary peritoneal macrophages under flow conditions were carried out with bEnd5 cells. bEnd5 cells were cultured in serum-free medium or serum-free medium containing 10 μg/ml FN in a μ-Slide I $^{0.4}$ Luer (Ibidi) over night. Primary macrophages were isolated and cultured in FN-free medium or medium containing 10 μg/ml FN. Macrophages were perfused at 2.5 dyne/cm^2 at 37°C over the endothelial monolayer for 10 min. Cells were washed with PBS, fixed with 4% PFA, stained for the Mac-1 antigen and the adherent macrophages were then counted in 10 microscopic fields per experiment.

Statistical analysis

The statistical analysis was performed using the Student's-*t*-test. The values are presented as mean ± SD.

Author contributions

The study was conceived by RF. IR, KB, EM performed most experiments and analyzed them together with RF. EB, PD and JN made cholesterol measurements and OS intravital microscopy experiments. RF and EM wrote the manuscript. All authors read and approved the manuscript.

Acknowledgements

The authors thank MSc Klaus Kemmerich for excellent technical assistance. KB was supported by EMBO. The work was funded by the Deutsche Forschungsgemeinschaft (SFB-914; to OS and RF) and the Max Planck Society (to RF).

Supporting Information is available at EMBO Molecular Medicine online.

The authors declare that they have no conflict of interest.

References

Astrof S, Hynes RO (2009) Fibronectins in vascular morphogenesis. Angiogenesis 12: 165-175

Babaev VR, Porro F, Linton MF, Fazio S, Baralle FE, Muro AF (2008) Absence of regulated splicing of fibronectin EDA exon reduces atherosclerosis in mice. Atherosclerosis 197: 534-540

Barringhaus KG, Phillips JW, Thatte JS, Sanders JM, Czarnik AC, Bennett DK, Ley KF, Sarembock IJ (2004) Alpha4beta1 integrin (VLA-4) blockade attenuates both early and late leukocyte recruitment and neointimal growth following carotid injury in apolipoprotein E (−/−) mice. J. Vasc. Res. 3: 252-260

Drechsler M, Megens RT, van Zandvoort M, Weber C, Soehnlein O (2010) Hyperlipidemia-triggered neutrophilia promotes early atherosclerosis. Circulation 18: 1837-1845

Dunér P, To F, Beckmann K, Björkbacka H, Fredrikson GN, Nilsson J, Bengtsson E (2011) Immunization of apoE−/− mice with aldehyde-modified fibronectin inhibits the development of atherosclerosis. Cardiovasc. Res. 91: 528-536

Feaver RE, Gelfand BD, Wang C, Schwartz MA, Blackman BR (2010) Atheroprone hemodynamics regulate fibronectin deposition to create positive feedback that sustains endothelial inflammation. Circ. Res. 106: 1703-1711

Fredrikson GN, Söderberg I, Lindholm M, Dimayuga P, Chyu KY, Shah PK, Nilsson J (2003) Inhibition of atherosclerosis in apoE-null mice by immunization with apoB-100 peptide sequences. Arterioscler. Thromb. Vasc. Biol. 23: 879-884

Funk SD, Yurdagul AJr, Green JM, Jhaveri KA, Schwartz MA, Orr AW (2010) Matrix-specific protein kinase A signaling regulates p21-activated kinase activation by flow in endothelial cells. Circ. Res. 106: 1394-1403

George EL, Georges-Labouesse EN, Patel-King RS, Rayburn H, Hynes RO (1993) Defects in mesoderm, neural tube and vascular development in mouse embryos lacking fibronectin. Development 119: 1079-1091

Georgiades P, Ogilvy S, Duval H, Licence DR, Charnock-Jones DS, Smith SK, Print CG (2002) VavCre transgenic mice: a tool for mutagenesis in hematopoietic and endothelial lineages. Genesis 34: 251-256

Glass CK, Witztum JL (2001) Atherosclerosis: the road ahead. Cell 104: 503-516

Glukhova MA, Frid MG, Shekhonin BV, Vasilevskaya TD, Grunwald J, Saginati M, Koteliansky VE (1989) Expression of extra domain A fibronectin sequence in vascular smooth muscle cells is phenotype dependent. J. Cell Biol. 109: 357-366

Goldbourt U, Neufeld HN (1986) Genetic aspects of arteriosclerosis. Arteriosclerosis 6: 357-377

Hahn C, Schwartz MA (2008) The role of cellular adaptation to mechanical forces in atherosclerosis. Arterioscler. Thromb. Vasc. Biol. 28: 2101-2107

Hahn C, Schwartz MA (2009) Mechanotransduction in vascular physiology and atherogenesis. Nat. Rev. Mol. Cell Biol. 10: 53-62

Hahn C, Orr AW, Sanders JM, Jhaveri KA, Schwartz MA (2009) The subendothelial extracellular matrix modulates JNK activation by flow. Circ. Res. 104: 995-1003

Hynes RO (2002) Integrins: bidirectional, allosteric signaling machines. Cell 110: 673-687

Kobayashi M, Inoue K, Warabi E, Minami T, Kodama T (2005) A simple method of isolating mouse aortic endothelial cells. J. Atheroscler. Thromb. 12: 138-142

Kuhn R, Schwenk F, Aguet M, Rajewsky K (1995) Inducible gene targeting in mice. Science 269: 1427-1429

Leiss M, Beckmann K, Giros A, Costell M, Fassler R (2008) The role of integrin binding sites in fibronectin matrix assembly in vivo. Curr. Opin. Cell Biol. 20: 502-507

Libby P, Ridker PM, Hansson GK (2011) Progress and challenges in translating the biology of atherosclerosis. Nature 473: 317-325

Lusis AJ (2000) Atherosclerosis. Nature 407: 233-241

Moretti FA, Chauhan AK, Iaconcig A, Porro F, Baralle FE, Muro AF (2007) A major fraction of fibronectin present in the extracellular matrix of tissues is plasma-derived. J. Biol. Chem. 21: 28057-28062

Nakashima Y, Plump AS, Raines EW, Breslow JL, Ross R (1994) ApoE-deficient mice develop lesions of all phases of atherosclerosis throughout the arterial tree. Arterioscler. Thromb. 1: 133-140

Newby AC (2007) Metalloproteinases and vulnerable atherosclerotic plaques. Trends Cardiovasc. Med. 17: 253-258

Newby AC, Zaltsman AB (1999) Fibrous cap formation or destruction–the critical importance of vascular smooth muscle cell proliferation, migration and matrix formation. Cardiovasc. Res. 41: 345-360

Newby AC, George SJ, Ismail Y, Johnson JL, Sala-Newby GB, Thomas AC (2009) Vulnerable atherosclerotic plaque metalloproteinases and foam cell phenotypes. Thromb. Haemost. 101: 1006-1011

Ni H, Yuen PS, Papalia JM, Trevithick JE, Sakai T, Fässler R, Hynes RO, Wagner DD (2003) Plasma fibronectin promotes thrombus growth and stability in injured arterioles. Proc. Natl. Acad. Sci. 100: 2415-2419

Oh E, Pierschbacher M, Ruoslahti E (1981) Deposition of plasma fibronectin in tissues. Proc. Natl. Acad. Sci. 78: 3218-3221

Orem C, Durmuş I, Kilinç K, Baykan M, Gökçe M, Orem A, Topbaş M (2003) Plasma fibronectin level and its association with coronary artery disease and carotid intima-media thickness. Coron. Artery Dis. 14: 219-224

Orr AW, Sanders JM, Bevard M, Coleman E, Sarembock IJ, Schwartz MA (2005) The subendothelial extracellular matrix modulates NF-kappaB activation by flow: a potential role in atherosclerosis. J. Cell Biol. 169: 191-202

Orr AW, Ginsberg MH, Shattil SJ, Deckmyn H, Schwartz MA (2006) Matrix-specific suppression of integrin activation in shear stress signaling. Mol. Biol. Cell 11: 4686-4697

Orr AW, Stockton R, Simmers MB, Sanders JM, Sarembock IJ, Blackman BR, Schwartz MA (2007) Matrix-specific p21-activated kinase activation regulates vascular permeability in atherogenesis. J. Cell Biol. 176: 719-727

Orr AW, Hahn C, Blackman BR, Schwartz MA (2008) p21-activated kinase signaling regulates oxidant-dependent NF-kappa B activation by flow. Circ. Res. 103: 671-679

Ozcelik F, Erdogan O, Aktoz M, Ekuklu G, Tatli E, Demir M (2009) Diagnostic value of plasma fibronectin level in predicting the presence and severity of coronary artery disease. Ann. Hematol. 88: 249-253

Sakai T, Johnson KJ, Murozono M, Sakai K, Magnuson MA, Wieloch T, Cronberg T, Isshiki A, Erickson HP, Fässler R (2001) Plasma fibronectin supports neuronal survival and reduces brain injury following transient focal cerebral ischemia but is not essential for skin-wound healing and hemostasis. Nat. Med. 7: 324-330

Schneider A, Zhang Y, Guan Y, Davis LS, Breyer MD (2003) Differential, inducible gene targeting in renal epithelia, vascular endothelium, and viscera of Mx1Cre mice. Am. J. Physiol. Renal Physiol. 284: 411-417

Song KS, Kim HK, Shim W, Jee SH (2001) Plasma fibronectin levels in ischemic heart disease. Atherosclerosis 154: 449-453

Steiner O, Coisne C, Engelhardt B, Lyck R (2010) Comparison of immortalized bEnd5 and primary mouse brain microvascular endothelial cells as in vitro blood–brain barrier models for the study of T cell extravasation. J. Cereb. Blood Flow Metab. 31: 315-327

Tan MH, Sun Z, Opitz SL, Schmidt TE, Peters JH, George EL (2004) Deletion of the alternatively spliced fibronectin EIIIA domain in mice reduces atherosclerosis. Blood 104: 11-18

Tzanatos HA, Tseke PP, Pipili C, Retsa K, Skoutelis G, Grapsa E (2009) Cardiovascular risk factors in non-diabetic hemodialysis patients: a comparative study. Ren. Fail. 31: 91-97

Tzima E, Del Pozo MA, Kiosses WB, Mohamed SA, Li S, Chien S, Schwartz MA (2002) Activation of Rac1 by shear stress in endothelial cells mediates both cytoskeletal reorganization and effects on gene expression. EMBO J. 24: 6791-6800

Vavalle JP, Wu SS, Hughey R, Madamanchi NR, Stouffer GA (2007) Plasma fibronectin levels and coronary artery disease. J. Thromb. Haemost. 4: 864-866

White ES, Baralle FE, Muro AF (2009) New insights into form and function of fibronectin splice variants. J. Pathol. 216: 1-14

Woollard KJ, Geissmann F (2010) Monocytes in atherosclerosis: subsets and functions. Nat. Rev. Cardiol. 7: 77-86

Zhang Y, Zhou X, Krepinsky JC, Wang C, Segbo J, Zheng F (2006) Association study between fibronectin and coronary heart disease. Clin. Chem. Lab. Med. 44: 37-42

Supplementary information:

Supplemental figure 1. Reduced incidence of atherosclerosis in ApoE$^{-/-}$FN^{MxCre} mice.

Supplemental figure 2. Normal levels of VCAM-1 and $\alpha4\beta1$ in ApoE$^{-/-}$FN^{MxCre} mice.

Supplemental figure 3. Monocyte/macrophages from ApoE$^{-/-}$FN^{MxCre} mice.

Supplemental figure 4. Atherosclerotic lesions of ApoE$^{-/-}$FN^{MxCre} mice lack fibrous caps.

Supplemental figure 1

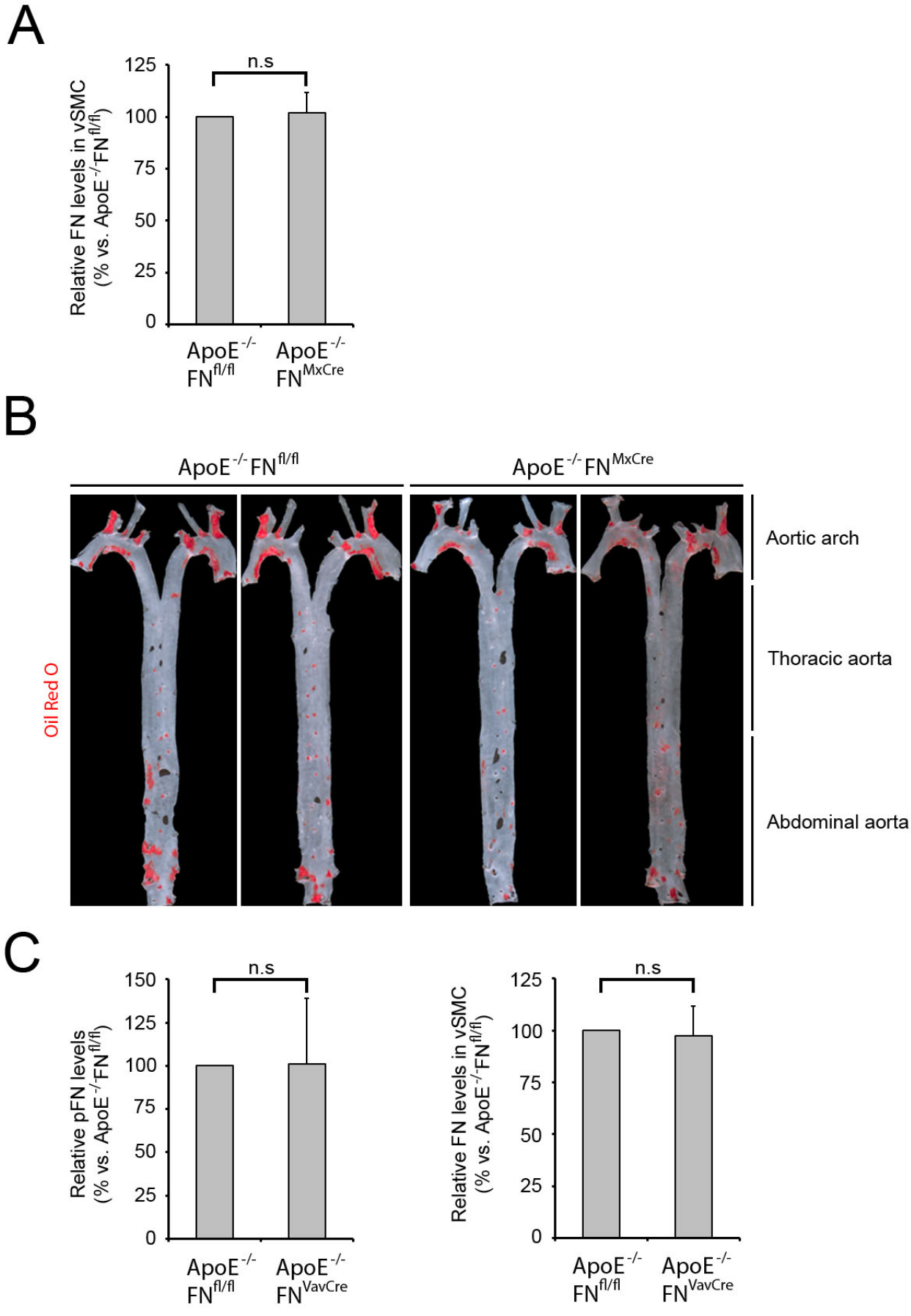

Supplemental figure 2

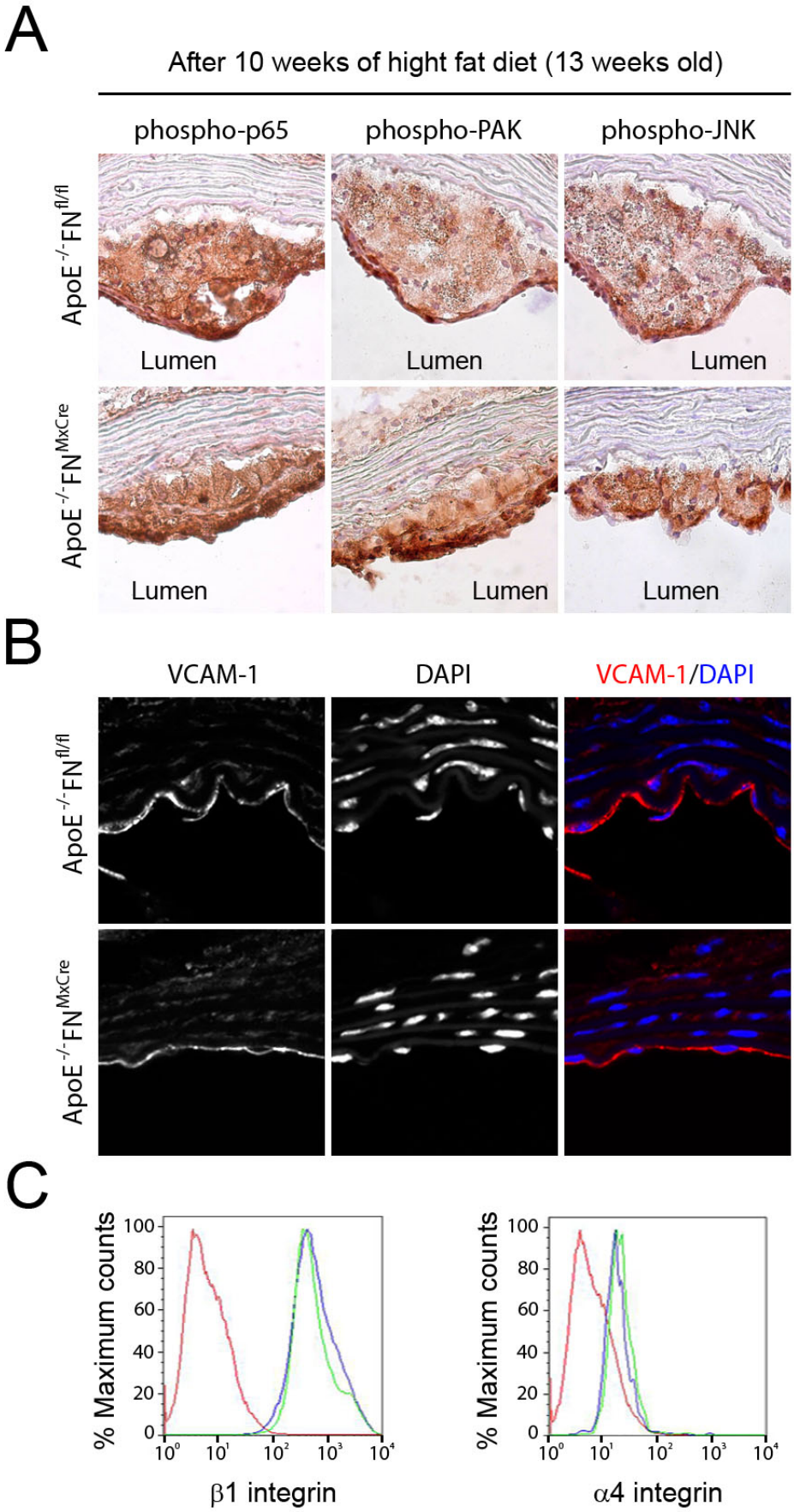

Supplemental figure 3

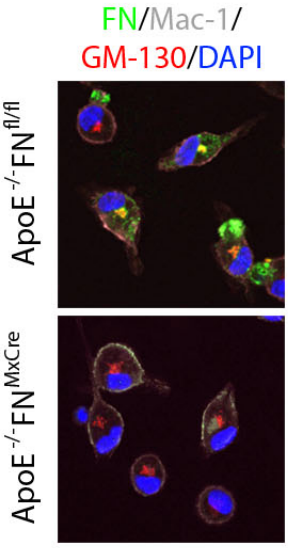

Supplemental figure 4

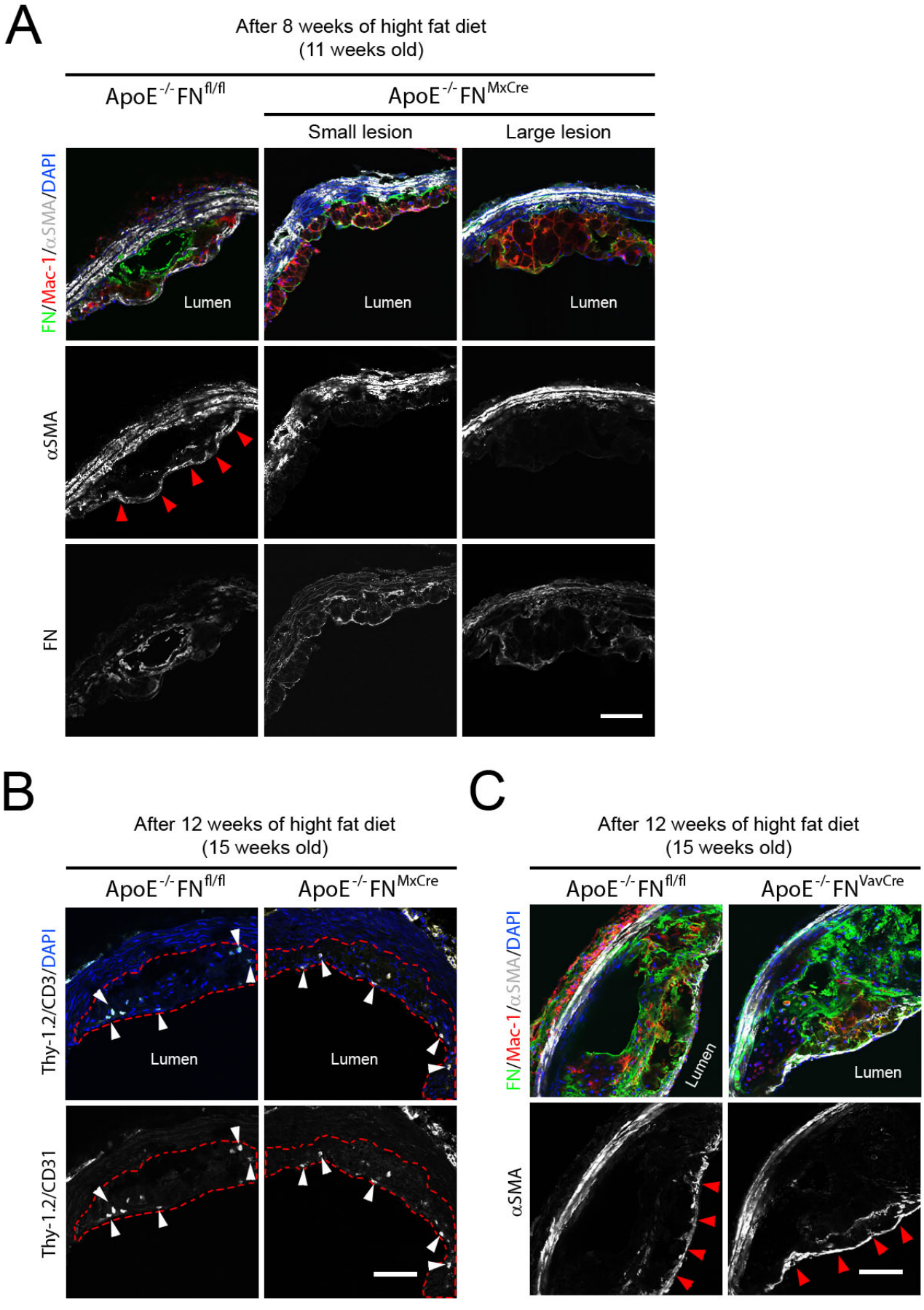

Supplemental figures

Supplemental figure 1. Reduced incidence of atherosclerosis in ApoE$^{-/-}$FN^{MxCre} mice

(A) Quantification of relative FN levels in vSMC lysates from ApoE$^{-/-}$FN$^{fl/fl}$ and ApoE$^{-/-}$FN^{MxCre} mice. Values are percentage ± SD; n.s.=not significant. (B) Whole-mount of longitudinally opened aortas from ApoE$^{-/-}$FN$^{fl/fl}$ and ApoE$^{-/-}$FN^{MxCre} mice stained with Oil red O after 12 weeks on a high-fat diet. (C) Quantification of relative FN levels vSMC lysates and in plasma from ApoE$^{-/-}$FN$^{fl/fl}$ and ApoE$^{-/-}$FN^{VavCre} mice. Values are percentage ± SD; n.s.=not significant.

Supplemental figure 2. Normal levels of VCAM-1 and α4β1 in ApoE$^{-/-}$FN^{MxCre} mice

(A) Immunostaining of phosho-NFκB/p65, phospho-PAK and phospho-JNK in the lesser curvature of the aortic arch from ApoE$^{-/-}$FN$^{fl/fl}$ and ApoE$^{-/-}$FN^{MxCre} mice fed with high fat diet for 10 weeks. (B) Immunostaining of VCAM-1 in the lesser curvature of the aortic arch from ApoE$^{-/-}$FN$^{fl/fl}$ and ApoE$^{-/-}$FN^{MxCre} mice. Nucleus was visualized with DAPI. (C) Integrin surface expression in monocytes from ApoE$^{-/-}$FN$^{fl/fl}$ (green) and ApoE$^{-/-}$FN^{MxCre} (blue) mice. A background control is shown in red.

Supplemental figure 3. Monocyte/macrophages from ApoE$^{-/-}$FN^{MxCre} mice

Immunostaining of freshly isolated peritoneal monocyte/macrophages from control and ApoE$^{-/-}$FN^{MxCre} mice for FN, GM-130 and Mac-1.

Supplemental figure 4. Atherosclerotic lesions of ApoE$^{-/-}$FN^{MxCre} mice lack fibrous caps

(A) Immunostaining of atherosclerotic plaques of control and ApoE$^{-/-}$FN^{MxCre} mice 8 weeks after a high-fat diet for FN, Mac-1 and αSMA. Arrowheads point to αSMA immunosignals in the fibrous cap. Nucleiare visualized with DAPI. (B) Immunostaining of atherosclerotic plaques of control and ApoE$^{-/-}$FN^{MxCre} mice 12 weeks after a high fat diet with Thy-1.2/CD3 antibodies (white arrowheads). Red dotted line displays plaque surface. Nuclei are visualized with DAPI (blue). (C) Immunostaining of atherosclerotic plaques of control and ApoE$^{-/-}$FN^{VavCre} mice 12 weeks after a high fat diet with antibodies against FN, Mac-1 and αSMA. Arrowheads point to αSMA immunosignals in the fibrous cap. Nuclei are visualized with DAPI. Scale bar represents 75μm in all images.

Publication 2 (in preparation)

α-Parvin controls contraction and actin organization in smooth muscle cells

published as

Rohwedder I; Tolde O; Zent R; Fässler R: ***α-Parvin controls contraction and actin organization in smooth muscle cells.*** Manuscript in preparation

α-Parvin controls contraction and actin organization in smooth muscle cells

Rohwedder I. [1]; Tolde O. [1]; Zent R. [2]; Fässler R. [1]

[1]Department of Molecular Medicine, Max-Planck Institute of Biochemistry, 82152 Martinsried, Germany;

[2] Vanderbilt Medical Center, Nashville, USA

Running title: Vessel stability depends on α-parvin in vascular smooth muscle cells

Key Words: vasculature, vSMC , integrin, parvin, contraction

Corresponding author: Reinhard Fässler (faessler@biochem.mpg.de)

ABSTRACT

α-parvin (αpv) is a focal adhesion (FA) protein that has been shown to be essential for blood vessel maturation during mouse development by regulating RhoA/ROCK signaling in vascular smooth muscle cells (vSMC). Here we report that a conditional deletion of the *αPv* gene in SMCs leads to lethality in mice around 4 weeks of age. The vasculature of mutant mice displays severe defects in the organization of the smooth muscle layer and spreading of single vSMC leading to dilations and aneurysm development in the aorta. Vessels are insufficiently covered by vSMCs and elastic fibers are degraded. In addition, the mutant mice suffer from intestinal pseudoobstruction and glomerulosclerosis in their kidneys. Deleting αpv from adult mice with an inducible knockout strategy leads to the death of homozygous mice 4-6 weeks after Cre induction, due to intestinal defects after the loss of αpv in the intestinal smooth muscle cell (iSMC) layer. Isolated primary vSMC and iSMC display a hypercontractile phenotype and fail to spread and polarize their cytoskeleton. We show that the loss of αpv in vSMC leads to higher activation of Myosin II, as well as elevated levels of MMP expression and matrix degradation. Our findings identify αpv as a key component for vessel integrity and a regulator of vSMC organization and contractility.

INTRODUCTION

The contractility of smooth muscle cells is important for maintaining organ function, including the regulation of the vascular tone, the motility of the gastrointestinal (GI) tract and the emptying of the bladder. Mural cells are one of these highly specialized cells that are associated to vessels, where they are of great importance for vascular maturation in development as well as for vessel maintenance in adult organism.

During embryogenesis, the formation of a mature vascular network involves three major steps. During vasculogenises the first vascular tubes are built *de novo* from angioblasts, which differentiate into endothelial cells (EC) and form the first primitive vascular plexus. In a second step angiogenesis is occurring, which defines the reorganization of this network and involves sprouting of new vessels from pre-existing ones (Risau et al. 1997). Vascular maturation as the final step involves the arterio-venous determination, the recruitment of mural cells and the development of the surrounding extracellular matrix (ECM) and elastic laminae (Jain et al. 2003). Mural cells are mostly derived from the mesenchyme (Beck and D'Amore 1997) and can be subdivided into two groups: pericytes (PC) and vascular smooth muscle cells (vSMC). PCs cover capillaries, small venules and immature vessels, where they contact the EC layer and enclosed by a basement membrane (BM). vSMC are associated with mature and larger blood vessels, where concentric layers of vSMC, ECM and elastin fibers are forming around the EC tube to resist shear stress and pulsatile flow. Mural cells are essential for blood vessel function, as they provide the required stability for the vessels to withstand blood pressure, to control EC proliferation and also to control the vascular tone with their ability to contract the vessels (Adams and Alitalo 2007).

PC/vSMCs are attracted to immature vessels by growth factors like PDGF-B (Lindahl et al.1997) and Ang 1 (Suri et al. 1996) and their migration from the mesenchyme highly dependent on ECM molecules and their receptors, the integrins. Integrins are heterodimeric transmembrane receptors, consisting of one α and one β subunit. With their extracellular domain, these receptors bind ECM molecules, subsequently cluster and form focal adhesions (FA), thereby stabilizing their adhesion to the ECM. With their intracellular tail these proteins bind adaptor and signaling proteins, which are important for maintaining cell shape (Hynes et al.2002, Legate et al. 2009). It has been shown in several *in vitro* and *in vivo* studies, that integrin mediated adhesion is crucial for vasculogenesis and vessel maturation. Angiogenesis defects and vessel malformations have been observed upon deletion of integrin α4 and α5 and the EC specific ablation of integrin β1 (Carlson et al. 2008, Malan et al. 2010, Grazioli et al. 2006, Francis et al. 2002). Likewise, ablation of extracellular ligands of integrins such as fibronectin (FN) (George et al. 1993), the laminin (LN) α4 chain (Thyboll et al. 2002) or collagen IV (Col IV) (Pöschl et al. 2004) lead to severe vascular phenotypes. Misregulation of ECM composition is associated with phenotypic switching of vSMC to a less contractile and more proliferative phenotype (Berk et al. 2001), which is associated with vessel abnormalities like aneurysm formation (Cheuk et al. 2004) and atherosclerosis (Owens et al. 2004). Also other smooth muscle tissues are strongly dependent of integrin signaling. For example, laminin α5 seems to be important for the proper development of intestinal musculature (Bolcato-Bellemin et al. 2003). Various publications also show that integrin-ECM interactions are important for the functional properties of mesangial cells (MC) in kidney glomeruli (Pröls et al. 1999).

The intracellular tail of integrins is short and without enzymatic activity. In order to regulate complex actions as adhesion and migration, integrins need to recruit kinases like FAK and Src or adaptor molecules like integrin-linked kinase (ILK), which is directly recruited to integrin β1 or β3 tails. ILK has N-terminal ankyrin repeats through which ILK binds PINCH1 and 2. With the C-terminal kinase-like domain ILK can bind to α-, β-, or γ-parvin. ILK, PINCH and parvin forms a protein complex (IPP-complex) that is assembled in the cytosol and is recruited to the FA upon assembly (Zhang et al. 2002). Deletion studies with each of these proteins have shown that the stability of the IPP complex is critically dependent on the presence of all three proteins, as it otherwise results in a proteasomal downregulation of the remaining partners (Fukuda et al. 2003). The parvins are a family of adaptor proteins which include an actin binding domain (ABD) consisting of two tandemly arranged calponin homology (CH) domains. Through this ABD, parvin can link the actin cytoskeleton to FAs and together with additional regulatory binding partners like Paxillin, Hic5 and α-actinin regulate cell adhesion, migration and cell survival (Legate et al. 2006). The three parvin family members are differently expressed in vertrebrate tissue: α-parvin/affixin/CH-ILKBP (αpv) is ubiquitously expressed, β-parvin (βpv) is enriched in heart and skeletal muscle and the expression of γ-parvin (γpv) is restricted to the hematopoietic system (Chu et al. 2006)].

The vascular tone, the peristaltic contraction of the intestine and the regulation of ultrafiltration of the urine in kidney glomeruli are performed by contracting α-smooth muscle actin (αSMA) filaments, an actin isoform which is unique for SMC. This contraction and relaxation of SMCs is regulated by phosphorylation of myosin light chain (MLC).This is mainly mediated by the myosin light chain kinase (MLCK) and can be reversed by dephosphorylation of MLC, which is achieved by myosin light chain phosphatase (MLCP). The RhoA effector ROCK can also directly phosphorylate MLC, but it mainly phosphorylates the myosin phosphatase target subunit 1 (MYPT1) and thus prevents the dephosphorylation of MLC by dislocating MLCP from MLC (Murthy et al. 2006).While normal RhoA/ROCK signaling is crucial for maintaining blood pressure, stabilizing vessels and also intestinal peristaltic, misregulation of this signaling in vSMC and other SMC in either direction is often leading to pathological conditions like hypertension (Mukai et al. 2001) and gut motility disorders (Rattan et al. 2010).

Genetic ablation of β1 integrin and its intracellular binding partner ILK in vSMCs results in late embryonic lethality (Abraham et al. 2008, Kogata et al. 2009) with strong vascular phenotypes. In both mouse models, vessels were dilated and poorly covered with MCs. Isolated vSMCs displayed spreading defects and in the case of ILK depleted vSMC a high RhoA / ROCK activity results in hypercontractility of vSMC. It was shown that the constitutive deletion of αpv in mice leads to embryonic lethality due to severe cardiovascular defects (Montanez et al. 2009).Homozygous embryos died between E10.5 to E14.5 and showed defective vSMC coverage of vessels and heart deformations. While EC were normally arranged and showed no abnormalities in culture, vSMC displayed a hypercontractile phenotype, increased RhoA /ROCK signaling with higher phosphorylation of MLC2. This suggested a role for αpv in vSMC recruitment as a negative regulator of RhoA/ROCK signaling in vSMC. To address the specific role of αpv in SMC, we generated αpv fl/fl mice and used tissue-specific (PDGFRβ-Cre) and inducible Cre (SMMHC-Cre-ER(T2)) lines to delete apv in SMCs. We show that deletion of αpv at embryonic age resulted in lethality of homozygous animals at the age of 4 weeks. Mice had dilated vessels with

aneurysm formation and defective vSMC coverage. Intestines of these mice showed symptoms of intestinal pseudoobstruction and in kidneys defective glomeruli were observed. Tamoxifen induced αpv deletion in adult mice led to death 4-6 weeks after induction. Mice developed pseudoobstruction and intestinal smooth muscle cell (iSMC) layer showed comparable signs of disorganization as for αpv deficient vSMC in vessels. *In vitro* isolated primary vSMC were hypercontractile, unpolarized and displayed elevated levels of pMLC2. Protein levels of ILK and PINCH were markedly reduced. In addition we show that αpv deletion in vSMCs resulted in higher expression of MMP9, but not in MMP2 along with stronger substrate degradation in *in vitro* experiments. This indicates that αpv deletion in vSMC leads to vessel destabilization in two independent ways: by disturbing vSMC alignement on the vessel and by promoting degradation of elastic fibres.

RESULTS

PDGFRβCre induced loss of αpv results in severe vascular, intestinal and renal defects

To analyze the specific function of αpv in vSMC we deleted the *αPv* gene conditionally in vSMC by intercrossing αpv fl/fl mice with mice expressing Cre-recombinase under the PDGFRβ promotor (PDGFRβCre). PDGFRβCre expressing control mice (αpv fl/+ PDGFRβCre) and knockout (αpv fl/fl PDGFRβCre) mice were born with a normal Mendelian ratio (data not shown) and were phenotypically normal until postnatal day (P) 21. Strikingly, at P30 αpv fl/fl PDGFRβCre mice became significantly smaller and lighter than their αpv fl/+ PDGFRβCre littermates and showed various signs of sickness like red skin, cramped posture, diarrhea and a bloated lower abdomen (Fig. 1A, B). First death of mutant mice was observed 18 days after birth and only 10% survived until P42 (Fig 1C). Heterozygous αpv fl/+ PDGFRβCre mice were vital and fertile. Aortas of αpv fl/fl PDGFRβCre mice displayed abdominal aortic aneurysms (AAA), visible already at P1 (Fig. 1D). Although aneurysms gained in diameter over time and thrombotic plaques were visible at the common iliac artery, no rupture of the aorta was detected. In smaller vessels dilations as well as bleedings were observed (data not shown). Frequently a persistent ductus arteriosus could be observed in αpv fl/fl PDGFRβCre mice at P30 (Fig. 1E). Additionally to vascular defects, the dissection of the gut of αpv fl/fl PDGFRβCre and αpv fl/+ PDGFRβCre mice revealed an extreme dilated food and gas filled caecum and colon after PDGFRβCre induced αpv deletion (Fig 1F), which are common symptoms of a paralytic ileus. In this case, symptoms mimic intestinal obstruction without physical blockage of the intestine. Interestingly, gross histological examination of kidney sections revealed, that PDGFRβCre induced deletion of αpv leads to cyst formation in the collecting ducts of the kidney in homozygous mutants (Fig. S1A).

SMC defects in vasculature and intestine of αpv fl/fl PDGFRβCre mice

To closer examine the vasculature in αpv fl/fl PDGFRβCre mice we performed whole mount immunostaining of ear vessels as well as of aorta using antibodies against αSMA and CD31/PECAM to visualize endothelial cells. As expected, CD31 staining showed no abnormalities in the EC layer of αpv fl/fl PDGFRβCre vessels, but αSMA gave only a punctuate staining and revealed a reduced coverage of vessels with vSMC (Fig. 2A). vSMC adherent to the EC layer were round and not stretched around the vessel (Fig. 2A middle row). Whole mounts immunostaining of αpv fl/fl PDGFRβCre aortas for αSMA showed an equivalent staining pattern for vSMC (Fig. 2A right row). Most vSMC were poorly spread and lacked the normal alignment with neighboring cells as observed in αpv fl/+ PDGFRβCre aortas, where cells aligned into parallel sheets perpendicular to the blood stream. This inhomogeneous distribution and the round cell shape suggest an insufficient support of the vasculature.

Immunostainings for αpv on aorta sections confirmed the loss of αpv in the vSMC layer of αpv fl/fl PDGFRβCre vessels (Fig. 2B). At higher magnification a round morphology of vSMC was detected. Interestingly, also HE staining of colon sections showed an unorganized layering of iSMC in the muscularis externa of αpv fl/fl PDGFRβCre mice characterized by an insufficient separation of circular and longitudinal smooth muscle (Fig. S1B). Immunostaining of these sections for the presence of αpv

produced a positive signal in the muscularis externa of αpv fl/+ PDGFRβCre mice but not in αpv fl/fl PDGFRβCre mice, indicating, that the PDGFRβCre-mediated deletion is also targeting iSMC.
To analyze the defect in vSMC *in vitro* we isolated primary vSMC from aorta. Although no differences were observed in adhesion of αpv fl/fl PDGFRβCre vSMC to FN-coated dishes (data not shown), these cells failed to spread within 4h of plaiting and remained in a round shape compared to the elongated αpv fl/+ PDGFRβCre vSMC (Fig. 2C). Immunostaing of primary αpv fl/fl PDGFRβCre vSMC for αpv confirmed the absence of αpv protein. αSMA staining revealed a different morphology of the actin cytoskeleton, with strong cortical actin fibers and a lack of the characteristic long stress fibers of vSMC as seen in αpv fl/+ PDGFRβCre vSMC. In addition, loss of αpv was confirmed by western blot analysis (Fig. 2D). Importantly, βpv was neither expressed nor upregulated in vSMC isolated from aorta of αpv fl/fl PDGFRβCre mice, and the levels of ILK and PINCH were reduced. Immunostainings of αpv deficient vSMC using antibodies against ILK and PINCH1 confirmed the absence of ILK and PINCH1 in FAs (Fig. 2E).

Loss of αpv in the mesangium results in glomerulus breakdown and interstitial fibrosis

PDGFRβ is strongly expressed on vSMC and therefore commonly used for conditional deletion approaches in the SMC layer of vessels. Beside vSMC also MC are highly dependent on PDGF/PDGFRβ signaling (Arar et al. 2000). These highly specific αSMA expressing cells are localized in the mesangium of kidney glomeruli and regulate the blood flow through the capillaries with their contractile abilities (Schlöndorff et al. 1987). A detailed examination of Hematoxilin & Eosin (HE) stained kidney sections revealed defective structure of glomeruli in αpv fl/fl PDGFRβCre mice (Fig. S1C). At higher magnification areas of hypercellularity as well as acellular areas and ECM accumulation can be seen. Immunostaining using antibodies against αpv and αSMA of kidney sections showed absence of αpv from glomeruli of αpv fl/fl PDGFRβCre mice in combination with a higher density of αSMA positive cells. αSMA is a widely accepted marker for myofibroblast formation in the glomerulus, which is regarded as an indication of glomerulosclerosis and nephritis. Further evidence for a decreased function of glomeruli is the secretion of protein such as albumin, into the urine of αpv fl/fl PDGFRβCre mice (Fig. S1D). In addition, we show areas in the kidney interstitium with high αSMA and colocalizing vimentin expression (Fig. S1E) indicating the formation of fibrotic tissue in the collecting ducts as a secondary effect of glomerulosclerosis.
Next, we performed blood sample analysis of αpv fl/fl PDGFRβCre mice and found evidence for acute (high levels of neutrophils) and chronic (high monocyte count) inflammation (Fig. S1F). This, together with the low red blood cell count and the resulting anemia in αpv fl/fl PDGFRβCre mice (Fig. S1G), is indicative for an inflammatory response by the kidney. Taken together we showed that PDGFRβCre mediated deletion of αpv is leading to glomerular destabilization resulting in proteinurea, tissue scarring and inflammation.

AAA formation in αpv fl/fl PDGFRβCre mice is accompanied by matrix degradation

We could show that αpv deficiency in vSMC results in the formation of abdomical aortic aneurysms (AAA). HE staining of aorta sections displayed dramatic derangements in the structure of the tunica media in αpv fl/fl PDGFRβCre aortas compared to αpv fl/+ PDGFRβCre aortas (Fig. S2A). vSMC layers

were disconnected and gaps suggested areas of cell loss or matrix degradation. In addition, the Verhoeff van Gieson (VVG) staining of aorta sections showed a strongly reduced black staining and therefore disrupted lamina fibers typical for AAA. Besides an increased vessel wall diameter and a reduced SMC density, infiltration of monocytes is a characteristic feature of AAA formation. We therefore immune-stained aorta sections for the presence of monocytes, using an antibody against Mac-1. While there were no Mac-1 positve cells in αpv fl/+ PDGFRβCre sections numerous positive signals, were observed in sections of αpv fl/fl PDGFRβCre aortas (Fig. S2B), indicating the presence of monocytes in the vessel wall of αpv fl/fl PDGFRβCre mice. Both, monocytes and vSMC are sources of matrix metalloproteinases (MMP) that can degrade ECM molecules. To test matrix degradation we performed *in situ* zymography with DQ-Gelatin on fresh aorta cryosections. A positive degradation signal distributed over all cells of the tunica media was only obtained in sections from αpv fl/fl PDGFRβCre mice (Fig. S2B). This indicates that not only monocytes are a source of MMPs but also αpv-deficient vSMC show high MMP expression. In agreement with this finding we also found a slightly stronger degradation signal in αpv fl/fl PDGFRβCre vSMC plated on DQ-Gelatin compared to αpv fl/+ PDGFRβCre vSMC (Fig. S2C). Because this method does not allow a distinction between the different MMPs that are involved in gelatin degradation, we additionally performed gelatin and casein zymography with primary vSMC lysates (Fig. S2D). Gelatin as well as casein zymography with vSMC lysates, isolated from αpv fl/fl PDGFRβCre mice gave a significantly stronger degradation signal than cells isolated from αpv fl/+ PDGFRβCre mice. A prominent band of around 100kDa was detected for MMP9 in gelatin gels and of 57 kDa for MMP12 in casein gels. In agreement with these findings we observed an upregulation for MMP9 as well as latent MMP1 protein levels in vSMC lysates of αpv fl/fl PDGFRβCre mice (Fig. S2E). Interestingly, MT1-MMP levels as well as their target MMP2 were not changed when compared to αpv fl/+ PDGFRβCre vSMC lysates. Taken together we show that deletion of αpv in vSMC leads to upregulated MMP expression by vSMC, invasion of monocytes and finally results in ECM degradation and AAA formation.

Inducible deletion of αpv results in smooth muscle defects in the GI tract

It was shown by previous publications (Montanez et al. 2009) and in this study, that αpv is playing a critical role in development of a mature vasculature, kidneys and GI tract. The function for αpv in SMC of the adult organism is unclear. We therefore intercrossed the αpv fl/fl mice with mice expressing a fusion protein of the Cre recombinase with the modified estrogen receptor binding domain ($CreER^{T2}$) under the control of the smooth muscle myosin heavy chain (SMMHC) promoter. Intraperitoneal injection of Tamoxifen induced deletion of αpv. Mice, expressing the SMMHC-$CreER^{T2}$ were phenotypically normal until day 30 to 35 after Tamoxifen induction, but then rapidly lost weight, developed a bloated abdomen and finally died 32-37 days after induction (Fig. 3A). No changes were observed in αpv fl/fl mice after Tamoxifen treatment, excluding Tamoxifen related toxiticity as a reason for lethality. Dissection of the GI tract of αpv fl/fl SMMHC-$CreER^{T2}$ mice revealed an extreme dilation of the small intestine and necrosis, suggesting that the loss of αpv in iSMC alters the motility of the GI tract and mice die from starvation (Fig. 3B). Whole mount immunostaining of small intestine for αSMA revealed a disorganized SMC layer with round iSMCs (Fig. S3A). HE staining of small intestine sections of αpv fl/fl SMMHC-$CreER^{T2}$ confirmed the disorganization of the iSMC layer, a closeup revealed mostly round cells (Fig. 3C).

Immunostainings of these sections confirmed the absence of αpv in the small intestine of αpv fl/fl SMMHC-CreER^{T2} mice after Tamoxifen induction. With immunostaining against Mac-1 we could demonstrate the presence of monocytes in the small intestine of αpv fl/fl SMMHC-CreER^{T2} mice, indicative of an inflammatory process taking place in the mutant intestine (Fig. S3B). Comparable to the phenotype of the aorta in αpv fl/fl PDGFRβCre mice, also in the intestine of αpv fl/fl SMMHC-CreER^{T2} mice a high proteolytic activity could be detected by i*n situ* zymography. Also higher levels of apoptotic cells were visible by TUNEL staining compared to αpv fl/fl mice.
A milder version of the observed intestinal phenotype was also visible in the SMC layer of the stomach (Fig. S3C). Although macroscopically no defects could be seen, in HE staining of stomach sections of αpv fl/fl SMMHC-CreER^{T2} mice we observed round and loosely connected SMC in αpv fl/fl mice.
Interestingly, no abnormalities were visible in the vasculature of αpv fl/fl SMMHC-CreER^{T2} mice, although αpv was absent from vSMC after Tamoxifen induction (data not shown). The vessel diameter of the aorta was unchanged and also a closer analysis of HE-stained sections revealed no defects comparable to αpv fl/fl PDGFRβCre aortas (Fig. S3D). vSMC were elongated and aligned, the elastic fibers were of normal thickness and not interrupted.
Since the most prominent defect in these mice was found in intestines, we isolated primary iSMC from small intestine of αpv fl/fl SMMHC-CreER^{T2} and αpv fl/fl mice. While αpv fl/fl iSMC had the typical stretched and elongated morphology of SMC, cultured iSMC from αpv fl/fl SMMHC-CreER^{T2} mice displayed a round phenotype, similar like in primary vSMC of αpv fl/fl PDGFRβCre mice (Fig. 3D). With immunostaining against αpv and αSMA we could confirm the deletion of αpv and an abrerrant reorganization of the actin cytoskeleton and the formation of multiple membrane protrusions. Loss of αpv was additionally confirmed by western blot analysis of iSMC lysate (Fig. 3E). PINCH1 levels were significantly reduced in αpv fl/fl SMMHC-CreER^{T2} iSMC, while ILK levels remained almost unchanged. Taken together we could demonstrate that αpv is of critical importance for the structure and functionality of iSMC in adult mice.

αpv deletion leads to hypercontractility in primary vSMC

Deletion of αpv in vSMC was shown to result in a hypercontractile phenotype and elevated RhoA and pMLC2 levels (Montanez et al. 2009). Likewise, the vSMC specific ILK-deletion resulted in an increased RhoA/ ROCK signaling (Kogata et al. 2009)]. We therefore analyzed the pMLC2 levels and distribution in primary vSMC from αpv fl/fl PDGFRβCre mice. Immunostainings against pMLC2 in primary αpv fl/+ PDGFRβCre vSMC showed a typical strong colocalization to actin stress fibers, whereas in αpv fl/fl PDGFRβCre vSMC pMLC2 localized to thick cortical actin bundles and no colocalization with stress fibers could be seen (Fig. 4A). Western blot analysis of pMLC2 protein levels in αpv fl/fl PDGFRβCre vSMC lysate showed a strong upregulation of pMLC2 levels compared to αpv fl/+ PDGFRβCre vSMC (Fig. 4B), while total MLC2 remained unchanged. This supports earlier findings showing that αpv regulates cell contractility in vSMC. Due to the fast dedifferenciation of cultured vSMC, we isolated SMC from the ureter (UC) of E14.5 αpv fl/fl animals and performed adenoviral Cre transduction to obtain αpv -/- cells. Two morphologically different subclones of αpv -/- cells (361 and 361) were used for further analysis. Prior to analyzing contractility we performed immunostainings against αSMA and αpv to characterize the phenotype of αpv -/- UC (Fig. S4A upper row). Loss of αpv led in both clones to significantly smaller

cells and strong cortical actin fibers. αpv -/- 361 UC tend to form colonies, while αpv -/- 369 cells remain singular. Along with the loss of αpv, also the localization of ILK and PINCH1 to FAs was lost (Fig. S4A lower row). Similarly, Western blot analysis showed a strong decrease of ILK and PINCH1 protein levels in the absence of αpv (Fig. S4B). Because of their phenotypic similarity to vSMC, we used immortalized UC for further biochemical studies including the analysis of αpv regulated contractility. In αpv fl/fl UC immunostainings the pMLC2 signal colocalized to the αSMA signal (Fig. 4C), while in both αpv -/- clones pMLC localized stronger to cortical actin bundles. In αpv -/- 361 UC pMLC2 signal orientated towards the outer borders of the cell colonies, whereas cell-cell connections remained pMLC2 free. In contrast to vSMC, UC did not show an αpv dependent regulation of MLC phosphorylation, since pMLC2 protein levels in αpv -/- UC remained unchanged compared to αpv fl/fl UC (Fig. 4D). Another method of quantifying pMLC2 intensity is by seeding cells on FN coated micropatterns. As the pattern itself is surrounded by PEG, cell spreading is restricted to the FN-coated shape which also reduces the variability of pMLC2 signal intensity due to absent size and shape differences between cells. For our assay we used umbrella shaped patterns which leads to cell contraction at the two legs of the pattern, while the upper part mimics the leading edge of cells and lamellopodia formation. In line with our observation on pMLC2 protein levels, we could not detect a clear upregulation of pMLC2 intensity in both UC αpv -/- clones (Fig. 4E). In αpv -/- 361 UC pMLC2 levels even seemed to be slightly downregulated. This suggests that although these cells phenotypically look like primary αpv deleted vSMC, the underlying molecular mechanisms leading to cell rounding are different.

Since the PDGFRβCre induced deletion of αpv is resulting in a destabilization of glomeruli we chose MC as a third cellular model for αpv related cell function. Unexpectedly αpv deletion in MC led only to a very mild spreading defect (data not shown) and immunostaining on normal 2D culture using antibodies against αSMA and pMLC2 showed no differences in cytoskeleton organization or in pMLC2 intensity and localization (Fig. S4C). Consistent with our previous findings in vSMC and UC, we could show that protein levels of ILK and PINCH1 in αpv -/- MC were significantly downregulated compared to αpv fl/fl MC (Fig. S4D). Surprisingly, this loss of the IPP complex was not causing dramatic changes in cell morphology. Also more detailed analysis of MC seeded on micropatterns revealed no significant differences in pMLC2 intensity (Fig. S4E), leading to the conclusion that despite the close relationship with SMC, their functionality seems not to be dependent on αpv and defects in glomeruli cannot be explained by hypercontractility of MC.

αpv controls cell migration in UC

In the developing embryo, vSMC as well as UC have to migrate from the mesenchyme to their destination on vessels or the ureter. We therefore wanted to determine, if this initial migration was impaired in the absence of αpv. To analyze possible migration defects we used an *in vitro* wound healing assay with αpv fl/fl and αpv -/- 361 and αpv -/- 369 UC (Fig. 5A). αpv fl/fl UC closed the wound within 24h, while αpv -/- 361 and αpv -/- 369 UC both failed to close the gap properly. Single cell tracking revealed two reasons for this observation: speed and directionality of migration. αpv -/- 361 UC were strongly impaired in velocity as well as directionality of migration and thus covered only a smaller distance during the given time period compared to αpv fl/fl UC. . αpv -/- 369 UC, although faster in migration than αpv fl/fl UC and as a consequence also able to cover a larger distance, had a strong

decrease in directionality. Therefore they closed the gap more than αpv -/- 361 UC, but even so failed to close the cleft completely, as do αpv fl/fl UC. In addition, we also tested the chemotaxis of UC, using FCS as attractant in a boyden chamber assay. No strong differences between αpv -/- 369, αpv -/- 361 and αpv fl/fl UC were observed (Fig. S5A). Cell migration is a highly regulated process, which involves the constant assembly of FAs at the cell front and disassembly at the rear of the cell. It was shown before that signaling molecules downstream of integrins, like FAK and ERK are involved in this regulation of adhesion formation (Webb et al. 2004). We therefore, analyzed if αpv deletion leads to changes in total and phosphorylation levels of FAK, Akt and Erk1/2 in primary vSMC, in UC and MC. No differences in phosphorylation of any of these three proteins were detected in primary vSMC lysates from αpv fl/fl PDGFRβCre mice (Fig. 5B) and also not in αpv deficient MC (Fig. S5B), consistent with findings in αpv null vSMC. In contrast, both αpv -/- UC clones displayed lower pFAK [Y397] levels, while pErk1/2 [T202/ Y204] levels were slightly higher(Fig. 5C). The protein level of pAkt [S473] was downregulated only in αpv -/- 369 cells.

Beside migration, also adhesion to the ECM is important for vSMC/PC coverage of vessels. Therefore, we tested if αpv deletion is resulting in a defective integrin-mediated adhesion by performing an *in vitro* adhesion assay with different substrates. In line with our *in vivo* observations on vSMC, αpv -/- 361 and αpv -/- 369 UC both display reduced adhesion to LN and especially FN, the two major components of vessel BM, compared to αpv fl/fl UC (Fig. 5D). No changes after αpv deletion were detected in adhesion to Col I. Interestingly, the αpv -/- 361 UC showed an increased ability over αpv fl/fl UC to adhere to Col IV. These changes in adhesion could be due to an altered integrin profile on αpv deleted UC and therefore, we tested the surface levels of various integrin subunits by FACS. Surprisingly, we could not detect major changes in LN or FN binding integrins (αvβ3 and α5β1) in αpv -/- 361 and αpv -/- 369 UC which could explain their reduced adhesion (Fig. 5E) to these substrates. Additionally, also surface levels of Col IV binding integrins (α1β1) were normal in αpv -/- 361 UC. This finding suggests that the main defects in these cells are probably in intracellular signaling rather than surface expression of integrins.

αpv deletion in MC but not in UC promotes matrix degradation

We could show that absence of αpv in vSMC results in upregulated MMP9 protein expression and as a consequence matrix degradation was higher. We wanted to know, if αpv deficient MC also showed higher matrix degradation ability, although these cells were not showing any contractility defects in the absence of αpv. Interestingly αpv deletion in UC leads to a strong downregulation of MMP9 and MT1-MMP (Fig. S5C). Consistently also MMP2 protein levels are reduced in αpv -/- 361 and αpv -/- 369 UC. In contrast to UC, MC deficient of αpv show upregulated MT1-MMP levels, whereas MMP9 and MMP2 levels remain unchanged. This tendency was also observed in the DQ-Gelatin degradation assay (Fig. S5D). Both, αpv -/- 361 and αpv -/- 369 UC show a strongly decreased ability to cleave Gelatin compared to αpv fl/fl UC. No changes were observed for MC in this assay. Overall these findings indicate that αpv deficiency is changing cell contractility and matrix degradation in two separate pathways, which are in addition cell type specific.

DISCUSSION

Integrins, their ligands as well as their intracellular binding partners at the FA sites are of critical importance for development of heart and vasculature. This was shown by several knockout approaches in mice where after deletion of FA proteins severe cardiovascular phenotypes were detected. Our study demonstrates a critical role for the FA protein αpv in SMC morphology and function *in vivo* and *in vitro*. We show that conditional deletion of αpv with PDGFRβCre results in lethality of homozygous mice at around 4 weeks of age. *In vitro* primary vSMC are poorly spread, contracted and show strong matrix degrading abilities. Closer analysis of immortalized UC revealed reduced adherence on the two BM compontens LN and FN and impaired directional migration in response to αpv deletion. This result suggests, although it was not proven experimentally, that intitial vSMC recruitment and attachment to the vessel wall is equally impaired. *In vivo* this leads to reduced coverage of vessels by vSMC and insufficient support of the vasculature, a phenotype reminiscent of instable and leaky tumor vasculature (Morikawa et al. 2002). Our proposed function for αpv is not exclusive for vSMC, as deletion of αpv results in similar defects in many SMC containing organs. iSMC from the intestinal wall also show a hypercontractile phenotype and lack the alignment with neighboring cells, which most likely affects motility and peristaltic of the intestine and explains the intestinal pseudoobstruction we observed in our mouse model. In addition also glomerulus morphology is altered in our αpv deficient mice, which can be explained by αpv deleted MC. The critical role for αpv in embryonic and postnatal organ has been shown in previous studies. Here we show that αpv has an equally important function for tissue homeostasis in an adult organism.

Vascular maturation describes the process which transforms the unorganized primitive vasculature in the early embryo into the hierarchical structure of arteries, veins and capillaries. One hallmark of this process is the recruitment of mural cells to the EC layer that forms the vessel lumen. vSMC are covering arteries in one or multiple layers and their recruitment involves differentiation, migration and adhesion from the surrounding mesenchyme to the vessel. Several mural knockout studies underscored the role of these processes for vessel development and especially for vSMC recruitment. The conditional knockout of integrin β1 in vSMC resulted in instable vessels, poorly covered by vSMC, similarly like the vSMC specific ablation of the IPP component ILK (Abraham et al. 2008, Kogata et al. 2009). Likewise to ILK, also the constitutive deletion of αpv primarily results in defective vSMC recruitment and heart malformations. Interestingly, while for ILK and β1 a constitutive knockout in mice results in early peri-implantation lethality (Sakai et al. 2003, Fässler et al. 1995), the constitutive αpv knockout mice survive until E10.5 to E14.5. This indicates, that αpv seems to have an important function in vSMC and heart development, but is of lesser significance in other cell types, thus allowing the embryo to proper develop until the cardiovascular defects become apparent. We therefore chose a conditional αpv deletion with PDGFRβ-Cre transgenic mice to investigate the specific role for αpv in SMC. Unexpectedly αpv fl/fl PDGFRβCre mice survived until birth and were free of symptoms until P21. Death of homozygous mice occurred latest at P30 most likely due to intestinal problems and only 10% of mice survived and were free of any phenotype. This discrepancy to the death of constitutive αpv null mice is most likely due to the normal heart development in αpv fl/fl PDGFRβCre mice, where the cardiomyocytes are not targeted by PDGFRβCre-mediated gene deletion. Furthermore it was postulated

that PDGFRβ expression and therefore strong vSMC recruitment starts at E11.5 (Hellström et al. 1999) a timepoint, where αpv null embryos already developed a strong phenotype. This can explain why the vSMC specific deletion of αpv with PDGFRβCre is not leading to perinatal lethality, although the vascular defects are comparable. Vessels of αpv fl/fl PDGFRβCre mice displayed only punctuated staining of αSMA and vessels were enlarged, which could be also observed in vasculature of αpv null mice. This suggests a contractility defect of vessels due to reduced vSMC investment into the vessel wall. Further evidence for this is the persistent ductus arteriosus that was frequently observed in αpv fl/fl PDGFRβCre mice at P30. This shunt vessel between pulmonary artery and aorta spontaneously closes in small rodents rapidly after birth, initially by contraction of the vSMC in the vessel. Thus a patent ductus arteriosus can be the result of a contractility defect of vSMC (Feng et al. 2010). In contrast to our findings, a study with SM22Cre+Ilk fl/fl conditional mutant mice came to the conclusion that the observed aneurysm formation and persistend ductus arteriosus in mutant mice is resulting of a downregulated contractility and reduced expression of SMC markers in vSMC after ILK depletion (Shen et al. 2011). Unfortunately, their study on RhoA activation was performed with passaged vSMC and Adeno virus treatment. It cannot be excluded that this leads to a switch of vSMC to a more synthetic phenotype, which probably masks the effects that ILK depletion has on vSMC *in vivo*.

We also show that vessel enlargement in αpv fl/fl PDGFRβCre mice is not only due to a defective vSMC recruitment and spreading failure of these cells, but they additionally show higher degradation abilities of ECM, finally resulting in AAA formation. Sections of AAA displayed invading macrophages, a typical observation in aneurysm (Brophy et al. 1991), but *in situ* zymogram revealed also high degradation in the whole tunica media, and thus a participation of vSMC in the degradation process. It was recently shown by Pignatelli et al (2012) that matrix degradation is dependent on αpv phosphorylation and especially on Rac1 activation which requires αpv phosphorylation, whereas the high RhoA activity observed in their non-phosphorylateable αpv is negatively regulating matrix degradation. Although the increased pMLC2 levels observed in our αpv null vSMC and the consequential hypercontractility seems to support their idea, we report that αpv deficient vSMC show increased secretion of MMPs, especially MMP9 along with higher matrix degrading ability compared to wildtype vSMC. Along with our observation in MC, which show only slightly higher matrix degradation and UC, where MMP secretion and matrix degradation is strongly decreased after αpv deletion, we believe that there is a connection, but most likely no direct link between αpv deletion and matrix degradation. The changed MMP expression is more likely a secondary effect of a different actin cytoskeleton and FA structure.

Beside vascular malformations, defects in kidney development are frequently observed, when deleting one of the components of integrin mediated adhesion and migration. For integrin β1 and also for the parvin binding partner ILK several severe abnormalities in kidney development have been reported, including the total absence of one or both kidneys (Wu et al. 2009, Lange et al. 2008). Likewise for αpv null mice, problems in proper kidney formation were detected. In αpv fl/fl PDGFRβCre mice kidneys formed normally and were of normal morphology and size until P14. At later age, development of cystic structures was observed, glomerulus architecture was highly altered and mice developed proteinurea together with symptoms of renal inflammation. An explanation for this finding is the αpv deletion in MC by PDGFRβCre. MC resemble SMC in morphology, protein expression pattern and contractile abilities.

According to Schlöndorff, these cells may function like specialized pericytes and are required for modulating glomerular hemodynamics by contraction (Schlöndorff et al. 1987). .It was observed in various nephrophathies, that MC can transdifferentiate from their mature contractile phenotype into an embryonic myofibroblast phenotype along with high proliferation rates and strong expression levels of αSMA (El-Nahas et al. 2003). In line with these clinical observations, we detected high levels of αSMA in glomeruli of αpv fl/fl PDGFRβCre mice, indicating that MC also switch to a myofibroblast phenotype after αpv deletion. According to the literature, this switch is accompanied with upregulated deposition of Col I, Col III and FN, instead of the normal ECM consisting of LN and Col IV. This new ECM is negatively regulating MC survival, as it was shown for rat MC, thus promoting cell apoptosis and cell depletion during progression of the disease (Mooney et al. 1999). This can very well explain our observation in αpv fl/fl PDGFRβCre glomeruli of either hypercellularity or areas of cell loss, depending on progression of the sclerosis. We additionally observed a tubulo-interstitial sclerosis, which is most likely a secondary effect of the glomerular malfunction and proteinurea (Christensen et al. 2008). Interestingly, isolated αpv deficient MC showed no phenotype beside a slight spreading defect and mild increase in matrix degradation, although not nearly comparable to αpv deficient vSMC. Also no upregulation of contractility markers were observed after αpv deletion. We therefore propose a specific role for αpv in MC that is well-defined from its function in regulation of contractility in other SMC subtypes and has to be revealed in further studies to explain the kidney phenotype in αpv fl/fl PDGFRβCre mice.

We were also asking the question, what function αpv has in adult SMC, where migration, adhesion and spreading processes have been already terminated. In our Tamoxifen inducible αpv fl/fl SMMHC-CreER^{T2} mice we observed major defects in the SMC layer of the small intestine, leading very rapidly to the death of homozygous mice. It is very likely that the loss of αpv in smooth muscle layers of the GI tract is disturbing peristalsis and leading to a paralytic ileus. This explains the failure to gain weight and would subsequently lead to death, as it is also described in other animal studies (Angstenberger et al. 2007, Mericskay et al. 2007). While αpv depleted iSMC behaved comparable to vSMC in αpv fl/fl PDGFRβCre, interestingly no phenotype was observed in the vasculature of induced αpv fl/fl SMMHC-CreER^{T2} mice, although it was shown that SMMHC-CreER^{T2} targets all SMC, including vSMC (Wirth et al. 2008). A possible explanation for this might be the severity of the pseudoobstruction and high lethality, which prevented prolonged studies of these mice. Another explanation might be a low protein turnover of FAs in vSMC. Migration of cells is depending on constant FA assembly and disassembly at the leading and lagging edge of the cell and therefore a constant need for FA proteins. Differentiated vSMC are in a resting, non-migratory state and not dependent on the formation of new FAs. Thus the loss of αpv expression would not become evident until de novo αpv incorporation into FAs would be required. This suggests that triggering angiogenesis in adult mice or vSMC migration like in atherosclerosis would cause a vascular defect in αpv fl/fl SMMHC-CreER^{T2} mice.

αpv is part of the ternary protein complex consisting of ILK, PINCH and parvin. The formation of the IPP complex is critically depending on the presence of all three proteins, and with one protein absent the other two undergo proteasomal degradation (Fukuda et al. 2003). In case of αpv it was described that βpv can rescue ILK and PINCH levels at the FAs, although the ILK-PINCH- βpv complex is unable to rescue the hypercontractility phenotype (Montanez et al. 2009). Our *in vitro* studies could show, that in general

primary αpv deleted vSMC isolated from aorta phenocopy the vSMC/PC after αpv deletion. They display the same round morphology with multiple retraction fibers and elevated pMLC2 levels also confirm the regulation of cell contractility by αpv. Unexpectedly in our system βpv expression is not upregulated in vSMC, resulting in a loss of the whole IPP complex at FAs and strongly decreased protein levels. Same results were obtained for MC and UC, after αpv deletion, suggesting, that βpv expression is absent in differentiated contractile SMC found in adult animals. Interestingly the loss of IPP in vSMC is not changing the phenotype, compared to vSMC obtained from αpv null mice, where ILK and PINCH levels were normal. Additionally no changes in integrin mediated signaling, like FAK and Erk phosphorylation were observed in αpv fl/fl PDGFRβCre vSMC upon loss of the IPP complex. Out of these findings we conclude, that in SMC especially αpv and the αpv containing IPP complex is of major importance for cell morphology and function. Further studies have to concentrate on αpv specific interaction partners to explain the regulation of contractility.

SMC have the ability to switch back and forth between a contractile quiescent state to a proliferative synthetic phenotype depending on extracellular stimuli, which goes hand in hand with loss of SMC specific proteins like smoothelin and αSMA (Rensen et al. 2007). This switching is necessary is situations, where migration and proliferation of SMC is necessary, like the formation of new vessels, or response to injury, but an unwanted feature when these cells are cultured for *in vitro* analysis. We therefore chose UC, which keep their contractile abilities also after immortalization and several passages in culture, to investigate the biochemical function of αpv on contractility regulation. We show that αpv deletion in UC resulted in poorly spread cells, defects in directed migration and adhesion to ECM proteins, especially to those present also in the vascular wall like FN and LN. Therefore these cells, unlike MC, seemed to be a suitable alternative to primary vSMC for *in vitro* studies. But in contrast to previous studies on αpv deficient vSMC and our results on αpv null vSMC, pMLC2 levels remained unchanged. SMC, even though performing similar functions in all organs are a heterogeneous cell type and thus conclusions drawn from one SMC subtype must not be true for all SMC. Unlike other cells, which derive from a distinct precursor cell like endothelial cells and myocytes, SMC can derive from different embryonic tissues (Gittenberger-de Groot et al. 1999). We think that this is the reason for the variability in phenotypes we observe in SMC after αpv deletion and we propose that αpv is regulating different signaling pathways depending on the origin of the SMC.

Taken together we confirm with the conditional deletion of αpv in SMC the vascular phenotype observed for the constitutive αpv deletion in mice. Although there are differences in lethality and in other organs, in both studies αpv regulates cell recruitment and spreading of vSMC and absence of αpv results in hypercontractility. We expand these findings to iSMC, which show comparable defects, but also show, that αpv is not performing the same function in all SMC related cells and that there might be another pathway involved. Further studies are necessary to resolve the critical difference in vSMC/iSMC to other SMC to finally present the signaling pathways αpv is regulating.

MATERIAL AND METHODS

Animal Procedures

α-parvin fl/fl mice (Altstätter et al., in preparation) were intercrossed with PDGFRβCre transgenic mice (Foo et al. 2006) to produce αpv fl/fl PDGFRβCre-mice or with SMMHC-CreERT2 transgenic mice (Wirth et a. 2008) to produce αpv fl/fl SMMHC-CreERT2 mice. Deletion of the αpv alleles was induced in 3 weeks old mice by intraperitoneal injection of 1mg Tamoxifen in peanut oil on 3 consecutive days. For experiments αpv fl/fl PDGFRβCre mice were compared to αpv fl/+ PDGFRβCre littermates and Tamoxifen induced male αpv fl/fl SMMHC-CreERT2 mice were compared to Tamoxifen induced αpv fl/fl female littermates, since the Cre is inherited via the y-Chromosome. All experiments with mice were performed in accordance to German guidelines and regulations.

Antibodies

The following antibodies were used: rabbit antibody against a-parvin (Cell Signaling); rabbit antibody against b-parvin (1453); biotinylated rat antibody agains-Mac-1 (Pharmingen); rat antibody against CD31 (PharMingen); Cy3-conjugated mouse antibody against aSMA (Sigma); mouse antibody against GAPDH (Calbiochem); rabbit antibody against ILK (Cell Signaling Technology); mouse antibody against ILK (Transduction Laboratories); mouse antibody against PINCH (Transduction Laboratories); rabbit antibody against myosin light chain (MLC2) (Santa Cruz); rabbit antibody against phospho-MLC2 (Cell Signaling); mouse antibody against paxillin (Transduction Laboratories); rabbit antibody against FAK (Cell Signaling); rabbit antibody against pFAK [Y397] (Invitrogen); rabbit antibody against Akt (Cell Signaling), rabbit antibody against pAkt [S473] (Cell Signaling); rabbit antibody against Erk ½ (Cell Signaling), rabbit antibody against pErk [T202/ Y204] (Cell Signaling); rabbit antibody against MMP9 (Millipore), goat antibody against MT1-MMP (Santa Cruz); rabbit antibody against pSrc [Y416] (Cell Signaling); rabbit antibody against pp38MAPK [T180/ Y182] (Cell Signaling); rabbit antibody against p38MAPK (Cell Signaling); mouse antibody against vimentin (Sigma), TRITC-conjugated phalloidin was used to detect F-actin (Molecular Probes; Eugene, OR, USA). Secondary antibodies were purchased from Jackson Immuno Research Laboratories, Molecular Probes or Invitrogen.

Histology and Immunohistochemistry

HE staining on organ sections was performed on tissue which was fixed overnight at 4°C in 4% PFA in PBS, dehydrated in a graded alcohol series and embedded in paraffin (Paraplast X-tra; Sigma-Aldrich) using a embedding machine (Shandon). For immunohistochemistry cryo-sections were used, therefore unfixed organs were embedded in OCT (Shandon Cryomatrix, Thermo) and rapidly frozen. Prior to staining, cryo-sections were fixed with PFA or acetone. For immunostaining on cells, primary vSMC, Mesangial Cells or Ureteric Cells were plated 4h or over night onto glass-coverslips coated with 2µg/ml FN. Cells were fixed in 3% PFA, permeabilized with 0.1% Triton-X100 and blocked with 3% BSA (all in PBS). Confocal images were acquired with a Leica TCS SP5 microscope (Leica Microsystems CMS, Mannheim, Germany), equipped with 20.0x NA 0.70, 40x NA 1.25, 63x NA 1.4 and 63x NA 1.2 objectives, using Leica Application Suite Advanced Fluorescence (LAS AF) software version 1.6.2. build 1110.

Whole mounts

Aorta and intestine were dissected and longitudinally opened. Ears were cut and the ventral half was separated from the dorsal half with the remaining cartilage. Samples were fixed over night in 2% PFA and blocked in 1% BSA for 1h at room temperature under constant agitation. Incubation with primary antibody was carried out over night at 4°C, incubation with secondary antibody for 1h at room temperature.

Micropattern analysis and immunostainings

Fabrication of FN-coated micropatterns: The micropatterns were generated on PEG-coated glass coverslips with deep UV lithography (Azioune et al. 2010). Briefly, glass coverslips were incubated in a 1mM solution of a linear PEG, CH3-(O-CH2-CH2)43-NH-CO-NH-CH2-CH2-CH2-Si(OEt)3, in dry toluene for 20 h at 80 °C under a nitrogen atmosphere. The substrates were removed, rinsed intensively with ethyl acetate, methanol and water, and dried with nitrogen. A pegylated glass coverslip and a chromium-coated quartz photomask (ML&C, Jena) were immobilized with vacuum onto a mask holder, which was immediately exposed to deep UV light using a low-pressure mercury lamp (Heraeus Noblelight GmbH, NIQ 60/35 XL longlife lamp, quartz tube, 60 W) at 5 cm distance for 7 min. The patterned substrates were subsequently incubated overnight with 100µL of fibronectin (20 µg/mL in PBS) at 4 °C and washed once with PBS before plating cells in culture medium with 0.5% serum. The patters were done by Dr. Julien Polleux.

Immunostaining: The cells were seeded on micropatterns in DMEM (GIBCO by life technologiesTM, Paisley, UK) supplemented with 0.5 % FBS at 37°C, 5% CO2 for 3h. Cells were fixed in 3% PFA in PBS and blocked with 1% BSA in PBS for 1h under constant agitation. Primary antibodies were incubated in 3% BSA, 0.1% TritonX-100 in PBS for 1h at 37°C. Staining intensity was quantified using Metamorph® software.

Zymography

Cells were lysed in buffer (50mM Tris pH 7.5, 100mM NaCl, 10mM CaCl2, 1% Triton-X, 0.01% Brij35) without protease inhibitors. Proteins were resolved on 10% SDS-PAA gel, substituted with 0.2% Gelatin or 0.2% Casein. After gelelectrophoresis, gels were washed in 0.2% Triton-X and incubated in MMP reaction buffer (50mM Tris pH 7.5, 200mM NaCl, 5mM CaCl2, 0.02% Na azide) for 24h – 3days. Gels were stained in Coomassie. Areas of degradation appear as white bands on blue background.

In situ zymogram

Fresh cryosections (8µm) were air dried and covered by a mixture of 1% low gelling agarose, 0.1mg/ml DQ-Gelatin and DAPI. After gelling of Agar at 4°C, sections were incubated at RT for minimum 1h. Sections were analyzed via confocal microscopy. Areas of degradation are vizualized at 488nm wavelength.

Coverslips were coated with 5% DQ-Gelatin in 10mg/ml Gelatin solution and air dried. After rehydration in PBS, Cells were seeded overnight on the Gelatin coated coverslips. After fixation in 3% PFA, coverslips were blocked in 3% BSA and incubated in primary antibody ON at 4°C. Cells were analyzed via confocal microscopy. Areas of degradation were visualized at 488nm wavelength.

Isolation of smooth muscle cells

Aortas were dissected, cut into smaller pieces and digested with digestion buffer (2 mg/ml collagenase type II and 0.5 mg/ml elastase in Dulbecco's modified Eagle medium (DMEM)) for 30 min at 37°C. Digestion was terminated with 10% foetal bovine serum (FBS) in DMEM. Released cells were centrifuged and re-suspended in DMEM containing 10% FBS and antibiotics, transferred to 6-well dishes and further expanded for analysis.

Small intestines were dissected, longitudinally opened and washed several times with HBSS. The luminal side was scratched with a sterile glass slide to remove epithelial layers. The intestine was minced into small pieces and digested for 30 min at 37°C in digestion buffer (0.35 mg/ml Papain, 0.35 mg/ml Collagenase type II, 0.25 mg/ml soybean trypsin inhibitor and 2 mg/ml BSA in Medium 199). The suspension was filtered, centrifuged and re-suspended in culture medium (Medium 199, 20% FBS, 2 mM L-Glutamin and antibiotics).

Isolation of Ureteric Cells and immortalization

Ureters were dissected from E14.5 αpv fl/fl embryos, and digested with digestion buffer (2 mg/ml collagenase type II and 0.5 mg/ml elastase in Dulbecco's modified Eagle medium (DMEM)) for 30 min at 37°C. Digestion was terminated with 10% foetal bovine serum (FBS) in DMEM. Released cells were transferred to DMEM containing 10% FBS and antibiotics and cultured in 6-well-dishes. Immortalization was achieved by retroviral transduction of SV40 large T antigen and immortalized cells were subsequently cloned. αpv null UC were derived from αpv fl/fl UC by adenoviral Cre transduction followed by cloning.

SDS–PAGE and immunoblotting

Cells were lysed in RIPA-Lysis buffer (150 mM NaCl, 1.0% IGEPAL® CA-630, 0.5% sodium deoxycholate, 0.1% SDS, and 50 mM Tris, pH 8.0, supplemented with protease inhibitors (Roche) and phosphatase inhibitors (SIGMA)), homogenized in Laemmli sample buffer and boiled for 5 min. Proteins were resolved by SDS–polyacrylamide gel electrophoresis (SDS–PAGE) gels and then electrophoretically transferred from the gels onto PVDF membranes, which were subsequently blocked in 5% BSA and incubated with antibodies. Bound antibodies were detected using chemiluminescence HRP substrate (Millipore Corporation, Billerica, USA).

FACS staining

UC were trypsinated and resuspended in FACS buffer (TBS; 3%BSA; 0,02%NaN3, 1mM MgCl2, 1mM CaCl2). Staining was performed in triplicates using >105 cells/well on 96-well plates. Antibodies used for FACS analyzes were FITC conjugated hamster antibody against integrin β1; biotinylated hamster antibody against integrin β3 (all from PharMingen, San Diego, CA); mouse antibody against integrin β5; rabbit antibody against integrin β8; FITC-conjugated hamster antibody against integrin α1 (Serotec); FITC-conjugated hamster antibody against integrin α2; biotinylated rat antibody against integrin α4;

biotinylated rat antibody against integrin α5; biotinylated rat antibody against integrin αv (all BD Biosciences); Cy5-conjugated Streptavidin (Jackson Immunochemicals Laboratories Inc.; West Grove, PA, USA); Integrin null cells served as negative control.

In vitro wound healing assay

After 4h incubation in DMEM complemented with 10%FCS and antibiotics, UC monolayers were gently scratched with a pipet tip. Subsequently, images were captured every 10 min for 24h at 37°C and 5% CO2 using a Zeiss Axiovert microscope equipped with 10× NA 0.3, 20× NA 0.4, 40× NA 0.6, and 100× NA 1.3 objectives, a motorized scanning table (Märzhäuser), a stage incubator (EMBL Precision Engineering) and a CCD camera (Roper Scientific MicroMAX). MetaMorph (Universal Imaging Corp.) software was used for microscope control and data acquisition. For single cell tracking and data analyzes, the ImageJ software-plugins “Manual Tracking” (Fabrice P. Cordelières) and “Chemotaxis and Migration Tool” (ibidi) were used. At least three independent experiments were performed and more than 10 individual cells were tracked for each experiment.

Boyden chamber assay

Chemotactic and chemokinetic migration assays were performed in 3-mm pore size chamber inserts (BD Falcon). For chemotaxis assays, $4x10^4$ cells were plated into the chamber and transferred into 24-well plates containing serum-free medium with or medium with 10% FCS. After overnight incubation, the cells in the bottom part of the chamber were stained with a crystal violet solution and counted. Five microscopic fields per chamber were analyzed. Data are represented as x-fold more cells when FCS was present to cell number in serum free medium.

Adhesion assay

96 well plates were coated with 2, 5, 10 [µg/ml] Fibronectin (Calbiochem, bovine); 2, 5, 10 [µg/ml] CollagenI (PureCol, Inamed Materials #5409); 2, 5, 10 [µg/ml] Laminin; 2, 5, 10 [µg/ml] CollagenIV; 1% BSA in PBS, or 0.1% PLL for 2h at RT and subsequently blocked with 1% BSA in PBS for 15 min at RT. 50.000 cells were used per well for 1h of adhesion. Wells were washed with PBS, dried and stained over night with 0.1% Crystal violet in 20% Methanol at 4°C. After washing with H_2O, permeabilization was performed with 0.1% Triton X-100 in dH_2O for several hours until the dye left the cells. Absorption was measured at absorption at 595nm wavelength in a plate reader.

REFERNECES

Abraham S, Kogata N, Fässler R, Adams RH.; Integrin beta1 subunit controls mural cell adhesion, spreading, and blood vessel wall stability.; Circ Res. 2008 Mar 14;102(5):562-70. doi: 10.1161/CIRCRESAHA.107.167908. Epub 2008 Jan 17.

Adams RH, Alitalo K.; Molecular regulation of angiogenesis and lymphangiogenesis.; Nat Rev Mol Cell Biol. 2007 Jun;8(6):464-78.

Angstenberger M, Wegener JW, Pichler BJ, Judenhofer MS, Feil S, Alberti S, Feil R, Nordheim A.; Severe intestinal obstruction on induced smooth muscle-specific ablation of the transcription factor SRF in adult mice.; Gastroenterology. 2007 Dec;133(6):1948-59. Epub 2007 Sep 5.

Arar M, Xu YC, Elshihabi I, Barnes JL, Choudhury GG, Abboud HE.; Platelet-derived growth factor receptor beta regulates migration and DNA synthesis in metanephric mesenchymal cells.; J Biol Chem. 2000 Mar 31;275(13):9527-33.

Azioune A, Carpi N, Tseng Q, Théry M, Piel M.; Protein micropatterns: A direct printing protocol using deep UVs.; Methods Cell Biol. 2010;97:133-46.

Berk BC.; Vascular smooth muscle growth: autocrine growth mechanisms.; Physiol Rev. 2001 Jul;81(3):999-1030.

Beck L Jr, D'Amore PA.; Vascular development: cellular and molecular regulation.; FASEB J. 1997 Apr;11(5):365-73.

Bolcato-Bellemin AL, Lefebvre O, Arnold C, Sorokin L, Miner JH, Kedinger M, Simon-Assmann P.; Laminin alpha5 chain is required for intestinal smooth muscle development.; Dev Biol. 2003 Aug 15;260(2):376-90.

Brophy CM, Reilly JM, Smith GJ, Tilson MD.; The role of inflammation in nonspecific abdominal aortic aneurysm disease.; Ann Vasc Surg. 1991 May;5(3):229-33.

Carlson TR, Hu H, Braren R, Kim YH, Wang RA.; Cell-autonomous requirement for beta1 integrin in endothelial cell adhesion, migration and survival during angiogenesis in mice.;Development. 2008 Jun;135(12):2193-202. doi: 10.1242/dev.016378. Epub 2008 May 14.

Cheuk BL, Cheng SW.; Differential expression of integrin alpha5beta1 in human abdominal aortic aneurysm and healthy aortic tissues and its significance in pathogenesis.;J Surg Res. 2004 May 15;118(2):176-82.

Christensen EI, Verroust PJ.; Interstitial fibrosis: tubular hypothesis versus glomerular hypothesis.; Kidney Int. 2008 Nov;74(10):1233-6. doi: 10.1038/ki.2008.421.

Chu H, Thievessen I, Sixt M, Lämmermann T, Waisman A, Braun A, Noegel AA, Fässler R.; gamma-Parvin is dispensable for hematopoiesis, leukocyte trafficking, and T-cell-dependent antibody response.; Mol Cell Biol. 2006 Mar;26(5):1817-25.

El-Nahas AM.; Plasticity of kidney cells: role in kidney remodeling and scarring.; Kidney Int. 2003 Nov;64(5):1553-63.

Fässler R, Meyer M.; Consequences of lack of beta 1 integrin gene expression in mice.; Genes Dev. 1995 Aug 1;9(15):1896-908.

Feng X, Krebs LT, Gridley T.; Patent ductus arteriosus in mice with smooth muscle-specific Jag1 deletion.; Development. 2010 Dec;137(24):4191-9. doi: 10.1242/dev.052043. Epub 2010 Nov 10.

Foo SS, Turner CJ, Adams S, Compagni A, Aubyn D, Kogata N, Lindblom P, Shani M, Zicha D, Adams RH.; Ephrin-B2 controls cell motility and adhesion during blood-vessel-wall assembly.; Cell. 2006 Jan 13;124(1):161-73.

Francis SE, Goh KL, Hodivala-Dilke K, Bader BL, Stark M, Davidson D, Hynes RO.; Central roles of alpha5beta1 integrin and fibronectin in vascular development in mouse embryos and embryoid bodies.; Arterioscler Thromb Vasc Biol. 2002 Jun 1;22(6):927-33.

Fukuda T, Chen K, Shi X, Wu C.; PINCH-1 is an obligate partner of integrin-linked kinase (ILK) functioning in cell shape modulation, motility, and survival.; J Biol Chem. 2003 Dec 19;278(51):51324-33. Epub 2003 Oct 8.George EL,

Georges-Labouesse EN, Patel-King RS, Rayburn H, Hynes RO.; Defects in mesoderm, neural tube and vascular development in mouse embryos lacking fibronectin.;Development. 1993 Dec;119(4):1079-91.

Gittenberger-de Groot AC, DeRuiter MC, Bergwerff M, Poelmann RE.; Smooth muscle cell origin and its relation to heterogeneity in development and disease.; Arterioscler Thromb Vasc Biol. 1999 Jul;19(7):1589-94.

Grazioli A, Alves CS, Konstantopoulos K, Yang JT.; Defective blood vessel development and pericyte/pvSMC distribution in alpha 4 integrin-deficient mouse embryos.; Dev Biol. 2006 May 1;293(1):165-77. Epub 2006 Mar 10.

Hellström M, Kalén M, Lindahl P, Abramsson A, Betsholtz C.; Role of PDGF-B and PDGFR-beta in recruitment of vascular smooth muscle cells and pericytes during embryonic blood vessel formation in the mouse.;Development. 1999 Jun;126(14):3047-55.

Hynes RO.; Integrins: bidirectional, allosteric signaling machines.; Cell. 2002 Sep 20;110(6):673-87.

Jain RK.; Molecular regulation of vessel maturation.; Nat Med. 2003 Jun;9(6):685-93.

Johnson RJ, Floege J, Yoshimura A, Iida H, Couser WG, Alpers CE.; J Am Soc Nephrol. 1992 Apr;2(10 Suppl):S190-7.; The activated mesangial cell: a glomerular "myofibroblast"?

Kogata N, Tribe RM, Fässler R, Way M, Adams RH.; Integrin-linked kinase controls vascular wall formation by negatively regulating Rho/ROCK-mediated vascular smooth muscle cell contraction.;Genes Dev. 2009 Oct 1;23(19):2278-83. doi: 10.1101/gad.535409.

Kurahashi M, Niwa Y, Cheng J, Ohsaki Y, Fujita A, Goto H, Fujimoto T, Torihashi S.; Platelet-derived growth factor signals play critical roles in differentiation of longitudinal smooth muscle cells in mouse embryonic gut.; Neurogastroenterol Motil. 2008 May;20(5):521-31.

Lange A, Wickström SA, Jakobson M, Zent R, Sainio K, Fässler R.; Integrin-linked kinase is an adaptor with essential functions during mouse development.; Nature. 2009 Oct 15;461(7266):1002-6. doi: 10.1038/nature08468.

Legate KR, Montañez E, Kudlacek O, Fässler R.; ILK, PINCH and parvin: the tIPP of integrin signalling.; Nat Rev Mol Cell Biol. 2006 Jan;7(1):20-31

Legate KR, Wickström SA, Fässler R.; Genetic and cell biological analysis of integrin outside-in signaling.; Genes Dev. 2009 Feb 15;23(4):397-418. doi: 10.1101/gad.1758709.

Levéen P, Pekny M, Gebre-Medhin S, Swolin B, Larsson E, Betsholtz C.; Mice deficient for PDGF B show renal, cardiovascular, and hematological abnormalities.; Genes Dev. 1994 Aug 15;8(16):1875-87

Li S, Bordoy R, Stanchi F, Moser M, Braun A, Kudlacek O, Wewer UM, Yurchenco PD, Fässler R.; PINCH1 regulates cell-matrix and cell-cell adhesions, cell polarity and cell survival during the peri-implantation stage.;J Cell Sci. 2005 Jul 1;118(Pt 13):2913-21.

Lindahl P, Johansson BR, Levéen P, Betsholtz C.; Pericyte loss and microaneurysm formation in PDGF-B-deficient mice.; Science. 1997 Jul 11;277(5323):242-5.

Malan D, Wenzel D, Schmidt A, Geisen C, Raible A, Bölck B, Fleischmann BK, Bloch W.; Endothelial beta1 integrins regulate sprouting and network formation during vascular development.;Development. 2010 Mar;137(6):993-1002. doi: 10.1242/dev.045377.

Mericskay M, Blanc J, Tritsch E, Moriez R, Aubert P, Neunlist M, Feil R, Li Z.; Inducible mouse model of chronic intestinal pseudo-obstruction by smooth muscle-specific inactivation of the SRF gene.; Gastroenterology. 2007 Dec;133(6):1960-70. Epub 2007 Sep 16.

Montanez E, Wickström SA, Altstätter J, Chu H, Fässler R.; Alpha-parvin controls vascular mural cell recruitment to vessel wall by regulating RhoA/ROCK signalling.; EMBO J. 2009 Oct 21;28(20):3132-44. doi: 10.1038/emboj.2009.295. Epub 2009 Oct 1.

Mooney A, Jackson K, Bacon R, Streuli C, Edwards G, Bassuk J, Savill J; Type IV collagen and laminin regulate glomerular mesangial cell susceptibility to apoptosis via beta(1) integrin-mediated survival signals.; Am J Pathol. 1999 Aug;155(2):599-606.

Morikawa S, Baluk P, Kaidoh T, Haskell A, Jain RK, McDonald DM.; Abnormalities in pericytes on blood vessels and endothelial sprouts in tumors.; Am J Pathol. 2002 Mar;160(3):985-1000.

Mukai Y, Shimokawa H, Matoba T, Kandabashi T, Satoh S, Hiroki J, Kaibuchi K, Takeshita A.; Involvement of Rho-kinase in hypertensive vascular disease: a novel therapeutic target in hypertension.; FASEB J. 2001 Apr;15(6):1062-4.

Murthy KS.; Signaling for contraction and relaxation in smooth muscle of the gut.; Annu Rev Physiol. 2006;68:345-74.

Owens GK, Kumar MS, Wamhoff BR.; Molecular regulation of vascular smooth muscle cell differentiation in development and disease.; Physiol Rev. 2004 Jul;84(3):767-801.

Pignatelli J, LaLonde SE, LaLonde DP, Clarke D, Turner CE.; Actopaxin (α-parvin) phosphorylation is required for matrix degradation and cancer cell invasion.; J Biol Chem. 2012 Oct 26;287(44):37309-20. doi: 10.1074/jbc.M112.385229. Epub 2012 Sep 6.

Pöschl E, Schlötzer-Schrehardt U, Brachvogel B, Saito K, Ninomiya Y, Mayer U.; Collagen IV is essential for basement membrane stability but dispensable for initiation of its assembly during early development.; Development. 2004 Apr;131(7):1619-28. Epub 2004 Mar 3.

Pröls F, Hartner A, Schöcklmann HO, Sterzel RB.; Mesangial cells and their adhesive properties.; Exp Nephrol. 1999 Mar-Apr;7(2):137-46.

Rattan S, Phillips BR, Maxwell PJ 4th.; RhoA/Rho-kinase: pathophysiologic and therapeutic implications in gastrointestinal smooth muscle tone and relaxation.; Gastroenterology. 2010 Jan;138(1):13-8.e1-3. doi: 10.1053/j.gastro.2009.11.016. Epub 2009 Nov 23.

Rensen SS, Doevendans PA, van Eys GJ.; Regulation and characteristics of vascular smooth muscle cell phenotypic diversity.; Neth Heart J. 2007;15(3):100-8.

Risau W.; Mechanisms of angiogenesis. Nature. 1997 Apr 17;386(6626):671-4

Sakai T, Li S, Docheva D, Grashoff C, Sakai K, Kostka G, Braun A, Pfeifer A, Yurchenco PD, Fässler R.; Integrin-linked kinase (ILK) is required for polarizing the epiblast, cell adhesion, and controlling actin accumulation.; Genes Dev. 2003 Apr 1;17(7):926-40.

Schlöndorff D.; The glomerular mesangial cell: an expanding role for a specialized pericyte.; FASEB J. 1987 Oct;1(4):272-81.

Shen D, Li J, Lepore JJ, Anderson TJ, Sinha S, Lin AY, Cheng L, Cohen ED, Roberts JD Jr, Dedhar S, Parmacek MS, Gerszten RE.; Aortic aneurysm generation in mice with targeted deletion of integrin-linked kinase in vascular smooth muscle cells.; Circ Res. 2011 Sep 2;109(6):616-28. doi: 10.1161/CIRCRESAHA.110.239343. Epub 2011 Jul 21.

Soriano P.; Abnormal kidney development and hematological disorders in PDGF beta-receptor mutant mice.; Genes Dev. 1994 Aug 15;8(16):1888-96.

Suri C, Jones PF, Patan S, Bartunkova S, Maisonpierre PC, Davis S, Sato TN, Yancopoulos GD.; Requisite role of angiopoietin-1, a ligand for the TIE2 receptor, during embryonic angiogenesis.;Cell. 1996 Dec 27;87(7):1171-80.

Thyboll J, Kortesmaa J, Cao R, Soininen R, Wang L, Iivanainen A, Sorokin L, Risling M, Cao Y, Tryggvason K.; Deletion of the laminin alpha4 chain leads to impaired microvessel maturation.; Mol Cell Biol. 2002 Feb;22(4):1194-202.

Webb DJ, Donais K, Whitmore LA, Thomas SM, Turner CE, Parsons JT, Horwitz AF.; FAK-Src signalling through paxillin, ERK and MLCK regulates adhesion disassembly. ; Nat Cell Biol. 2004 Feb;6(2):154-61. Epub 2004 Jan 25.

Wirth A, Benyó Z, Lukasova M, Leutgeb B, Wettschureck N, Gorbey S, Orsy P, Horváth B, Maser-Gluth C, Greiner E, Lemmer B, Schütz G, Gutkind JS, Offermanns S.; G12-G13-LARG-mediated signaling in vascular smooth muscle is required for salt-induced hypertension.; Nat Med. 2008 Jan;14(1):64-8. Epub 2007 Dec 16.

Wu W, Kitamura S, Truong DM, Rieg T, Vallon V, Sakurai H, Bush KT, Vera DR, Ross RS, Nigam SK.; Beta1-integrin is required for kidney collecting duct morphogenesis and maintenance of renal function.; Am J Physiol Renal Physiol. 2009 Jul;297(1):F210-7. doi: 10.1152/ajprenal.90260.2008. Epub 2009 May 13.

Zhang Y, Chen K, Tu Y, Velyvis A, Yang Y, Qin J, Wu C.; Assembly of the PINCH-ILK-CH-ILKBP complex precedes and is essential for localization of each component to cell-matrix adhesion sites.; J Cell Sci. 2002 Dec 15;115(Pt 24):4777-86.

.

AUTHOR CONTRIBUTIONS

The study was conceived by RF. IR performed most of the experiments and analyzed them together with OT and RF. OT made UC isolation, immortalization and Adeno-Cre treatment and performed wound healing assay, Boyden chamber assay, adhesion assay and integrin profile with these cells. RZ provided MC and performed and analyzed HE staining of glomeruli. IR and RF wrote the manuscript. All authors read and approved the manuscript.

FIGURE LEGEND

Figure 1: PDGFRβCre induced deletion of αpv leads to vascular and intestinal defects. **(A)** Representative images of αpv fl/+ PDGFRβCre and αpv fl/fl PDGFRβCre mice at the age of 30 days. **(B)** Weight gaining curve of αpv fl/+ PDGFRβCre and αpv fl/fl PDGFRβCre mice. Values are mean weight of 10 animals per genotype. **(C)** Kaplan-Meier-survival curve of αpv fl/+ PDGFRβCre and αpv fl/fl PDGFRβCre mice. Values are based on 20 mice per genotype. **(D)** Dissected aorta from αpv fl/+ PDGFRβCre and αpv fl/fl PDGFRβCre mice at day 1 and day 30 after birth. αpv fl/fl PDGFRβCre mice display large abdominal aortic aneurysms. Star points to atheroma formation. Scale bar: 0.25cm and 1cm. **(E)** HE staining of ductus arteriosus sections from αpv fl/+ PDGFRβCre and αpv fl/fl PDGFRβCre mice at day 30 after birth. Note the persistent ductus arteriosus in αpv fl/fl PDGFRβCre mice. Scale bar: 100µm. **(F)** Dissected digestion tract from αpv fl/+ PDGFRβCre and αpv fl/fl PDGFRβCre mice at day 30 after birth. Note the enlarged large intestine and caecum. si = small intestine, li = large intestine, c = caecum. Scale bar: 1cm

Figure 2: PDGFRβCre deletion of αpv results in impaired cell spreading and cell shape. **(A)** Whole mount immunostaining of the vasculature in the ear and aorta of αpv fl/+ PDGFRβCre and αpv fl/fl PDGFRβCre mice Scale bar: 100µm and 75µm. SMCs are labeled with αSMA (red/white) and ECs with CD31/PECAM (green). **(B)** Immunostaining of aorta sections of αpv fl/+ PDGFRβCre and αpv fl/fl PDGFRβCre mice. αpv (green) is absent from the smooth muscle cell containing layer in αpv fl/fl PDGFRβCre mice. Nuclei are visualized with DAPI. Note the round smooth muscle cells in the aorta of αpv fl/fl PDGFRβCre mice. Scale bar: 75µm and 50µm. **(C)** Brightfield images and immunostainings against αpv (green) and αSMA (red) of isolated primary vSMC from αpv fl/+ PDGFRβCre and αpv fl/fl PDGFRβCre mice seeded on 2µg/ml FN. Nuclei are visualized with DAPI. Scale bar: 50 and 20µm. **(D)** Protein levels of αpv, β-parvin, ILK and PINCH1 from primary vSMC. Gapdh levels served as loading control. **(E)** Immunostainings for ILK (red), PINCH1 (red) and αpv (green) in primary vSMC from αpv fl/+ PDGFRβCre and αpv fl/fl PDGFRβCre mice seeded of 2µg/ml FN. Scale bar: 20µm.

Figure 3: Tamoxifen induced deletion of αpv in SMCs leads to severe intestinal defects. **(A)** Representative images of αpv fl/fl and αpv fl/fl SMMHC-CreER^{T2} mice at day 35 after Tamoxifen treatment. **(B)** Dissected digestion tract from αpv fl/fl and αpv fl/fl SMMHC-CreER^{T2} mice at day 35 after Tamoxifen treatment. Note the enlargement of the small intestine together with the black discoloration. si = small intestine, li = large intestine, c = caecum. Scale bar: 1cm. **(C)** HE staining of small intestine sections of αpv fl/fl and αpv fl/fl SMMHC-CreER^{T2} mice at day 35 after Tamoxifen treatment. Closeup of the SMC layer shows round SMCs in αpv fl/fl SMMHC-CreER^{T2} mice. Immunostainings against αSMA (red) and αpv (green) show absence of αpv in αpv fl/fl SMMHC-CreER^{T2} mice. Scale bar: 100µm and 75µm. **(D)** Brightfield images and immunostainings against αpv (green) and αSMA (red) of isolated primary iSMC from αpv fl/fl and αpv fl/fl SMMHC-CreER^{T2} mice seeded on 2µg/ml FN. Nuclei are visualized with DAPI. Scale bar: 50µm and 20µm. **(E)** Protein levels of αpv, βpv, ILK and PINCH1 from primary vSMC. Gapdh levels served as loading control.

Figure 4: Deletion of αpv leads to increased cell contraction of SMC. **(A)** Immunostainings of primary vSMC against pMLC2 (green) and αSMA (red). Nuclei are visualized with DAPI. Scale bar: 20µm. **(B)**.Protein levels of pMLC2 and MLC2 in vSMC lysates from αpv fl/+ PDGFRβCre and αpv fl/fl PDGFRβCre

mice. **(C)** Immunostainings of immortalized UC against pMLC2 (green) and αSMA (red). Nuclei are visualized with DAPI. Scale bar: 20µm **(D)** Protein levels of pMLC2 and MLC2 from of αpv fl/fl UC, αpv -/- 361 and αpv -/- 369 UC. **(E)** Immortalized αpv fl/fl and αpv -/- UC on FN coated umbrella shaped micropatterns and immunostained for pMLC2 (green), Phalloidin (red) and Paxillin (white). Nuclei are visualized with DAPI. Single channels are shown in black and white.

Figure 5: αpv regulates migration and adhesion of UC (A) *In vitro* wound healing assay with αpv fl/fl UC, αpv -/- 361 and αpv -/- 369 UC. Representative images at t=0 and at t=24h show inability of αpv -/- 361 and αpv -/- 369 UC to close the scratch after 24h. Graphs display average distance after 13h in µm, average velocity in µm/min and directionality of cells. 10 cells were tracked for analysis. Bars represent SEM. **(B)** Protein levels of FAK, pFAK [Y397], Akt, pAkt [S473], Erk1/2, pErk 1/2 [T202/ Y204] of primary vSMC from αpv fl/+ PDGFRβCre and αpv fl/fl PDGFRβCre mice. Gapdh levels served as loading control. **(C)** Protein levels of FAK, pFAK [Y397], Akt, pAkt [S473], Erk 1/2, pErk1/2 [T202/ Y204] of αpv fl/fl UC, αpv -/- 361 and αpv -/- 369 UC. Gapdh levels served as loading control **(D)** Adhesion assay using αpv fl/fl UC, αpv -/- 361 and αpv -/- 369 UC on Laminin, Collagen I and IV and Fibronectin [numbers represent concentrations]. Adhesion was allowed for 1h. Graph shows x-fold increase of adhesion over background adhesion and represents data of technical triplicates. Bars represent SD. **(E)** FACS analysis of Integrin surface expression from αpv fl/fl UC, αpv -/- 361 and αpv -/- 369 UC. Integrin null cells were used as control

Figure S1: Loss of αpv in the mesangium results in glomerulus breakdown and interstitial fibrosis (A) HE staining of kidney sections from αpv fl/+ PDGFRβCre and αpv fl/fl PDGFRβCre mice at embryonic stage 17 and 30 days after birth. Note kidney cysts in P30 kidneys from αpv fl/fl PDGFRβCre mice. Scale bar: 500µm **(B)** HE staining and immunostaining against αpv (green) and αSMA (red) of large intestine sections of αpv fl/+ PDGFRβCre and αpv fl/fl PDGFRβCre mice. Scale bar: 50µm and 75µm **(C)** HE stainings of glomeruli and closeup of single glomerulus. Arrowhead indicates areas of cell loss, rectangle indicates area of matrix accumulation, star indicates hypercellular area. Scale bar: 200µm. Immunostaining of kidney sections from αpv fl/+ PDGFRβCre and αpv fl/fl PDGFRβCre mice against αpv (green) and αSMA (red) reveal loss of αpv in glomeruli of αpv fl/fl PDGFRβCre mice. Nuclei are visualized with DAPI. Scale bar: 75µm. **(D)** Urine samples taken from αpv fl/+ PDGFRβCre and αpv fl/fl PDGFRβCre mice were analysed by coomassie stained 12% SDS-Page. **(E)** Immunostaining of kidney sections from αpv fl/+ PDGFRβCre and αpv fl/fl PDGFRβCre mice against αSMA (red) and Vimentin (green) reveal fibrotic areas in αpv fl/fl PDGFRβCre mice. Nuclei are visualized with DAPI. Scale bar: 75µm. **(F)** Hemavet analysis of blood samples of αpv fl/+ PDGFRβCre and αpv fl/fl PDGFRβCre mice. Panel shows average white blood cell counts of 5 mice of each genotype. Bars represent standard deviation. **(G)** Hemavet analysis of blood samples of αpv fl/+ PDGFRβCre and αpv fl/fl PDGFRβCre mice. Panel shows average red blood cell counts of 5 mice of each genotype. Bars represent standard deviation.

Figure S2: Deletion of αpv in vSMC leads to degradation of laminar fibers in the aorta. **(A)** HE staining and Verhoeff van Gieson staining of abdominal aorta sections of αpv fl/+ PDGFRβCre and αpv fl/fl PDGFRβCre mice. Scale bar: 75µm. **(B)** Immunostaining against Mac1 (white) and *in situ* zymogram of aorta sections of αpv fl/+ PDGFRβCre and αpv fl/fl PDGFRβCre mice. Green staining indicates areas of proteolytic activity. Pictures were taken with the same laser intensity. Nuclei are visualized with DAPI. Scale bar: 75µm **(C)** *In situ* zymogram with DQ-Gelatin (green) and phalloidin (red) in αpv fl/+ PDGFRβCre

and αpv fl/fl PDGFRβCre vSMC. Green fluorescence marks areas of proteolytic activity. Nuclei are visualized with DAPI. Pictures were taken with same the laser intensity. Scale bar: 20µm **(D)** Zymogram of vSMC lysates of αpv fl/+ PDGFRβCre and αpv fl/fl PDGFRβCre mice with Gelatin (2mg/ml) and Casein (2mg/ml) as substrate. White bands indicate areas of MMP induced degradation. **(E)** Protein levels of MMP9, MMP1, MT1-MMP and MMP2 in vSMC lysates of αpv fl/+ PDGFRβCre and αpv fl/fl PDGFRβCre mice. Gapdh served as loading control.

Figure S3: Tamoxifen induced deletion of αpv in SMCs results in gastrointestinal defects. (A) Whole mount immunostaining of small intestine of αpv fl/fl and αpv fl/fl SMMHC-CreER^{T2} mice against αSMA (white). Images are maximum projections of multiple stack images. Scale bar: 75µm. **(B)** Immunostaining against Mac1 (white), *in situ* zymogram with DQ-Gelatin (green) and Tunel (green) assay for apoptotic cells on small intestine sections of αpv fl/fl and αpv fl/fl SMMHC-CreER^{T2} mice. Nuclei are visualized with DAPI. Scale bar: 75µm. **(C)** HE staining of stomach sections of αpv fl/fl and αpv fl/fl SMMHC-CreER^{T2} mice. Closeup shows increased thickness of SMC layer and round SMCs. Scale bar: 100µm. **(D)** HE staining of aorta sections of αpv fl/fl and αpv fl/fl SMMHC-CreER^{T2} mice. Closeup shows no changes in number or shape of SMCs. Scale bar: 100µm.

Figure S4: αpv deletion does not change contractility of MC. (A) Immunostaining against αpv (green) and αSMA (red) (upper row)and ILK (green) and PINCH1 (red) (lower row) of αpv fl/fl UC, αpv -/- 361 and αpv -/- 369 UC seeded on 2µg/ml FN. Nuclei are visualized with DAPI. Scale bar: 20µm. **(B)** Protein levels of αpv, ILK and PINCH1 of αpv fl/fl UC, αpv -/- 361 and αpv -/- 369 UC. Gapdh levels served as loading control. **(C)** Immunostaining against αpv (green) and αSMA (red) of αpv fl/fl and αpv -/- MC seeded on 2µg/ml FN. Nuclei are visualized with DAPI. Immunostaining against pMLC2 (green) and αSMA (red) of αpv fl/fl and αpv -/- MC seeded on 2µg/ml FN. Nuclei are visualized with DAPI. Scale bar: 20µm. **(D)** Protein levels of αpv, ILK and PINCH1 of αpv fl/fl UC, αpv -/- 361 and αpv -/- 369 UC. Gapdh levels served as loading control. **(E)** Immortalized αpv fl/fl and αpv -/- MC seeded on FN coated umbrella shaped micropatterns and immunostained for pMLC2 (green), Phalloidin (red) and Paxillin (white). Nuclei are visualized with DAPI. Single channels are shown in black and white.

Figure S5: αpv deletion enhances degradation activity of MC. **(A)** Representative pictures of a boyden chamber assay using αpv fl/fl UC, αpv -/- 361 and αpv -/- 369 UC. Cells were stained by crystal violet Pure medium was used as a control. Graph displays fold increase of cell number stimulated by 10% FCS against pure medium. **(B)** Protein levels of FAK, pFAK [Y397], Akt, pAkt [S473], Erk 1/2, pErk1/2 [T202/ Y204] of αpv fl/fl and αpv -/- MC. Gapdh levels served as loading control **(C)** Protein levels of MMP9, MT1-MMP and MMP2 in αpv fl/fl UC, αpv -/- 361 and αpv -/- 369 UC and αpv fl/fl and αpv -/- MC. Tubulin levels served as loading control. **(D)** *In situ* zymogram with DQ-Gelatin (green) using αpv fl/fl UC, αpv -/- 361 and αpv -/- 369 UC and αpv fl/fl and αpv -/- MC. Green fluorescence marks areas of proteolytic activity. Nuclei are visualized with DAPI. Pictures were taken with the same laser intensity. Scale bar: 20µm.

Figure 1

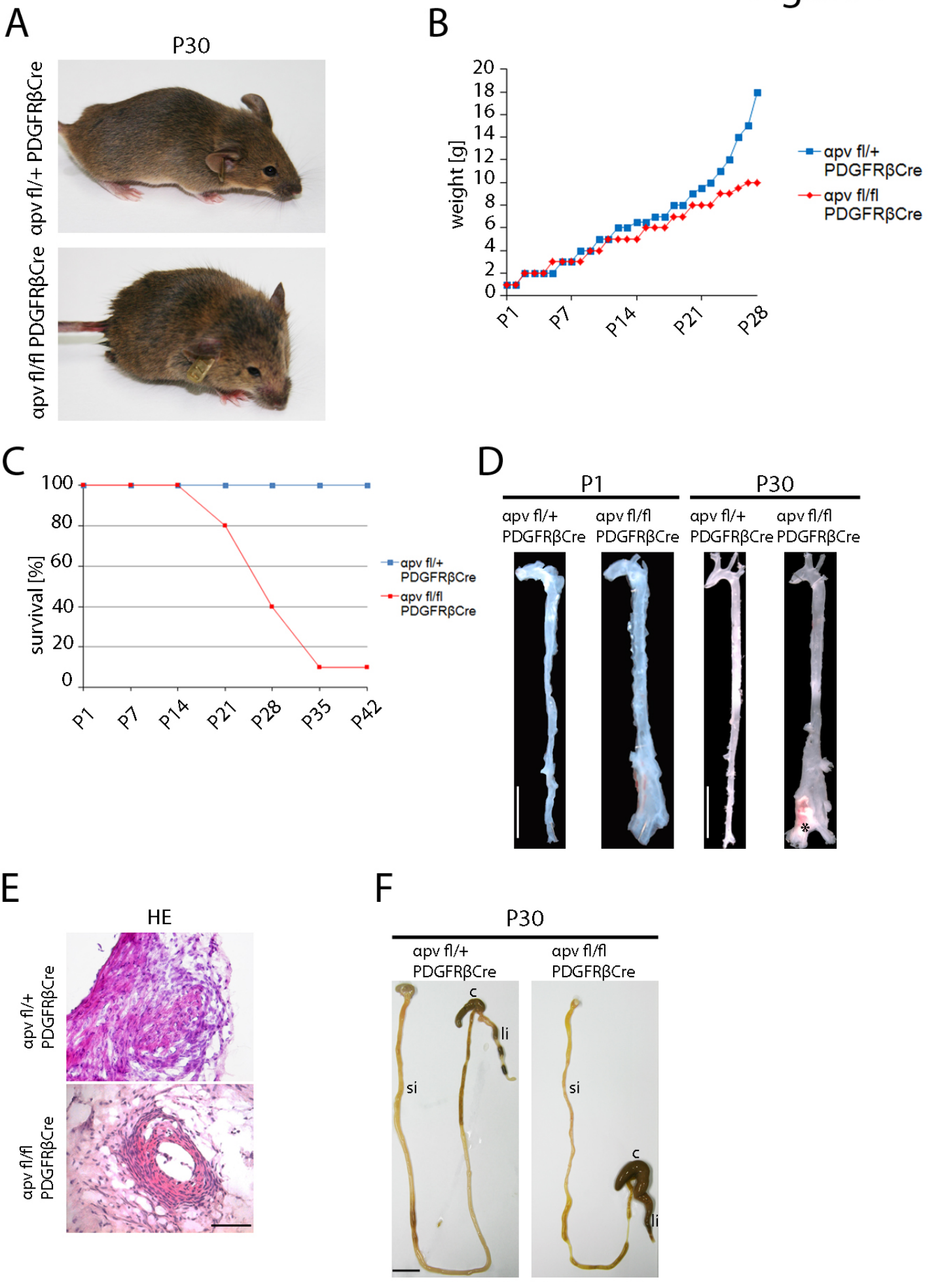
A
P30
apv fl/+ PDGFRβCre
apv fl/fl PDGFRβCre
B
weight [g]
20
18
16
14
12
10
8
6
4
2
0
P1
P7
P14
P21
P28
apv fl/+ PDGFRβCre
apv fl/fl PDGFRβCre
C
survival [%]
100
80
60
40
20
0
P1
P7
P14
P21
P28
P35
P42
apv fl/+ PDGFRβCre
apv fl/fl PDGFRβCre
D
P1
P30
apv fl/+ PDGFRβCre
apv fl/fl PDGFRβCre
apv fl/+ PDGFRβCre
apv fl/fl PDGFRβCre
E
HE
apv fl/+ PDGFRβCre
apv fl/fl PDGFRβCre
F
P30
apv fl/+ PDGFRβCre
apv fl/fl PDGFRβCre
c
li
si
si
c
li

Figure 2

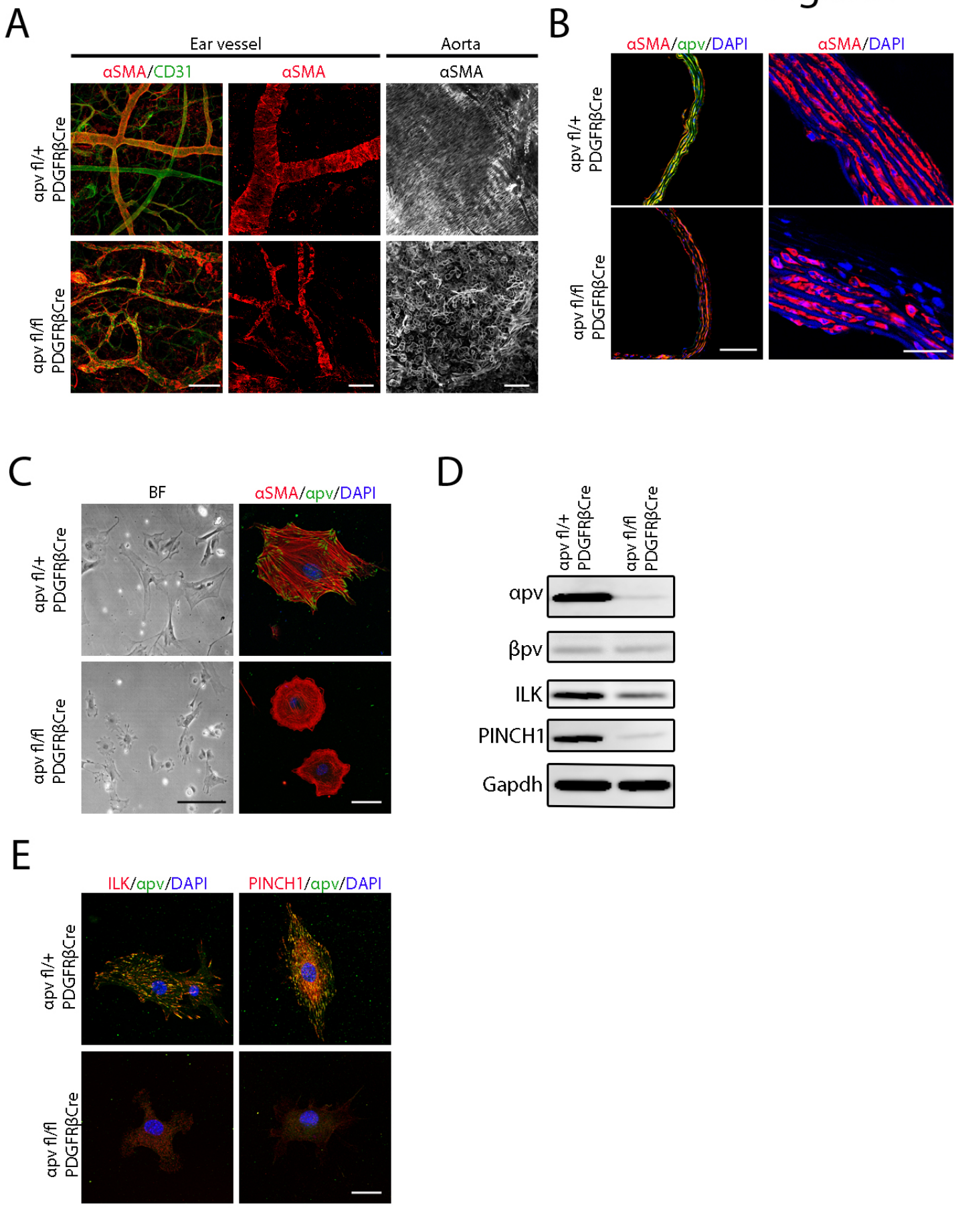
A
Ear vessel
Aorta
αSMA/CD31
αSMA
αSMA
apv fl/+ PDGFRβCre
apv fl/fl PDGFRβCre
B
αSMA/apv/DAPI
αSMA/DAPI
apv fl/+ PDGFRβCre
apv fl/fl PDGFRβCre
C
BF
αSMA/apv/DAPI
apv fl/+ PDGFRβCre
apv fl/fl PDGFRβCre
D
apv fl/+ PDGFRβCre
apv fl/fl PDGFRβCre
αpv
βpv
ILK
PINCH1
Gapdh
E
ILK/apv/DAPI
PINCH1/apv/DAPI
apv fl/+ PDGFRβCre
apv fl/fl PDGFRβCre

Figure 3

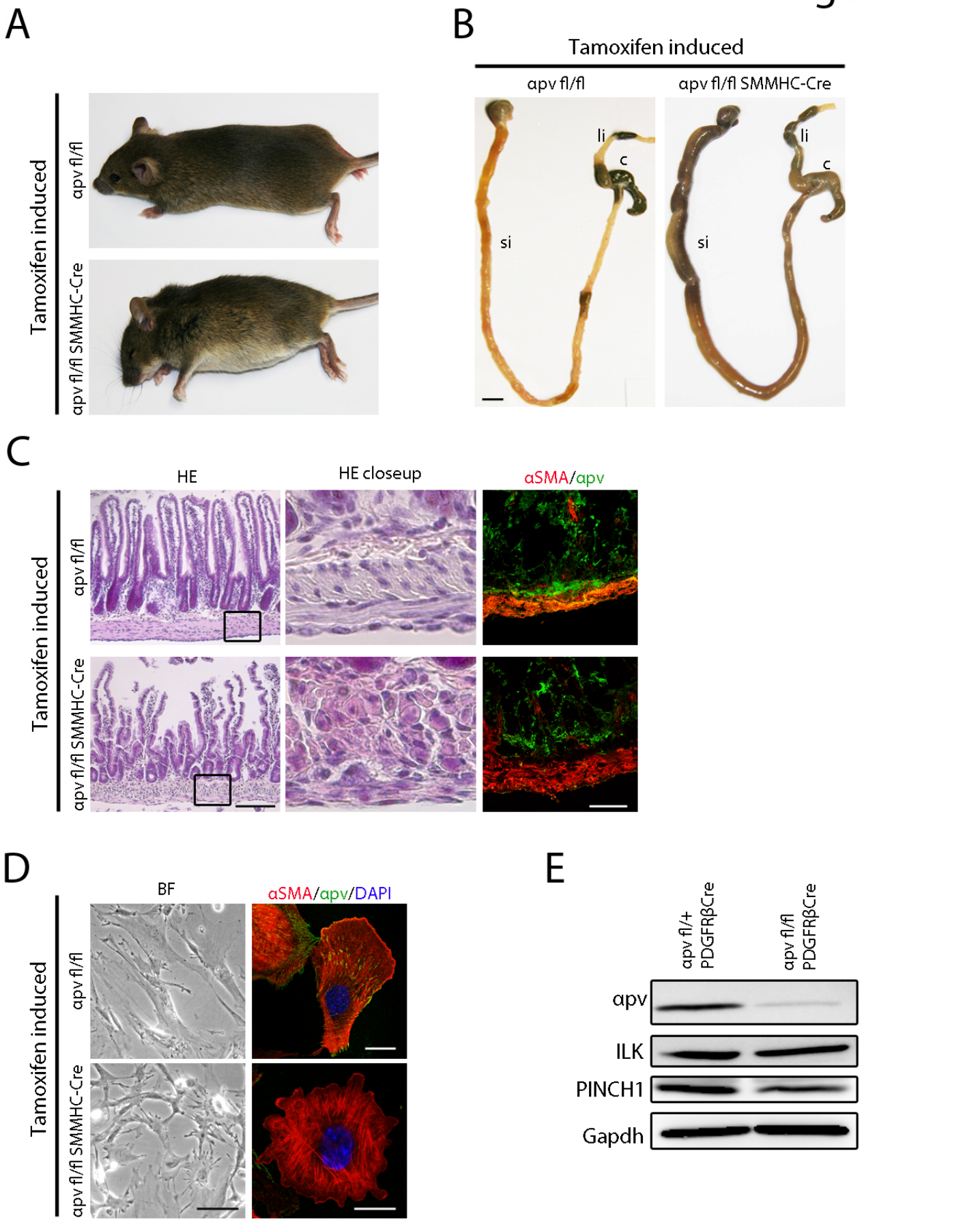
A
Tamoxifen induced
apv fl/fl
apv fl/fl SMMHC-Cre
B
Tamoxifen induced
apv fl/fl
apv fl/fl SMMHC-Cre
li
c
si
C
HE
HE closeup
αSMA/apv
D
BF
αSMA/apv/DAPI
E
apv fl/+ PDGFRβCre
apv fl/fl PDGFRβCre
apv
ILK
PINCH1
Gapdh

Figure 4

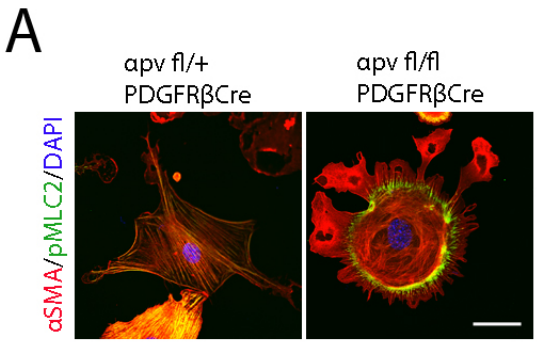
A
apv fl/+
PDGFRβCre
apv fl/fl
PDGFRβCre
αSMA/pMLC2/DAPI

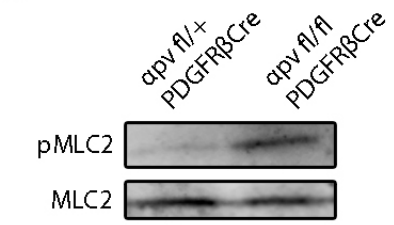
B
apv fl/+
PDGFRβCre
apv fl/fl
PDGFRβCre
pMLC2
MLC2

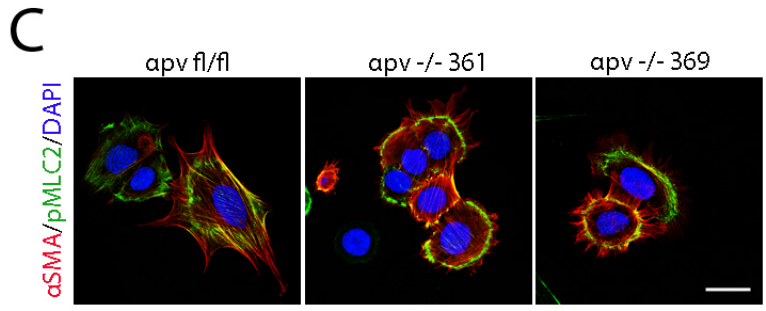
C
apv fl/fl
apv -/- 361
apv -/- 369
αSMA/pMLC2/DAPI

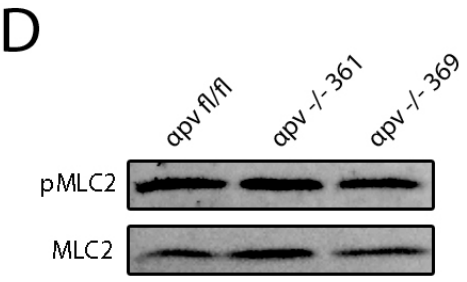
D
apv fl/fl
apv -/- 361
apv -/- 369
pMLC2
MLC2

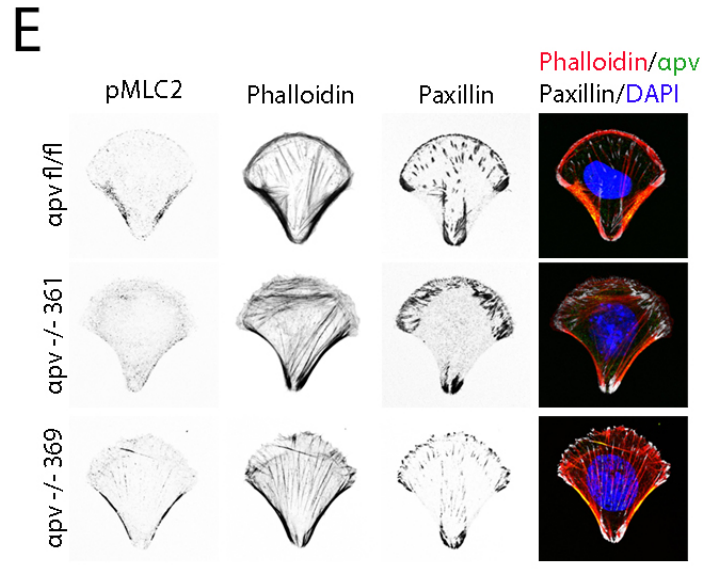
E
pMLC2
Phalloidin
Paxillin
Phalloidin/apv
Paxillin/DAPI
apv fl/fl
apv -/- 361
apv -/- 369

Figure 5

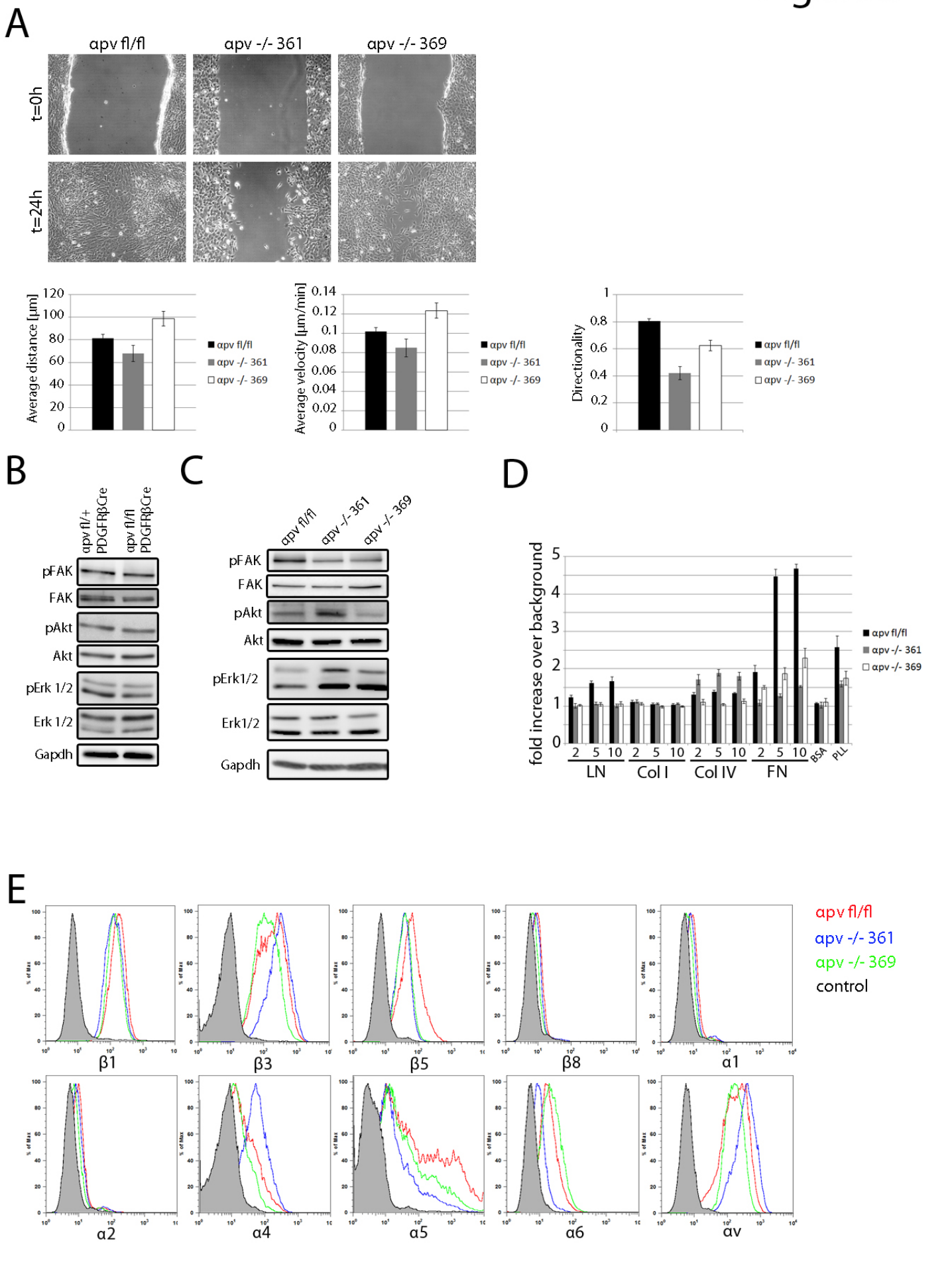
A
αpv fl/fl
αpv -/- 361
αpv -/- 369
t=0h
t=24h
Average distance [µm]
Average velocity [µm/min]
Directionality
αpv fl/fl
αpv -/- 361
αpv -/- 369
B
αpv fl/+ PDGFRβCre
αpv fl/fl PDGFRβCre
pFAK
FAK
pAkt
Akt
pErk 1/2
Erk 1/2
Gapdh
C
αpv fl/fl
αpv -/- 361
αpv -/- 369
pFAK
FAK
pAkt
Akt
pErk1/2
Erk1/2
Gapdh
D
fold increase over background
2 5 10 2 5 10 2 5 10 2 5 10 BSA PLL
LN
Col I
Col IV
FN
αpv fl/fl
αpv -/- 361
αpv -/- 369
E
αpv fl/fl
αpv -/- 361
αpv -/- 369
control
β1
β3
β5
β8
α1
α2
α4
α5
α6
αv

Figure S1

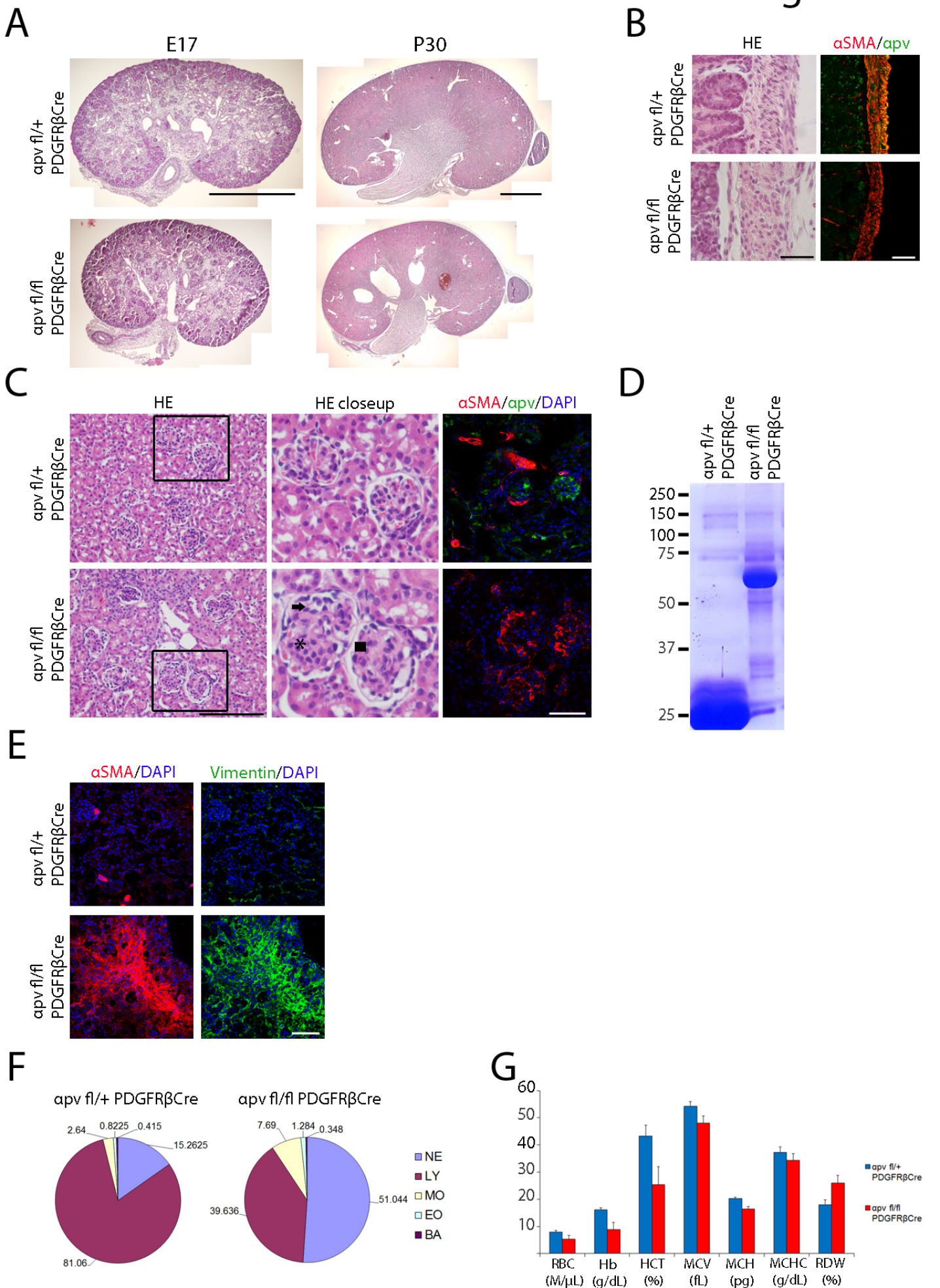
A
E17
P30
apv fl/+ PDGFRβCre
apv fl/fl PDGFRβCre
B
HE
αSMA/apv
C
HE
HE closeup
αSMA/apv/DAPI
D
250
150
100
75
50
37
25
E
αSMA/DAPI
Vimentin/DAPI
F
apv fl/+ PDGFRβCre
apv fl/fl PDGFRβCre
2.64
0.8225
0.415
15.2625
81.06
7.69
1.284
0.348
51.044
39.636
NE
LY
MO
EO
BA
G
60
50
40
30
20
10
RBC (M/μL)
Hb (g/dL)
HCT (%)
MCV (fL)
MCH (pg)
MCHC (g/dL)
RDW (%)

Figure S2

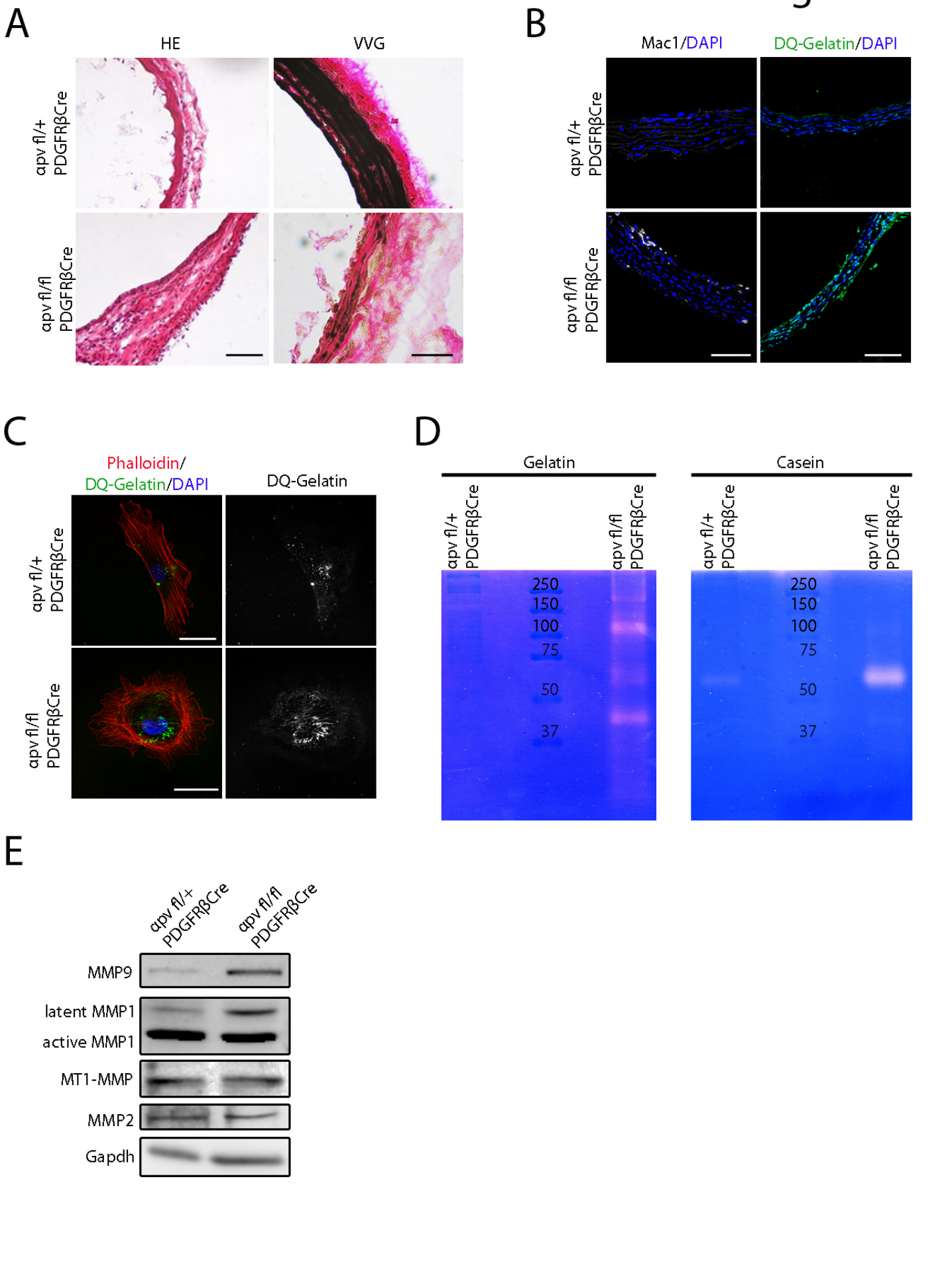
A
HE
VVG
αpv fl/+ PDGFRβCre
αpv fl/fl PDGFRβCre
B
Mac1/DAPI
DQ-Gelatin/DAPI
αpv fl/+ PDGFRβCre
αpv fl/fl PDGFRβCre
C
Phalloidin/ DQ-Gelatin/DAPI
DQ-Gelatin
αpv fl/+ PDGFRβCre
αpv fl/fl PDGFRβCre
D
Gelatin
Casein
αpv fl/+ PDGFRβCre
αpv fl/fl PDGFRβCre
250
150
100
75
50
37
E
αpv fl/+ PDGFRβCre
αpv fl/fl PDGFRβCre
MMP9
latent MMP1
active MMP1
MT1-MMP
MMP2
Gapdh

Figure S3

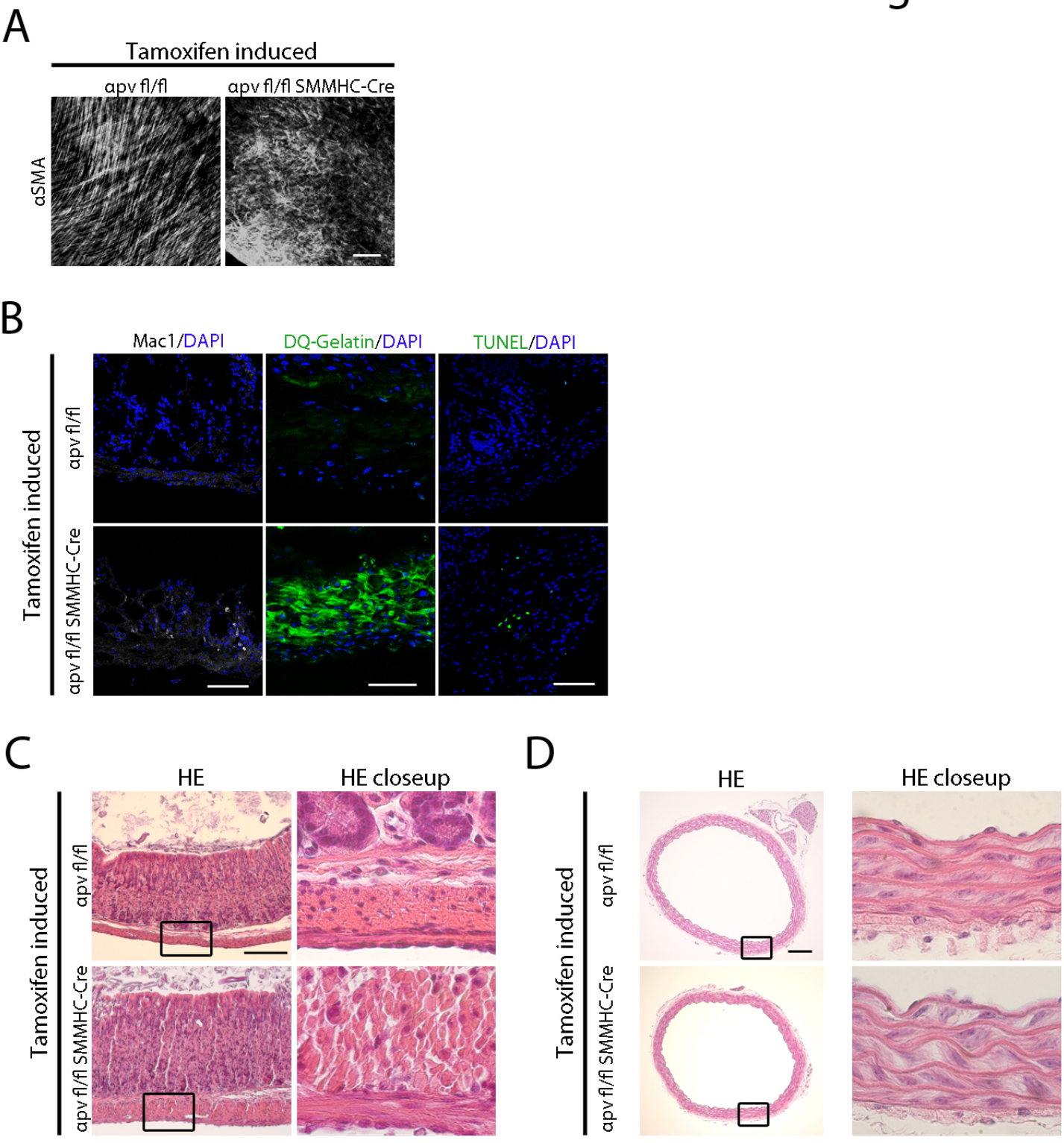
A
Tamoxifen induced
αpv fl/fl
αpv fl/fl SMMHC-Cre
αSMA
B
Mac1/DAPI
DQ-Gelatin/DAPI
TUNEL/DAPI
Tamoxifen induced
αpv fl/fl
αpv fl/fl SMMHC-Cre
C
HE
HE closeup
Tamoxifen induced
αpv fl/fl
αpv fl/fl SMMHC-Cre
D
HE
HE closeup
Tamoxifen induced
αpv fl/fl
αpv fl/fl SMMHC-Cre

Figure S4

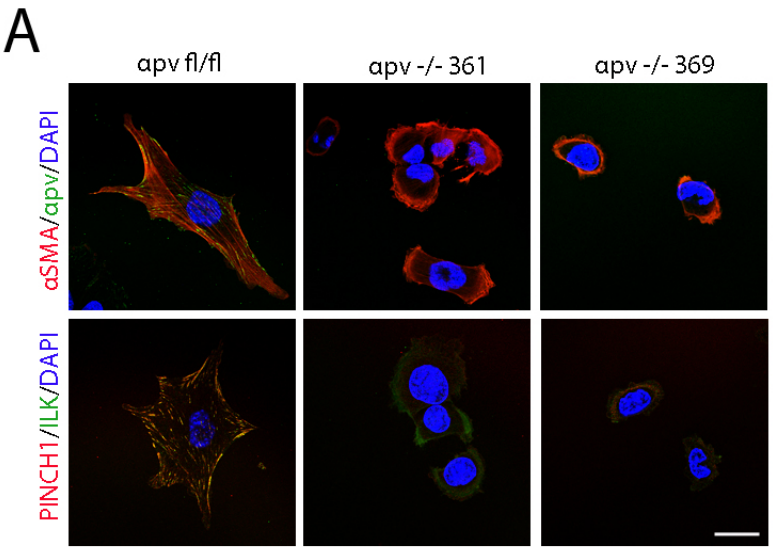
A
apv fl/fl
apv -/- 361
apv -/- 369
αSMA/apv/DAPI
PINCH1/ILK/DAPI

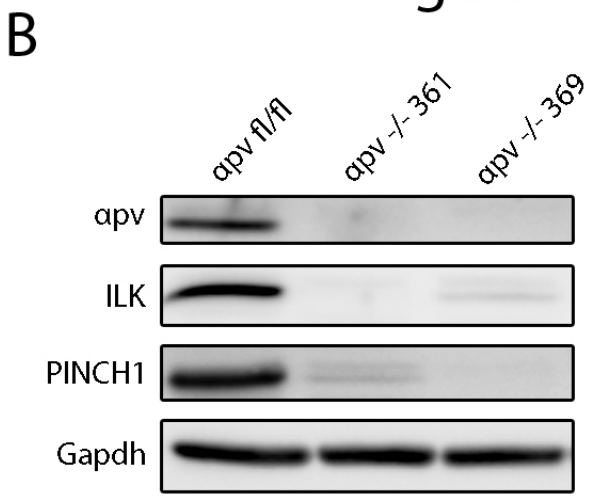
B
apv fl/fl
apv -/- 361
apv -/- 369
apv
ILK
PINCH1
Gapdh

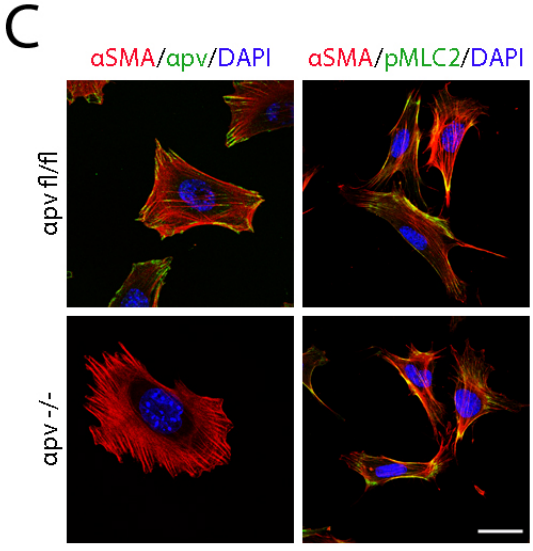
C
αSMA/apv/DAPI
αSMA/pMLC2/DAPI
apv fl/fl
apv -/-

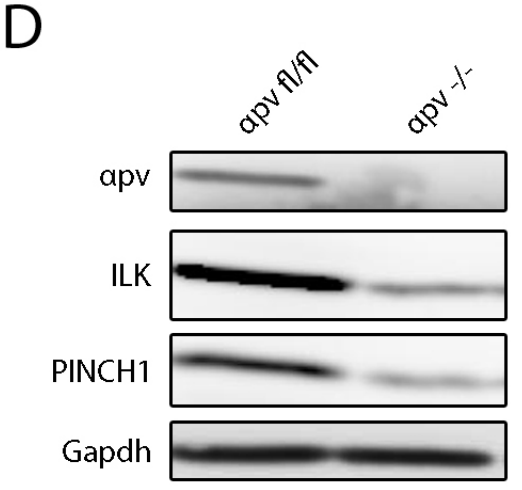
D
apv fl/fl
apv -/-
apv
ILK
PINCH1
Gapdh

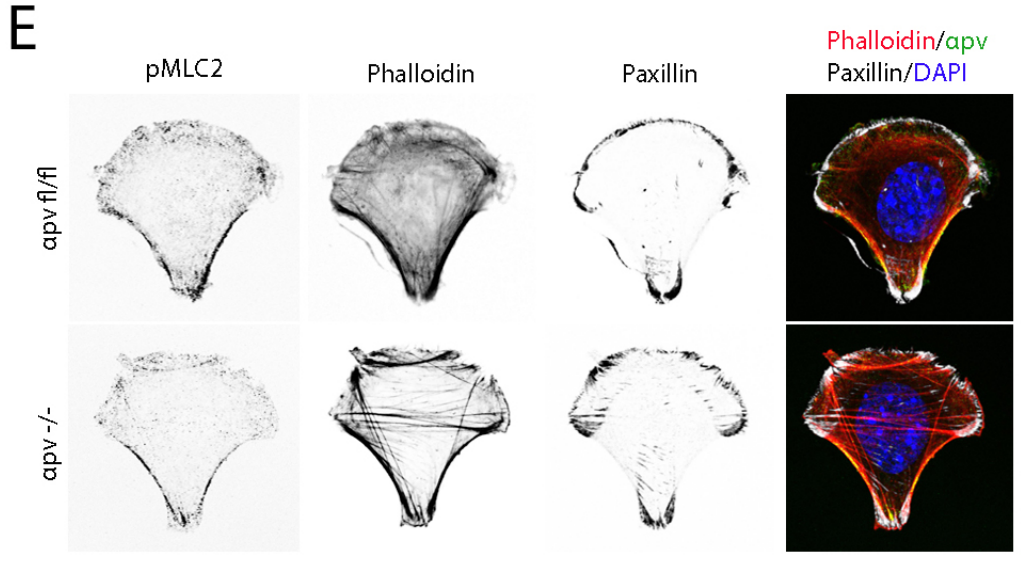
E
pMLC2
Phalloidin
Paxillin
Phalloidin/apv
Paxillin/DAPI
apv fl/fl
apv -/-

Figure S5

A

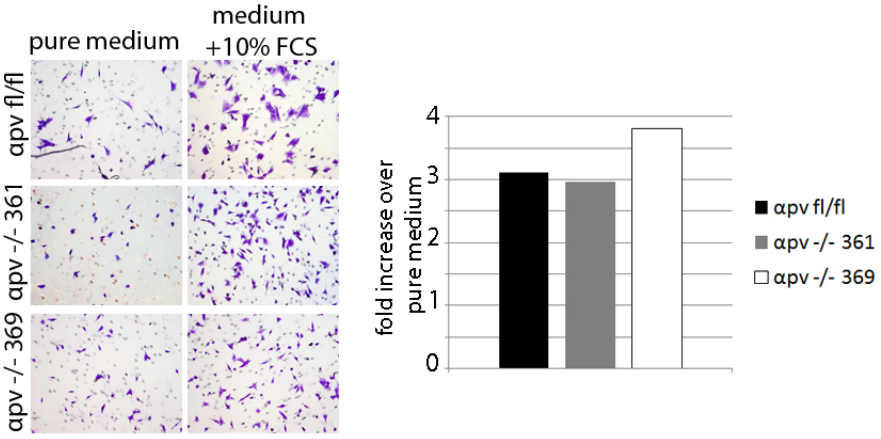

B

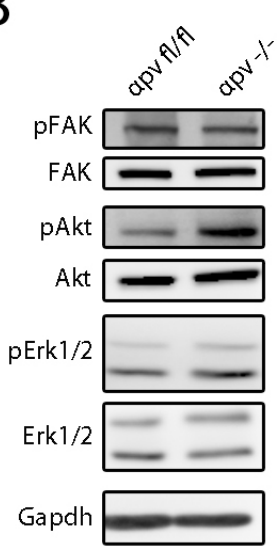

C

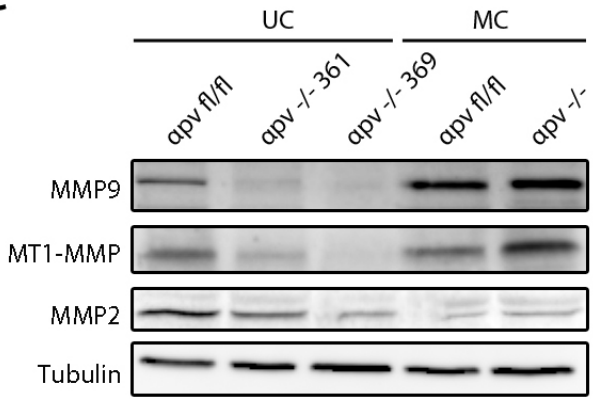

D